The Cloning and Characterization of a Profilin Homolog Encoded by Orthopoxviruses

by

Christine Kathrine Butler-Cole
B.Sc., University College of the Fraser Valley, 2002

A Thesis Submitted in Partial Fulfillment of the
Requirements for the Degree of

MASTER OF SCIENCE

in the Department of Biochemistry and Microbiology

Supervisor: Dr. Chris Upton

Abstract

This thesis focuses on the characterization of a gene in ectromelia virus that encodes a homolog of profilin, a cellular actin-binding protein. The profilin homolog protein family is found exclusively within the orthopoxviruses, and orthologs share greater than 90% amino acid identity. The conservation of the gene in orthopoxviruses, in addition to its location in the variable terminal region of the genome, suggests that it is important for increasing viral fitness during infection. A homology model of the ECTV-Mos 141 protein, suggests that although the profilin homolog and mammalian profilin share only 30% amino acid identity, the three-dimensional structures of the proteins are similar. There are differences at the amino acid level, however, which may have important implications in the localization and function of the profilin homolog *in vivo*. Interestingly, ECTV-Mos 141 associates with cellular tropomyosin and viral A-type inclusion proteins in virus infected cells. Colocalization of ECTV-Mos 141, tropomyosin and truncated A-type inclusion protein at putative actin tails and CEV-induced protrusions from the cell surface, suggests a role for these proteins in intercellular spread of the virus. Additionally, ECTV-Mos 141 associates with A-type inclusion bodies formed by both truncated and full-length A-type inclusion proteins; these structures are important in the protection and dissemination of the virus outside the host. The formation of these bodies may be facilitated by the action of the profilin homolog and utilization of the microtubule cytoskeleton.

Table of Contents

Abstract *ii*
Table of Contents *iii*
List of Tables *iv*
List of Figures *v*
List of Abbreviations *vi*
Acknowledgments *vii*

Chapter 1 – Introduction 1

History of Poxviruses 1
Classification of Poxviruses 2
Biology and Life Cycle of Poxviruses 3
Virion Structure 3
Genome 4
Replication Cycle 6
Motility 10
Dissemination 13
Poxvirus Virulence Factors 13
Host Immune Evasion 13
A-type Inclusion Bodies 15
Profilin Homolog 16
Significance of Poxvirus Research 19
Thesis Rationale 21
Contributors to Work Presented in this Thesis 23

Chapter 2 – Materials and Methods 24

Chapter 3 – Results 62

Selection of Gene Targets 62
Cloning of Gene Targets 66
Location of Gene Target ortholog ORFs in the ECTV-Mos genome 70
Expression of Recombinant Proteins 73
Purification of ECTV-Mos 141 protein, a profilin homolog 76
Analysis of the Orthopoxvirus Profilin Homolog Protein Family 79
Homology Model of ECTV-Mos 141 protein 82
Coimmunoprecipitation of ECTV-Mos 141 and ECTV-Mos 141-interacting proteins from poxvirus-infected cells 85
ECTV-Mos 141 and tropomyosin interact directly 89
Analysis of Orthopoxvirus A-type Inclusion Proteins 92
Localization of ECTV-Mos 141 and A-type Inclusion Proteins *in vivo* 94
Localization of ECTV-Mos 141 and cellular tropomyosin *in vivo* 101

Chapter 4 – Discussion 104

Concluding Remarks 115

Literature Cited 117

List of Tables

Table 1	Complete poxvirus genomes in the Viral Orthologous Clusters (VOCs) database.	25
Table 2	Oligonucleotide primers used for PCR-amplification of gene targets.	31
Table 3	Selection of 56 conserved orthopoxvirus gene families for characterization.	64
Table 4	PCR-amplified gene targets sent to the University of Alberta for cloning and characterization.	67
Table 5	PCR-amplified gene targets retained for cloning and characterization.	69
Table 6	The orthopoxvirus profilin homolog protein family.	80

List of Figures

Figure 1	Replication cycle of vaccinia virus.	9
Figure 2	Overview of intracellular and intercellular virion movement.	12
Figure 3	Cellular profilin performs a diversity of functions.	19
Figure 4	Design of oligonucleotide primers for PCR-amplification of gene targets.	29
Figure 5	Cloning strategy for the production of pDEST14 expression clones.	43
Figure 6	Organization of gene target ORFs in the ECTV-Mos genome.	72
Figure 7	SDS-PAGE analysis of recombinant protein expression in *E.coli*.	75
Figure 8	SDS-PAGE and western blot analysis of purified ECTV-Mos 141 protein.	78
Figure 9	Protein sequence alignment of the orthopoxvirus profilin homolog protein family.	81
Figure 10	Homology model of ECTV-Mos 141 protein.	83
Figure 11	Coimmunoprecipitation and identification of proteins interacting with ECTV-Mos 141 during infection.	87

Figure 12 Western blot to detect actin in coimmunoprecipitated proteins. 89

Figure 13 Far western analysis of the interaction between ECTV-Mos 141 and tropomyosin. 91

Figure 14 Graphical representation of sequence alignment of A-type inclusion proteins. 93

Figure 15 Colocalization of ECTV-Mos 141 and VACV-WR 148 in virus-infected cells. 97

Figure 16 Colocalization of ECTV-Mos 141 and ECTV-Mos 128 in virus-infected cells. 100

Figure 17 Colocalization of ECTV-Mos 141 and tropomyosin in virus-infected cells. 103

List of Abbreviations

α, alpha

aa, amino acid(s)

Amp^R, ampicillin resistant

araBAD, arabinose operon

ATI, A-type inclusion

ATPase, adenosine triphosphate phosphatase

β, beta

BS-C-1, African green monkey cells

BLASTP, Basic Local Alignment Search Tool-Protein

bp, basepair

BSA, bovine serum albumin

C-terminus, carboxy terminus

CEV, cell-associated enveloped virus

CMLV, camelpox virus

CO_2, carbon dioxide

CPXV, cowpox virus

DAPI, 4',6'-diamidino-2-phenylindole

DMEM, Dulbecco's minimal essential medium

DMSO, dimethyl sulphoxide

DNA, deoxyribonucleic acid

dNTP, deoxyribonucleotide triphosphate

DTT, dithiothreitol

EB, elution buffer

EDTA, ethylenediaminetetraacetic acid

EEV, extracellular enveloped virion

ECTV, ectromelia virus

FBS, fetal bovine serum

FITC, fluorescein isothiocyanate

γ, gamma

HA, haemagglutinin

HBS, HEPES-buffered saline solution

HEPES, N-2-hydroxyethylpiperazine-N' -2' -ethanesulfonic acid

HGT, horizontal gene transfer

His, histidine

IFN, interferon

IL, interleukin

IMV, intracellular mature virion

Kan^R, kanamycin resistant

kb, kilobasepair

kDa, kiloDalton

LB, Luria-Bertani

MALDI-TOF, Matrix Assisted Laser Desorption Ionization-Time of Flight

ml, millilitre

μg, microgram

μl, microlitre

mM, millimolar

MOI, multiplicity of infection

MPXV, monkeypox virus

mRNA, messenger ribonucleic acid

N-terminus, amino terminus

ng, nanogram

NMR, Nuclear Magnetic Resonance

NTP-PPH, nucleoside triphosphate pyrophosphohydrolase

OD, optical density

ORF, open reading frame

PAGE, polyacryalamide gel electrophoresis

PBS, phosphate buffered saline

PCR, polymerase chain reaction

PEG, polyethylene glycol

pfu, plaque forming units

PH-PPH, nucleophosphohydrolase-pyrophosphohydrolase downregulator

PIP_2, phosphatidylinositol 4,5-bisphosphate

PKR, RNA-dependent protein kinase

PMSF, phenyl methyl sulfonyl fluoride

RNA, ribonucleic acid

rpm, revolutions per minute

RPXV, rabbitpox virus

SDS, sodium dodecylsulfate

SSC, standard saline citrate

TAE, tris, acetic acid, EDTA

TBS, tris buffered saline

VARV, variola virus

VACV, vaccinia virus

VASP, Vasodilator Stimulated Phosphoprotein

VOCs, Viral Orthologous Clusters

N-WASP, neural Wiskott-Aldrich syndrome protein

WIP, WASP-interacting protein

Acknowledgments

I thank my supervisor Dr. Chris Upton for his guidance on this project throughout the previous three years and in supporting my decision to complete my Masters and pursue a degree in law. I appreciate your understanding. I thank my committee members Dr. Nano and Dr. Koop for their help throughout my studies. Thank you to all of the individuals who have contributed to the work presented in this thesis, including: Dr. Mark Buller, Arwen Hunter, Roderick Haesevoets, Guiyun Lee, Dr. David Esteban, and Shan Sundararaj. I would also like to express my gratitude to Melisa Da Silva and Angelika Ehlers for their friendship and computer expertise. Thanks are also extended to Scott Scholz, Albert Labossiere and Stephen Horak for their technical support and to Melinda Powell and Deb Penner for their help through the administrative process. Finally I would like to thank my family, friends and my husband Chris for their love and support.

Chapter 1: Introduction

I. History of Poxviruses

Smallpox was once the most serious disease faced by mankind; it has had an enormous impact on human history. It claimed the lives of hundreds of millions of people between its first recorded out break in Ancient Egypt and its eradication in 1979 (Mahalingam et al., 2004). Variola virus, the causative agent of smallpox, is speculated to have emerged in Africa or Asia some 5,000 years ago (Moss, 2001). Although its exact origins remain obscure, an ancestral virus of variola present in a wild animal reservoir likely adapted to the human population through an intermediate host such as cattle or small rodent. Large high-density populations and the domestication of animals are thought to have been necessary for the emergence and continuance of this pathogen (Ellner, 1998).

In about 1000 A.D., one of the first effective preventative measures against an infectious disease was initiated against smallpox. Variolation, a risky procedure in which people were inoculated with material collected from individuals infected with smallpox, offered some protection against smallpox infection (Moss, 2001). In 1796 Edward Jenner demonstrated that cowpox virus, which is less virulent to humans, could be used to protect against contraction of smallpox and marked the beginning of a scientific investigation into vaccination (Ellner, 1998). Global eradication of smallpox was declared in 1979 following a World Health Organization (WHO)-led vaccination program (Ellner, 1998). The vaccine against smallpox contained vaccinia virus, now considered the prototypic poxvirus. The absence of a non-human reservoir for variola

virus in addition to sociopolitical factors contributed to the successful eradication of this disease (Mahalingam et al., 2004).

Due to its role in the eradication of smallpox, vaccinia virus has the longest and most extensive history of use in humans compared to any other virus and has been studied extensively in the laboratory. It was the first animal virus seen microscopically, grown in tissue culture, accurately titered, physically purified, and chemically analyzed (Shen and Nemunaitis, 2004). Poxvirus research has, and continues to be, an active area of investigation.

II. Classification of Poxviruses

The *Poxviridae,* as a family, are ubiquitous, infecting mammals, birds, reptiles and invertebrates. Two members of this family, variola virus and molluscum contagiousum virus, are obligate human pathogens although many other poxviruses can be transmitted to humans from other animal hosts. Poxviruses can be divided into two subfamilies based on their ability to replicate within vertebrates (*Chordopoxvirinae*) and insects (*Entomopoxvirinae*). The *Chordopoxvirinae* consists of eight genera: *Orthopoxvirus* (camelpox, cowpox, ectromelia, monkeypox, raccoonpox, skunkpox, vaccinia, variola, volepox), *Parapoxvirus* (ecthyma, orf, pseudocowpox, parapox of deer, sealpox), *Avipoxvirus* (canarypox, fowlpox, juncopox, mynahpox, pigeonpox, psittacinepox, quailpox, sparrowpox, starlingpox, turkeypox), *Capripoxvirus* (goatpox, lumpy skin disease, sheeppox), *Leporipoxvirus* (myxoma, hare fibroma, rabbit fibroma, squirrel fibroma), *Suipoxvirus* (swinepox), *Molluscipoxvirus* (molluscum contagiosum) and

Yatapoxvirus (tanapox, Yaba monkey tumor). Viruses belonging to the same genus are genetically and antigenically related and have a similar morphology and host range (Moss, 2001). The *Entomopoxvirinae* subfamily contains three genera, which are distinguished from one another by their insect host range and virion morphology (Moss, 2001; Arif, 1984). Genus A viruses infect coleopterans, genus B viruses infect lepidopterans and orthopterans, and genus C viruses infect dipterans. Insects are the only known hosts of entomopoxviruses, and their viral host range is restricted to a small number of related species (Afonso et al., 1999).

III. Biology and Life Cycle of Poxviruses

Virion Structure

Poxviruses are the largest known animal viruses, and are discernable by light microscopy (Dubochet et al., 1994). The structure of poxvirus virions has been studied extensively using vaccinia virus, the prototypic virus of the family, although the basic features may largely apply to other family members as well. Vaccinia virions are oval or brick-shaped, approximately 300 x 240 x 120 nm in size, and consist of a lipoprotein envelope surrounding a complex core structure (Moss, 2001). The virion core contains the viral genome associated with a number of virus-encoded enzymes required for transcription; including the multisubunit DNA dependent RNA polymerase, early transcription factor (VETF), enzymes for methylation and capping of mRNA, a poly (A) polymerase and nucleoside triphosphate phosphohydrolase (NTP-PPH) (Moss, 2001; Smith et al., 2002).

Vaccinia virus produces four different types of virion from each infected cell that have different abundance, structure, location and roles in the virus life cycle (Husain and Moss, 2005). First, intracellular mature virus (IMV) particles are formed within cytoplasmic factors from non-infectious precursors and represent the majority of infectious progeny. IMV are released from the cell during cell lysis and are important for viral transmission from one host to another (Moss, 2001). The majority of IMV remain in the cell until lysis, however, some IMV become wrapped by a double layer of intracellular membrane to form intracellular enveloped virus (IEV) (Hiller and Weber, 1985). The composition of this membrane is different from that of the host, and contains at least seven poxvirus-encoded polypeptides (Husain and Moss, 2005; Lorenzo et al., 1998). IEV then move to the cell periphery where the outer membrane fuses with the plasma membrane exposing a cell-associated enveloped virus (CEV) on the surface. CEV are involved in actin tail formation that is instrumental in the intercellular spread of the virus (Blasco and Moss, 1992). CEV released from the cell surface are called extracellular enveloped virus (EEV). Although less abundant than IMV or CEV, EEV play a role in the long range dissemination of the virus within tissue culture and the host (Payne, 1980). CEV and EEV are physically indistinguishable and contain one fewer membrane that IEV and one more membrane than IMV, respectively (Smith et al., 2002).

Genome

The poxvirus genome is not infectious and consists of a linear, double-stranded DNA molecule with covalently closed ends (Baroudy et al., 1982). The size of the poxvirus genome varies from approximately 130 kbp in parapoxviruses (Delhon et al., 2004) to

about 380 kbp in avipoxviruses (Laidlaw and Skinner, 2004). Like many other viruses, poxviruses have inverted terminal repeats (ITRs), which are identical but oppositely oriented sequences at either end of the genome and are required for poxvirus DNA replication. The ITRs are variable in length due to deletions, repetitions, and transpositions. The general composition of ITRs is: an A+T rich hairpin loop at each end of the genome that links the two DNA strands together; a sequence of approximately 100 bp important for the disassociation of concatemers during viral replication; variable-length sets of short, tandemly repeated sequences; and up to several open reading frames (ORFs). Examination of poxvirus genomic maps reveals a high degree of utilization of the genomic DNA, with few, if any, non-coding sequences. ORFs are present on both strands and are organized in clusters that are predominantly transcribed toward the closest end of the genome (Moss, 2001).

To date, 49 absolutely conserved poxvirus genes have been identified in 42 sequenced poxvirus genomes, while the vertebrate-infecting chordopoxviruses share 90 conserved genes (Upton et al., 2003). Analysis of complete poxvirus genomes have demonstrated that the poxvirus genome consists of a highly conserved central region that contains genes essential for replication, and more variable terminal regions containing genes involved in virulence and host interaction. Additionally, the localization of individual ORFs in this central region is largely preserved in chordopoxviruses (Upton et al., 2003; Moss, 2001).

The genomes of poxviruses are not static, but are subject to frequent events of gene duplication, deletion, and horizontal gene transfer (HGT) from their hosts (Hughes and Friedman, 2005). These gene loss and gene gain events have been consistent characteristics of poxvirus genome evolution. Genes that are acquired and lost during poxvirus evolution are likely to have host specific effects such as host range or evasion of host antiviral defense mechanisms (McLysaght et al., 2003). These fluctuations in the content of the genome, therefore, are likely opportunities for virus adaptation. Interestingly, the rate of gene acquisition is not constant over time, and it has increased in the orthopoxviruses. Although it is not yet clear what has changed the rate of gene acquisition and retention in orthopoxviruses it has been suggested that this is associated with the unique features of orthopoxvirus infection, replication, and virulence (Hughes and Friedman, 2005; McLysaght et al., 2003).

Replication Cycle

Poxvirus genomes are large and complicated by the standards of many other viruses and their life cycle reflects this. Poxviruses are unique among the DNA viruses in that their replication cycle occurs exclusively within the cytoplasm of the infected host cell and therefore must encode all of the enzymes and factors necessary for genome replication and transcription of viral mRNAs (Moss, 2001). The details of poxvirus replication have been obtained primarily by studying vaccinia virus infections of tissue culture cells. The time required to complete a single replication cycle varies considerably from virus to virus and ranges from 12 to 24 hours by vaccinia and up to 75 hours by Yaba virus (Buller and Palumbo, 1991).

The poxvirus replication cycle begins with the entry of the virus into the host cell (Figure 1). The mechanism by which poxviruses penetrate cells is poorly understood, in part because the complexity of the virus makes it difficult to determine which of the numerous known or predicted membrane proteins are involved (Senkevich and Moss, 2005). Vaccinia produced two forms of infectious virions: enveloped extracellular virus (EEV) and intracellular mature virus (IMV) that bind to different receptors (Vanderplasschen and Smith, 1997) and use different mechanisms for entry into the host cell (Moss, 2001; Vanderplasschen and Smith, 1997). IMV attachment is enhanced by viral proteins in the viral membrane that bind to proteoglycans on the cell surface (Senkevich and Moss, 2005). Entry of IMV occurs by fusion with the plasma membrane or vesicles that are formed by surface invaginations in a pH-independent manner (Doms et al., 1990), although non-fusion mechanisms have also been suggested (Locker et al., 2000). EEV entry into cells is dependant on low pH, suggesting that an endocytic pathway is used, although vaccinia virus may be too large for internalization through clathrin pits (Husain and Moss, 2005). Once inside the vesicle, low pH disruption of the outer membrane results in the release of the IMV particle which then fuses to the vesicle membrane (Husain and Moss, 2005; Ichihashi, 1996).

Upon entry into the cell, virus particles undergo two stages of disassembly. During the first stage, the nucleoprotein core is released from the outer coat and early mRNA is synthesized. Viral gene expression is tightly controlled and the three classes of genes, early, intermediate and late, are expressed in a temporal cascade with the transcription of each gene class being dependent upon prior expression of genes of the previous class

(Smith et al., 2004). Within 20 minutes of infection, early transcription begins, generating capped, polyadenylated mRNAs that encode proteins required for intermediate gene transcription, viral genome replication, nucleotide biosynthesis and the down-regulation of a variety of host immune functions. Approximately 50% of the poxvirus genome consists of early genes that are characterized by an A/T rich promoter region that is bound and transcribed by a virus-encoded transcription factor and RNA polymerase (Moss, 2001). Early gene expression is followed by a second round of uncoating that facilitates replication of the virus genome. DNA synthesis occurs in discrete areas of the cytoplasm called factories or virosomes, and results in thousands of genome copies per cell only half of which are packaged into mature virus particles. Although specific origin sequences have not been defined, synthesis appears to start near the ends of the genome because a 200 bp sequence in the ITR is required for optimal template replication (De Silva and Moss, 2005; Du and Traktman, 1996). The onset of replication varies considerably for individual poxviruses, anywhere from 4 to 16 hours post-infection, and is influenced by cell type and multiplicity of infection. Genome replication produces concatameric intermediates that are not resolved until the products of late genes are synthesized (Beaud, 1995).

Viral DNA replication is followed by sequential transcription of intermediate and late genes, processes that are dependent upon the presence of naked DNA template (Keck et al., 1990). Intermediate mRNAs appear approximately 100 minutes post infection and are translated into late transcription factors that regulate late stage transcription. Transcription and translation of late mRNAs produces early gene transcription factors,

virion structural proteins and several enzymes that are later incorporated with viral genomes into viral particles (Moss, 2001). The first visible structures are crescent-shaped and are composed of virus protein and host-derived lipid. These structures grow to form immature virus (IV) particles that are initially non-infectious but gain infectivity during a process that involves condensation of the virus core and proteolytic processing of several major structural proteins to produce IMV (Smith and Law, 2004).

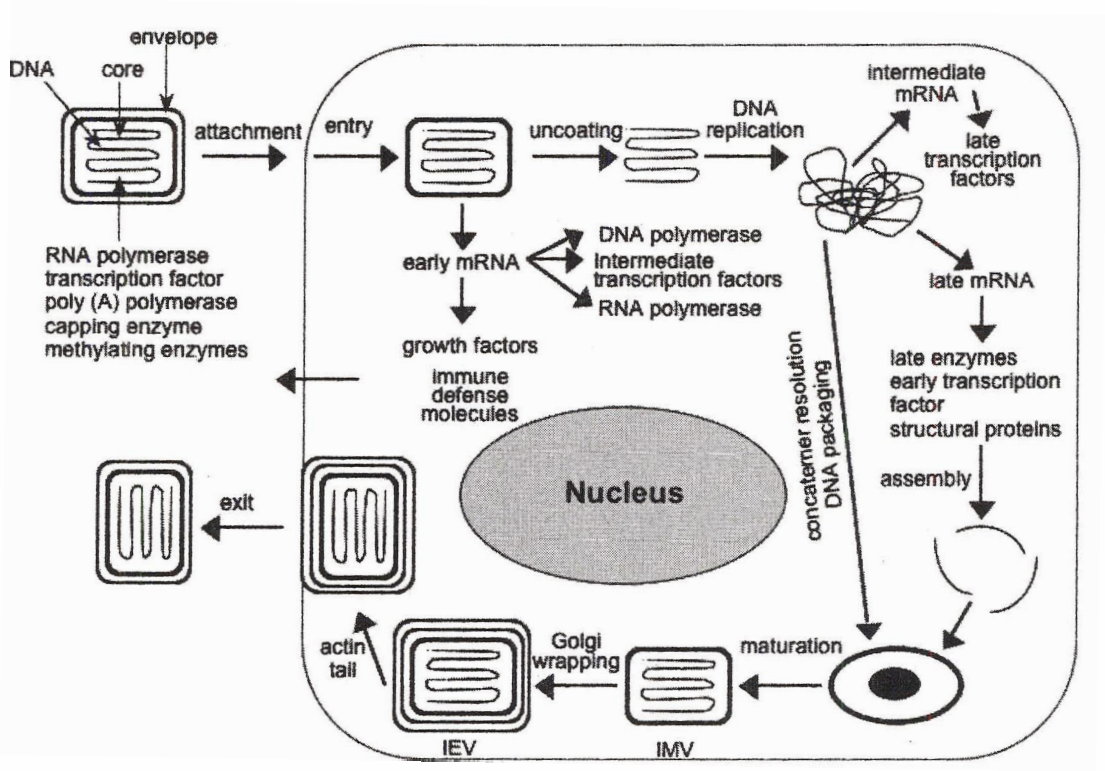

Figure 1 (adapted from Moss, 2001). Replication of vaccinia virus.

Motility

Poxviruses utilize the actin and microtubule cytoskeletons for the intracellular and intercellular movement of virions and viral components (Figure 2). It has been estimated that if poxviruses relied on diffusion through the viscous cytoplasm it would take 10 hours to move from the site of replication to the cell periphery; however by exploiting the host cell transport machinery, it takes less than one minute (Hall, 2004). After entering the cell, the viral core attaches to microtubules and moves to the perinuclear region of the host cell where the virus then replicates its DNA within viral factories. The core proteins that interact with microtubules remain to be defined, but *in vitro* studies have suggested that vaccinia (strain Copenhagen) A10L and L4R might be involved (Smith et al., 2003; Ploubidou et al., 2000). A subset of IMVs are transported away from the viral factory on microtubules to the site of wrapping near the microtubule organizing centre (MTO) where they are enveloped by an extra double membrane to become IEV (Smith et al., 2002). This process requires the A27L protein because if the A27L gene not is expressed, IMV are not transported away from factories (Sanderson et al., 2000). The host protein(s) required for attachment of the IMVs to the microtubule is currently unknown, although recent evidence suggests the involvement of both kinesin and dynein microtubule motors (Ward, 2005). IEVs are then transported from the site of wrapping to the cell periphery on microtubules by kinesin, a protein normally involved in transporting cellular cargo (protein complexes or vesicles) from the Golgi network to the plasma membrane. The interaction between the IEV and kinesin is mediated through the vaccinia envelope protein, A36R, which binds directly to the kinesin light chain through its amino terminus (Ward and Moss, 2004). Another protein present on the IEV

envelope, vaccinia F12R, has also been implicated in the movement of IEV, although a specific role for the encoded protein has not yet been identified (Smith and Law, 2004).

Once at the cell periphery, the outermost IEV membrane fuses with the plasma membrane depositing the cell-associated enveloped virus (CEV) on the cell surface. The vaccinia A36R protein, in addition to its vital role in microtubule-based motility of IEVs, is necessary for the formation of actin tails that promote intercellular spread of the virus. After CEV are deposited on the cell surface, vaccinia A36R is situated just underneath of the CEV with the majority of the protein on the cytosolic side of the plasma membrane and becomes phosphorylated on certain serine, threonine, and tyrosine residues by a host cell tyrosine kinase called Src (Gouin et al., 2005; Frischknecht et al., 1999). A viral protein, vaccinia B5R, which is associated with the membrane of the CEV, interacts with an unknown host-cell protein to promote Src activation and phosphorylation of A36R (Gouin et al., 2005). Once phosphorylated, it has been proposed that A36R triggers dissociation of the IEV from kinesin (Newsome et al., 2004). Phosphorylation of A36R also results in the recruitment of a complex of cellular proteins composed of Nck, N-WASP and WASP-interacting protein (WIP) that stimulates the actin-nucleating activity of the cellular Arp2/3 complex. Actin polymerization occurs directly beneath the CEV on the cytosolic side of the membrane resulting in thick actin structures known as actin tails. As the viral particle sits at the tip of these finger-like membrane extensions of actin filaments, it is propelled into neighbouring cells (Ward, 2005). The importance of actin tail formation in the intercellular spread of vaccinia virus is highlighted by the fact that all mutant viruses unable to form actin tails have a reduced plaque size (Smith et al.,

2003). As such, inhibition of intracellular movements provides a potential strategy to limit pathogenicity. The viral factors that interact with host cell motors and the microtubule and actin filament tracks are potential therapeutic targets (Bearer and Satpute-Krishnan, 2002).

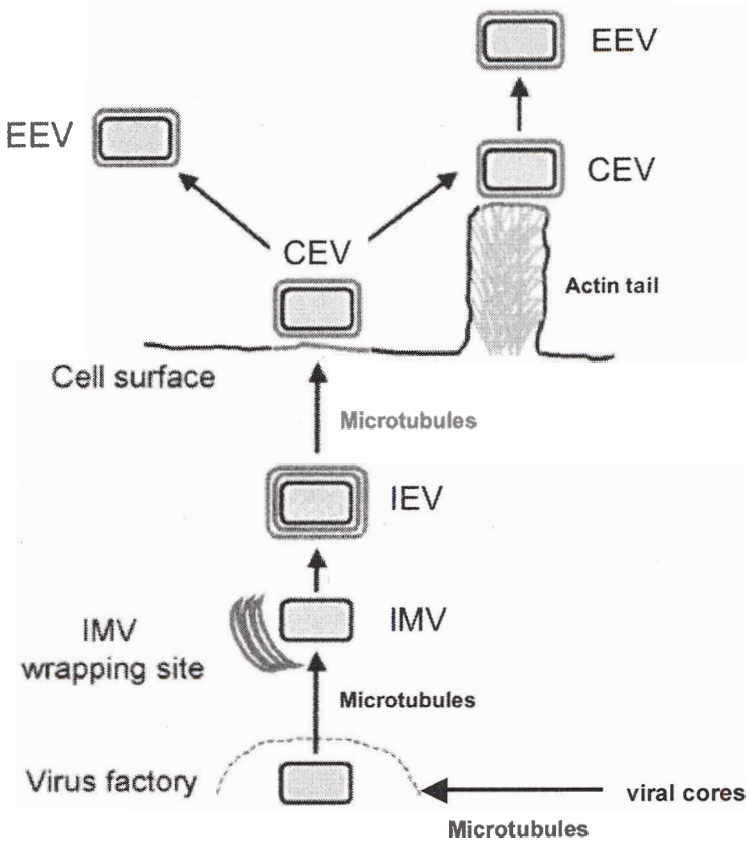

Figure 2 (adapted from Smith et al., 2002). Intracellular and extracellular virion movement. After entry, the viral cores move on microtubules to the perinuclear region. IMV are made in a virus factory and move on microtubules to the wrapping membranes derived from the trans-Golgi network or early endosomes. IMV are wrapped by a double membrane to form IEV that move to the cell surface on microtubules. At the cell surface the outermost IEV membrane fuses with the plasma membrane to form CEV that induce actin tail formation to drive the virion away from the cell. CEV may also be released to form EEV (Smith et al., 2002).

Dissemination

Poxviruses, as a family, infect a wide range of hosts and thus use a variety of different routes to facilitate their transmission. Myxoma and shope fibroma viruses are transmitted between their rabbit hosts through insect vectors such as fleas and mosquitoes (Willer et al., 1999) while swinepox is transmitted primarily through lice (Afonso et al., 2002b). Smallpox is spread by one of two mechanisms, either by inhalation of aerosols directly from an infected person or indirectly through fomites (Buller and Palumbo, 1991). Several orthopoxvirus species, not including vaccinia virus, form proteinaceous bodies in the host cell cytoplasm late in infection that may contain IMV. These 'A-type' inclusions are thought to prolong survival and more efficient dissemination of the virions outside the host after lysis of the cell (Meyer and Rziha, 1993).

IV. Poxvirus Virulence Factors

Host Immune Evasion

The successful propagation of poxviruses within the mammalian host requires the evasion or manipulation of the hosts' immune defenses (Seet et al., 2003). Mechanisms of immune evasion have been characterized for several poxviruses including the orthopoxviruses vaccinia, cowpox, ectromelia, and rabbitpox and the leporipoxvirus myxoma. The process of immune evasion in variola virus, the causative agent of smallpox, is one of the least understood among the orthopoxviruses, in part because of the difficulty in finding an appropriate animal model and because variola DNA is not available to the general scientific community. Therefore, much of what is known about

the mechanisms of immune evasion is inferred from studies of orthologous genes, particularly in vaccinia and ectromelia viruses (Dunlop et al., 2003; Buller and Palumbo, 1991). Approximately 25% of the 200 open reading frames (ORFs) present in vaccinia are 'nonessential' for virus replication in cell culture, however, some have been demonstrated and many others proposed to express important functions which modulate host responses during the virus life cycle. These host-response modifiers (HRMs), or virulence factors, are located in the terminal regions of the genome and show much variability among the poxvirus species in function and specificity (Chen et al., 2000). No single immunomodulatory ortholog is common to every poxvirus, a property that highlights differences in pathogenesis and host tropism among viruses (Seet et al., 2003; Chen et al., 2000).

Vaccinia has accumulated a wide range of immune evasion strategies. Soon after entry into the host cell, the virus arrests DNA, RNA and protein synthesis of cellular origin (Boone and Moss, 1978; de Gouttes Olgiati et al., 1976; Esteban et al., 1973), effectively preventing class I and class II major histocompatability complex (MHC) molecule production and presentation. Interference with MHC presentation leads to poor recognition of the virus infected cells by T cells. Vaccinia virus also blocks the function of many immune defense molecules by secreting truncated, soluble receptors for these molecules to prevent them from binding to their natural cell surface receptors, including: interleukin (IL)-1β, IL-18, interferon (IFN)-α, IFN-β, IFN-γ, tumor necrosis factor (TNF)-α, TNF-β and a chemokine-binding protein (Seet et al., 2003).

Additionally, poxviruses manipulate a variety of intracellular signal transduction pathways such as the apoptotic response and the complement cascade (Dunlop et al., 2003). Many of the poxvirus genes that disrupt these pathways have been "captured" directly from the host, while others have demonstrated no clear resemblance to any known host genes (Seet et al., 2003). Apoptosis is a mechanism by which the host eliminates infected cells, thereby terminating further replication and spread of the virus. Poxviruses prevent this host response by producing viral proteins that are rapidly expressed during the early stages of replication. These anti-apoptotic proteins have different modes of action. They can be secreted and neutralize signals emanating from the extracellular environment, such as the TNF decoy, or they can act to manipulate transduction of cell death pathways within the cell, such as the virus-encoded serpins and PRK inhibitors. Complement is another means by which the host organisms inactivate and clear viruses, and vaccinia encodes a secreted complement control protein (VCP) that inhibits pathways of complement activation (Seet et al., 2003). Furthermore, vaccinia incorporates host complement control proteins in the outer envelope of EEV, allowing the virus to evade the consequences of complement activation (Shen and Nemunaitis, 2004).

A-type Inclusion Bodies

In addition to the immunomodulatory proteins encoded by poxviruses, there are a number of other viral proteins that increase the fitness of the virus both inside and outside of host cells and can be considered virulence factors. In certain orthopoxvirus species including cowpox, ectromelia and raccoonpox viruses, A-type inclusion proteins form large

cytoplasmic inclusions late in infection that may contain IMV (Funahashi et al., 1988). It has been assumed, by analogy with the inclusions of insect viruses, that such bodies allows the prolonged survival of the virus outside the host and results in more efficient dissemination of the virions (Meyer and Rziha, 1993; Funahashi et al., 1988). A-type inclusion bodies can be classified into two groups according to whether they contain virus particles (V^+) or whether they contain few if any virus particles (V^-) and is a strain specific phenotype (Patel et al., 1986). The P4c protein, present on the surface of IMV appears to have a role in directing the insertion of the virus particles into the A-type inclusion bodies (McKelvey et al., 2002). Interestingly, orthopoxvirus species that do not produce large A-type inclusion bodies, such as vaccinia, variola, monkeypox and camelpox viruses, maintain a truncated version of the full-length A-type inclusion protein found in cowpox virus, suggesting an alternative role for the truncated A-type inclusion protein during the virus life cycle.

Profilin Homolog

The coevolution of viruses and their hosts has had a significant impact on how each has evolved, and the consequences of this interaction are evident in both host and viral genomes. The presence of cellular gene homologs in the genome of poxviruses suggests these viruses occasionally acquire genes from their host and retain those that confer a selective advantage to the virus (Hughes and Friedman, 2005; McLysaght et al., 2003; Bugert and Darai, 2000). During infection, poxviruses utilize the cellular cytoskeleton to move virus components and virions to different locations throughout the cytoplasm, and to enhance intercellular virus spread. An intensive area of poxvirus research has been

delineating the mechanisms by which these viruses are able to control the actin and microtubule cytoskeletons to facilitate their own life cycle (Newsome et al., 2004). Orthopoxviruses encode a homolog of cellular profilin, a protein intimately involved in the regulation of the actin cytoskeleton. Although the profilin homolog is 'nonessential' for virus replication in tissue culture, the gene may increase the fitness of the virus during natural infection (Blasco et al. 1991).

Profilins are small actin-regulating proteins that are essential in all organisms examined to date. Once thought to bind only to actin, it is now recognized that they function as hubs that control a complex network of molecular interactions, the importance of which is just beginning to be understood (Witke, 2004). Profilins mediate these cellular processes through interactions with ligands at three conserved domains that bind actin, poly (L-proline) or phosphoinositides (Figure 3) (Witke, 2004).

In addition to their role in regulating actin polymerization (Carlsson et al., 1997) and modulating the activity of actin regulatory proteins (Yamamoto et al., 2001), profilins have been implicated in a wide variety of other cellular processes. In mammalian cells, profilins are involved in membrane trafficking, as indicated by the presence of profilin 1 at budding Golgi vesicles and the profilin-1-dependent recruitment of dynamin 2 to the Golgi that is required for vesicle budding (Dong et al., 2000). Further, a role for profilins in endocytosis is suggested by experiments showing that profilin 1 forms complexes with clathrin, a protein that assembles at membrane sites of endocytosis to form coated pits, and valosine-containing protein (VCP), a protein involved in vesicle

transport (Witke et al., 1998). The interaction of profilin with scaffolding proteins in neurons suggests that profilins may be involved in formation of receptor scaffolds in both the presynaptic and the postsynaptic compartments (Miyagi et al., 2002; Wang et al., 1999). Interestingly, profilin 1 has been shown to distribute to the nucleus and associate with subnuclear structures (ribonuclear particles and Cajal bodies) and has been implicated in pre-mRNA processing; although the significance of these findings is not yet known (Skare et al., 2003). In recent years, the number of known profilin-binding proteins from different organisms has increased to more than fifty characterized ligands, although this is probably only a fraction of the number of actual profilin-binding partners. The binding of profilin to such a variety of ligands might provide a means of linking different pathways to cytoskeletal dynamics. Alternatively, the profilin –ligand interaction might work in an actin-independent manner to regulate the ligands directly (Witke, 2004). Whichever is the case, given the activities of profilins and their involvement in such a variety of cellular processes and the requirement for utilization of the host cytoskeleton during the virus life cycle, one can envision how the acquisition of a profilin protein could contribute to the evolutionary success of orthopoxviruses.

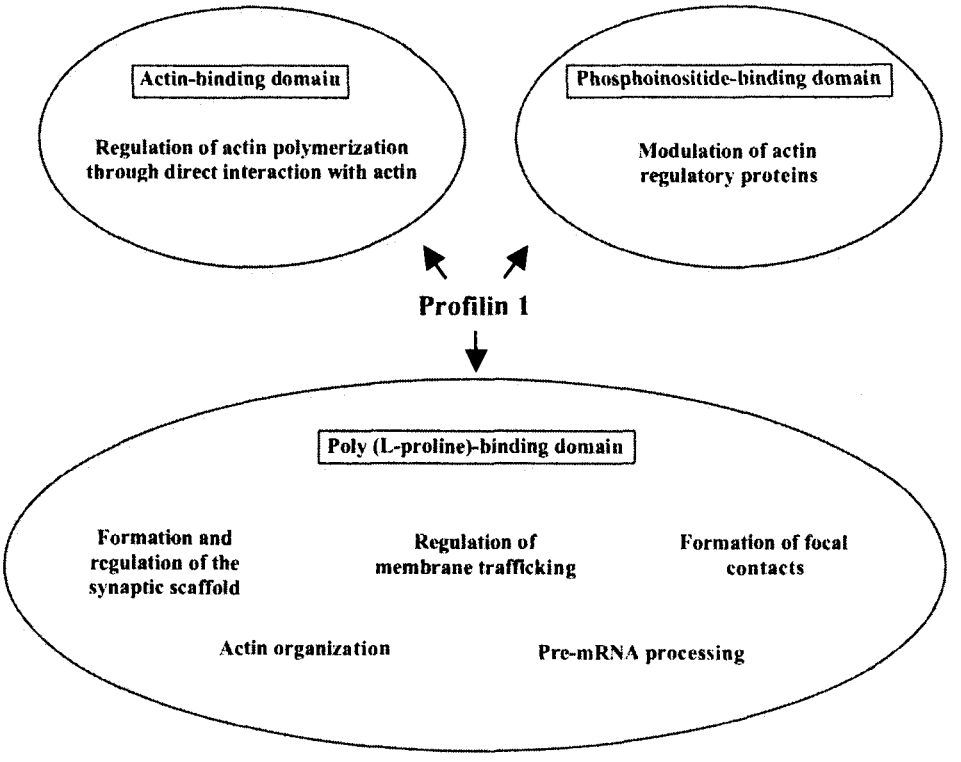

Figure 3 (adapted from Witke, 2004). Cellular profilin performs a diversity of functions. Profilin 1 contains actin, phosphoinositide and poly (L-proline)-binding domains. Interaction with ligands at these domains influences a variety of cellular processes (Witke, 2004).

V. Significance of Poxvirus Research

The study of poxviruses has been and continues to be a highly worthwhile endeavor. Biotechnological and medical applications resulting from the study of poxvirus virulence factors are apparent. Recombinant poxvirus expression vectors have been used successfully as tools to study protein processing and intracellular trafficking, antigen

presentation, cell fusion, protein-protein interactions, structure/function relationships and determinants of humoral and cellular immunity (Carroll, 1997; Miner and Hruby, 1990). There has also been considerable interest in the development of recombinant poxvirus vaccines to prevent infectious diseases and in cancer therapy. Several aspects of poxvirus vectors make this a promising prospect from a safety perspective; they are non-oncogenic and can be engineered to reduce disseminated infections after immunization, and block spread to non-vaccinated contacts. Concerns regarding the safety of poxviruses for human and veterinary applications have been largely addressed by creating attenuated vaccina virus strains, such as vaccinia Ankara (MVA) and NYVAC (Sutter and Moss, 1992; Tartaglia et al., 1992). Both these viruses have proven to be immunogenic and effective, despite a highly attenuated phenotype in immunocompetent and immunocompromised animal models (Perkus, 1995). Recently, vaccinia virus has become the platform of many exploratory approaches to treat cancer, and has been used as a delivery vehicle for anti-cancer transgenes, as vaccine carrier for tumor-associated antigens and immunoregulatory molecules in cancer therapy, and as an oncolytic agent that selectively replicates in and lyses cancer cells (Shen and Nemunaitis, 2004).

Additionally, there is still an abundance of proteins encoded in the poxvirus genome for which there is no known function. The analysis of these poxviral proteins may provide insight into aspects of the poxvirus life cycle that are still not well understood, and may not only result in a deeper understanding of the poxvirus life cycle and virus-host interactions, but may also aid in identification of drug, antibody, vaccine and detection targets (Upton et al., 2003).

VI. Thesis Rationale

The object of this project was to identify and begin preliminary characterization of genes conserved within the orthopoxviruses. Although the genomes of 42 poxviruses have been completely sequenced, there are many genes for which no function has yet been determined, or merely a prediction of function made based on sequence similarity. In order to gain a clearer picture of poxvirus biology and virus-host interactions, it is critical that the function of these genes be determined. The initial high-throughput cloning and expression of 56 conserved orthopoxvirus genes was undertaken in this project. The focus of this thesis, however, is the characterization of the ECTV-Mos 141 gene from ectromelia virus, a virulent orthopoxvirus. This gene encodes a protein that is homologous to cellular profilin 1, a protein involved in the regulation of the cellular cytoskeleton. Vaccinia virus utilizes both the actin and microtubule cytoskeletons to facilitate its own life cycle. It is therefore predicted that the viral profilin homolog has a function in viral manipulation of the host cytoskeleton during infection.

Thus, the research objectives are as follows:

1) Identify conserved orthopoxvirus genes with little or no previous characterization
2) Determine location of gene target ORFs in the genome of ECTV-Mos to predict the 'essential' or 'non-essential' function of the encoded proteins in the virus life cycle
3) Amplify gene targets from ectromelia virus DNA, clone gene targets into Gateway Technology and express the recombinant proteins
4) Purify the profilin homolog for structural analysis by NMR
5) Build a homology model of the ECTV-Mos 141 protein to begin structural analysis

6) Determine what protein(s) the profilin homolog associates with *in vivo* and where this co-localization occurs in the cell

VII. Contributors to work presented in this thesis

I would like to specially thank the following people for their contribution to the work presented in my thesis.

a) Dr. R. Mark Buller (Department of Molecular Microbiology and Immunology, Saint Louis University of Health Sciences Center, St. Louis, USA) for preparing the ECTV-Mos genomic DNA fragments.

b) Arwen Hunter (present address: Department of Pathology and Laboratory Medicine, University of British Columbia, Vancouver, Canada) assisting in choosing gene targets.

c) Roderick Haesevoets (Department of Biology, University of Victoria, Victoria, Canada) performed the automated sequencing of plasmid constructs.

d) Guiyun Lee (Department of Biochemistry and Microbiology, University of Victoria, Victoria, Canada) for assisting with the cloning of ECTV-Mos 118 and ECTV-Mos 123.

e) Dr. David Esteban (Department of Biochemistry and Microbiology, University of Victoria, Victoria, Canada) for assisting with the immunofluorescence microscopy experiments.

f) Shan Sundararaj (current address: Department of Computing Science and Biological Sciences, University of Alberta, Edmonton, Alberta, Canada) for constructing the homology model of ECTV-Mos 141.

Chapter 2: Materials and Methods

Oligonucleotide primers were obtained from Invitrogen Life Technologies (Carlsbad, CA, USA). Unless otherwise indicated, chemicals were obtained from Sigma-Aldrich Canada Ltd. (Oakville, ON, Canada).

Database search for conserved gene families in orthopoxviruses[1]

The Viral Orthologs Clusters (VOCs) database version 2.0 (Ehlers et al., 2002), which is available from the Poxvirus Bioinformatics Resource Center (http://www.poxvirus.org), was used to search for gene families conserved between 40 complete chordopoxvirus genomes (including 18 complete orthopoxvirus genomes) and 2 entomopoxvirus genomes (Table 1). This database groups all poxvirus protein orthologs into separate families that are then assessed by a human database curator.

---

[1] This work was performed in part by Arwen Hunter (current address: Department of Pathology and Laboratory Medicine, University of British Columbia, Vancouver, Canada)

Table 1: Complete poxvirus genomes in the Viral Orthologs Clusters Database (VOCs).

Genome	Abbreviation	GenBank no.	Reference
Chordopoxviruses			
Bovine papular stomatitis virus (AR02)	BPSV-AR02	NC_005337	(Delhon et al., 2004)
Camelpox virus (CMS)	CMLV-CMS	AY009089	(Gubser and Smith 2002)
Camelpox virus (Kazakhstan M-96)	CMLV-M96	AF438165	(Afonso et al., 2002a)
Canarypox virus (ATCC VR-111)	CNPV	NC_005309	(Tulman et al., 2004)
Cowpox virus (Brighton Red)	CPXV-BR	AF482758	Unpublished
Cowpox virus (GRI-90)	CPXV-GRI	X94355	Unpublished
Deerpox virus (W-848-83)	DPV-W83	NC_006966	(Alfonso et al., 2005)
Deerpox virus (W-1170-84)	DPV-W84	NC_006966	(Alfonso et al., 2005)
Ectromelia virus (Moscow)	ECTV-Mos	AF012825	Unpublished
Ectromelia virus (Naval)	ECTV-Nav	NC_004105	Unpublished
Fowlpox virus (Virulent-Iowa)	FWPV-Vir_Iowa	AF198100	(Afonso et al., 2000)
Fowlpox virus (HP1-438 Munich)	FWPV-Munich	AJ581527	(Laidlaw and Skinner, 2004)
Goatpox virus (G20-LKV)	GTPV-G20LKV	AY077836	(Tulman et al., 2002)
Goatpox virus (Pellor)	GTPV-Pellor	AY077835	(Tulman et al., 2002)
Lumpy skin disease virus (Neethling vaccine LW 1959)	LSDV-1959	AF409138	(Kara et al., 2003)
Lumpy skin disease virus (Neethling 2490)	LSDV-Neeth	NC_003027	(Tulman et al., 2001)
Lumpy skin disease virus (Neethling Warmbaths LW)	LSDV-Warm	AF409137	(Kara et al., 2003)
Molluscum contagiosum virus subtype 1	MOCV-1	U60315	(Senkevich et al., 1997)
Monkeypox Virus (Walter Reed 267)	MPXV-WRAIR	AY603973	Unpublished
Monkeypox virus strain (Zaire)	MPXV-Zre	AF380138	(Shchelkunov et al, 2001)
Myxoma virus (Lausanne)	MYXV-Laus	NC_001132.2	(Cameron et al., 1999)
Orf virus (OV-IA82)	ORFV-IA82	AY386263	(Delhon et al., 2004)

Genome	Abbreviation	GenBank no.	Reference
Orf virus (NZ2)	ORFV-NZ2	AX754989	Unpublished
Orf virus strain OV-SA00	ORFV-SA00	AY386264	(Delhon et al., 2004)
Rabbitpox virus (Utrecht)	RPXV-Utr	To be submitted	Unpublished
Shope Rabbit fibroma virus (Kasza)	SFV-Kas	AF170722	(Willer et al., 1999)
Sheeppox virus (A)	SPPV-A	AY077833	(Tulman et al., 2002)
Sheeppox virus (NISKHI)	SPPV-NISKHI	AY077834	(Tulman et al., 2002)
Sheeppox virus (Turkey-TU-V02127)	SPPV-TU	NC_004002	(Tulman et al., 2002)
Swinepox virus (Nebraska 17077-99)	SWPV-Neb	AF410153	(Afonso et al., 2002b)
Vaccinia virus (Acambis 3000 Modified Virus Ankara)	VACV-Acambis	AY603355	Unpublished
Vaccinia virus (Copenhagen)	VACV-Cop	M35027	(Goebel et al., 1990)
Vaccinia virus (Modified Vaccinia Ankara)	VACV-MVA	U94848	(Antoine et al., 1998)
Vaccinia virus (Tian Tan)	VACV-Tan	AF095689	Unpublished
Vaccinia virus (Western Reserve)	VACV-WR	AF411104	(Szajner et al., 2001)
Variola major virus (Bangladesh-1975)	VARV-Bsh	L22579	(Massung et al., 1994)
Variola minor virus (Garcia-1966)	VARV-Gar	Y16780	Unpublished
Variola major virus (India 3 major-1967)	VARV-Ind	X69198	(Shchelkunov et al., 1996a,b)
Yaba-like Disease Virus (Smith)	YLDV	NC_002642	(Lee et al, 2001)
Yaba monkey tumor virus	YMTV	NC_005179	(Brunetti et al., 2003)
Entomopoxviruses			
Melanoplus sanguinipes	MsEPV	NC_001993	(Afonso et el., 1999)
Amsacta moorei	AmEPV	NC_002520	(Bawden et al., 2000)

Ectromelia virus DNA purification and amplification[2]

A plaque-purified isolate of the ECTV-Mos (ATCC VR-1374) was propagated in an African green monkey kidney cell line, BS-C-1 (ATCC CCL 26) (Chen et al., 1992). The viral DNA was extracted from virions by an SDS and proteinase K treatment followed by phenol-chloroform purification (Moss and Earl, 1998). The ECTV-Mos genome, except the hairpin loops, the 32 kbp of the right-hand end (Chen et al., 2000) and the 1.5 kbp right hand terminal repeat, was split into 16 overlapping fragments of approximately 11 kb. Each fragment was amplified from purified genomic DNA using Expand Long Template PCR System (Roche Diagnostics Corp., Indianapolis, IN, USA) following the manufacturer's instructions. In order to ensure sequence accuracy, each base position was sequenced at least once on both forward and reverse strands. Sequencing reactions were carried out using CEQ 2000 Dye Terminator Cycle Sequencing with Quick Start Kit (Beckman Coulter Inc., Fullerton, CA, USA), and run on CEQ 2000XL DNA Analysis System (Beckman Coulter Inc.).

---

[2] This work was performed by Dr. R. Mark. L. Buller (Department of Molecular Microbiology and Immunology, Saint Louis University Health Sciences Center St. Louis, Missouri, USA).

Vaccinia virus DNA isolation

VACV genomic DNA was used as template in PCR reactions to amplify the gene encoding the VACV-WR 148 A-type inclusion protein and was prepared by a method adapted from Roper, 2004. Approximately 2.48 x 10^7 pfu (~100 µl), of the recombinant VACV-WR strain vTF7-3 (passage 3, ATCC VR-2153) were aliquoted into a 1.5 ml Micro Tube (Cat # 72690, SARSTEDT AG & Co., Nümbrecht, Germany). Viral aggregates and cellular debris were broken up or removed by sonication for 60 pulses at output level 8 followed by centrifugation for 10 seconds at 14,000 x g in a microfuge (Eppendorf centrifuge 5415C; Brinkmann Instruments). Supernatant was removed and dispensed into a new 1.5 ml Micro Tube to which 100 µl 2 x PCR detergent (100 mM KCl, 20 mM Tris pH 8.3, 3 mM $MgCl_2$, 0.01% gelatin, 0.9% TWEEN-20 and 0.9% IGEPAL) and 12 µl proteinase K (2 µg/ml in: 10 mM Tris-HCl pH 7.5, 20 mM $CaCl_2$, 50% glycerol) were added. The tube was incubated at 37°C for 1 hour, followed by heat inactivation of the proteinase K by incubation at 95°C for 5 minutes. 1µl of the resulting crude viral genomic DNA preparation was used directly in PCR reactions.

Polymerase chain reaction (PCR)

ORFs corresponding to orthologs of the 56 conserved orthopoxvirus genes in addition to the gene encoding the ECTV-Mos 128 A-type inclusion protein were amplified from ECTV-Mos genomic DNA fragments provided by Dr. Mark Buller. The gene encoding the VACV-WR 148 A-type inclusion protein was amplified from a crude VACV-WR genomic DNA preparation. Oligonucleotide primers were designed from genomic DNA

sequences using NetPrimer (PREMIER Biosoft International, Palo Alto, CA, USA) (Table 2). The nucleotide sequence CACC was incorporated onto the 5' end of the N-primers to facilitate cloning of the genes into TOPO Cloning Technology by topoisomerase. An epitope tag was also incorporated into the N-primer or C-primer to aid in purification or localization studies of the encoded protein (Figure 4). A 6 x histidine tag, CACCATCACCACCATCAT, was integrated into the N-primer of each of the 56 conserved genes to facilitate purification of the protein by metal chelation chromatography. In addition, the conserved ECTV-Mos 141 gene, encoding a profilin homolog, was also amplified using a N-primer, which had an incorporated myc tag, GAGCAGAAACTCATCTCTGAAGAGGATCTG, for use in immunofluorescence studies. The two genes encoding A-type inclusion proteins, ECTV-Mos 128 and VACV-WR 148, had an influenza haemagglutin (HA) tag, TACCCATACGATGTTCCAGATTACGCT, incorporated into the C-primer for immunofluorescence studies.

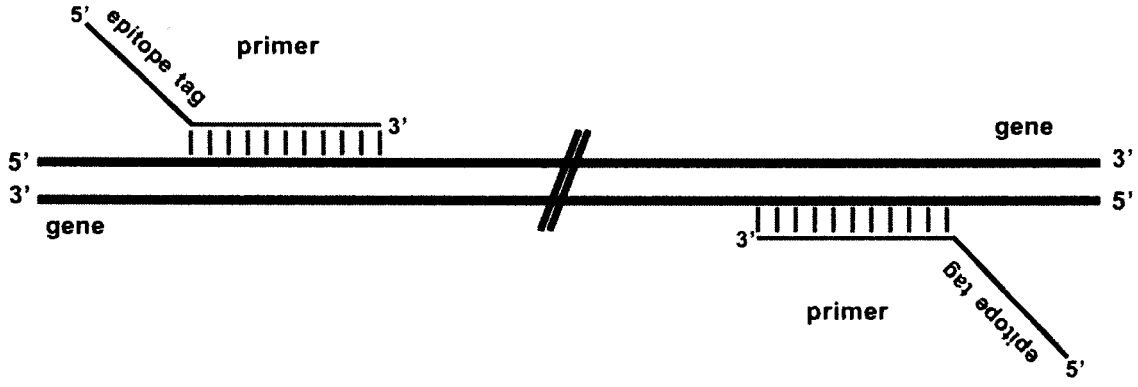

Figure 4. Design of oligonucleotide primers. Epitope tags were incorporated onto the 5' end of genes via PCR. Nucleotide sequences encoding epitope tags (6 x histidine, myc, haemagglutinin) were added to the 5' end of primers, resulting in an overhang when the 3' end of the primer annealed to the complementary sequence at the 5' end of the gene.

PCR reactions (50 µl total volume) were performed in 200 µl thin-walled PCR tubes (Cat # TW6200, Gordon Technologies, Mississauga, ON, Canada) in Minicycler PTC-150-25 (MJ Research, Watertown, MA, USA). Reaction mixes consisted of 1xPCR buffer (50 mM KCl, 10 mM Tris pH 8.3, 1.5 mM $MgCl_2$, 0.01% gelatin), 0.1 mM dNTP mix (Invitrogen Life Technologies, Carlsbad, CA, USA), 0.1 µM each of the forward and reverse primer, 1 ng template DNA and 1 unit *Pfu* polymerase (Cat # 600135, Stratagene, San Diego, CA, USA). Reactions were overlaid with two drops of mineral oil to prevent evaporation of the reaction mixture. The following thermocycler conditions were used to amplify the 56 conserved genes: initial denaturation at 94°C for 30 seconds; 26 cycles at 94°C for 30 seconds, 50°C for 30 seconds, 72°C for 2 minutes; a final extension at 72°C was performed for 10 minutes and then samples were held at 4°C.

The genes encoding the A-type inclusion proteins, ECTV-Mos 128 and VACV-WR 148, were amplified using similar PCR conditions as for the 56 conserved genes except the extension time was 5 minutes.

Table 2. Oligonucleotide primers used for PCR-amplification of gene targets.

Primer Name	Epitope Tag	Sequence 5' → 3'
ECTV-Mos 012		
ECTV-Mos 012 - N	6 x histidine	CACCATGGCACACCATCACCACCATCATATGGAATTCGATCCTGCC
ECTV-Mos 012 - C		TTAGTTAACTAGCTTATAGAACTTGCTCATTGTTATG
ECTV-Mos 018		
ECTV-Mos 018 - N	6 x histidine	CACCATGGCACACCATCACCACCATCATATGACTAATGCTATGCGCAAT
ECTV-Mos 018 - C		CTATTGTAGGAATTTTTTTTCACAGTTGCT
ECTV-Mos 023		
ECTV-Mos 023 - N	6 x histidine	CACCATGGCACACCATCACCACCATCATATGATTGCGTTATTGATATTAT
ECTV-Mos 023 - C		TTAAGGAGATTCCACCTTACCCATAAAC
ECTV-Mos 024		
ECTV-Mos 024 - N	6 x histidine	CACCATGGCACACCATCACCACCATCATATGAGTGCAAACTGTATGTTCAA
ECTV-Mos 024 - C		TTATAACTTTACTCTATTAAAAATCCAAGTTTCTATTTCT
ECTV-Mos 026		
ECTV-Mos 026 - N	6 x histidine	CACCATGGCACACCATCACCACCATCATATGTTCAACATGAATATTAACTCACC
ECTV-Mos 026 - C		TTATCTAAGTCCAGTTGATCCAAATCCTT

Primer Name	Epitope Tag	Sequence 5' → 3'
ECTV-Mos 027		
ECTV-Mos 027 - N	6 x histidine	CACCATGGCACACCATCACCACCATCATATGAACATGGATCAAATTATAGATAT
ECTV-Mos 027 - C		TTACCATCTTATCCCATTCCATATATTCC
ECTV-Mos 028		
ECTV-Mos 028 - N	6 x histidine	CACCATGGCACACCATCACCACCATCATATGGAACCGATCCTTGCA
ECTV-Mos 028 - C		TTAAAAGTCAACATCTAAAGAAAAATGATTGTC
ECTV-Mos 029		
ECTV-Mos 029 - N	6 x histidine	CACCATGGCACACCATCACCACCATCATATGAGTAAAATACTCACATTTGTTAAA
ECTV-Mos 029 - C		TCAATTTATTGTAAAAAAAGAATCGGTTTTATAC
ECTV-Mos 031		
ECTV-Mos 031 - N	6 x histidine	CACCATGGCACACCATCACCACCATCATATGGAGGGATCTAAACGCA
ECTV-Mos 031 - C		CTATTTTGGTGGAGGATTATATGATATAATTCG
ECTV-Mos 032		
ECTV-Mos 032 - N	6 x histidine	CACCATGGCACACCATCACCACCATCATATGGCGGAAACTAAAGAGTTT
ECTV-Mos 032 - C		TTAAACGTATAAAAACGTTCCGTATCTGTATTT
ECTV-Mos 033		
ECTV-Mos 033 - N	6 x histidine	CACCATGGCACACCATCACCACCATCATATGGGTGTTGCCAATGATT
ECTV-Mos 033 - C		TTAGTTTCCGCCATTTATCCAGTCTG

Primer Name	Epitope Tag	Sequence 5' → 3'
ECTV-Mos 037		
ECTV-Mos 037 - N	6 x histidine	CACCATGGCACACCATCACCACCATCATATGAAACACAGAGTGTATTCTGAAG
ECTV-Mos 037 - C		TTATACATCCTGTTCTACCAACG
ECTV-Mos 038		
ECTV-Mos 038 - N	6 x histidine	CACCATGGCACACCATCACCACCATCATATGAGGAGTATTGCGGGG
ECTV-Mos 038 - C		TTATTCTATTTCGAATTTAGGCTTCCAAA
ECTV-Mos 039		
ECTV-Mos 039 - N	6 x histidine	CACCATGGCACACCATCACCACCATCATATGAAAGTGGTGATTGTGACTAGT
ECTV-Mos 039 - C		TCATTTTTTGTCTAGAATATCCATTTTGTTC
ECTV-Mos 043		
ECTV-Mos 043 - N	6 x histidine	CACCATGGCACACCATCACCACCATCATATGTCTAAGATCTATATTGACGAGTG
ECTV-Mos 043 - C		TCAGAATCTAATGATGACGTAACCAAGAAG
ECTV-Mos 044		
ECTV-Mos 044 - N	6 x histidine	CACCATGGCACACCATCACCACCATCATATGGAAAATGTATACATTAGTAG
ECTV-Mos 044 - C		TTATTCATCATCCTCTGGCGGTTCGTCGTT
ECTV-Mos 053		
ECTV-Mos 053 - N	6 x histidine	CACCATGGCACACCATCACCACCATCATATGGCCGAGGAATTTGTAC
ECTV-Mos 053 - C		TCAACAAGTTCTCAATACACCAATAGATGATAG

Primer Name	Epitope Tag	Sequence 5' → 3'
ECTV-Mos 058		
ECTV-Mos 058 - N	6 x histidine	CACCATGGCACACCATCACCACCATCATATGGCGGATGCTATAACC
ECTV-Mos 058 - C		TTAACTTTTCATTAATAGGGACTTGACGTAC
ECTV-Mos 059		
ECTV-Mos 059 - N	6 x histidine	CACCATGGCACACCATCACCACCATCATATGAATAACTTTGTTAAACAAGTAGC
ECTV-Mos 059 - C		TCAAAGAATATGTGACAAAGTCCTAGTTGTATAC
ECTV-Mos 064		
ECTV-Mos 064 - N	6 x histidine	CACCATGGCACACCATCACCACCATCATATGCCATTTAGAGATCTAATTTT
ECTV-Mos 064 - C		CTATGGAGTTTGGCCACCTGTTACCGAATA
ECTV-Mos 067		
ECTV-Mos 067 - N	6 x histidine	CACCATGGCACACCATCACCACCATCATATGGTGTTCCAATTAGTGTGTTC
ECTV-Mos 067 - C		TTAGTTTATATCCAATAGAGGTTGCACTGT
ECTV-Mos 068		
ECTV-Mos 068 - N	6 x histidine	CACCATGGCACACCATCACCACCATCATATGGATCCGGTTGATTTTAT
ECTV-Mos 068 - C		TCACCCTTTAAGGTAATCAATTTGCC
ECTV-Mos 070		
ECTV-Mos 070 - N	6 x histidine	CACCATGGCACACCATCACCACCATCATATGAGCATCCGTATAAAAATCG
ECTV-Mos 070 - C		TTAGTCTAAAAACGCCATAAAGATGTTAATCTT

Primer Name	Epitope Tag	Sequence 5' → 3'
ECTV-Mos 073		
ECTV-Mos 073 - N	6 x histidine	CACCATGGCACACCATCACCACCATCATATGGAAGTTATCGCTGATCG
ECTV-Mos 073 - C		TTATAGTATAAAGTAATAAAAAATAGTTAATGTGATGACTTG
ECTV-Mos 075		
ECTV-Mos 075 - N	6 x histidine	CACCATGGCACACCATCACCACCATCATATGAGTCTACTGCTAGAAAACCTC
ECTV-Mos 075 - C		TCAATCCTTTGTTGGAATATCTGTTAGAGG
ECTV-Mos 080		
ECTV-Mos 080 - N	6 x histidine	CACCATGGCACACCATCACCACCATCATATGAACCAATACAACGTAAAATATC
ECTV-Mos 080 - C		TTAATCAGCGACTGAAATAACAGATCTATCG
ECTV-Mos 083		
ECTV-Mos 083 - N	6 x histidine	CACCATGGCACACCATCACCACCATCATATGGATAAGAAAAGTTTGTATAAATACT
ECTV-Mos 083 - C		TTAATTCTTATCAATCACATATTTTTCTATGATGTCT
ECTV-Mos 084		
ECTV-Mos 084 - N	6 x histidine	CACCATGGCACACCATCACCACCATCATATGGATAAAACTACTTTATCAGTAAAC
ECTV-Mos 084 - C		CTATTCCATATTACTAAGATCGGAACACCA
ECTV-Mos 087		
ECTV-Mos 087 - N	6 x histidine	CACCATGGCACACCATCACCACCATCATATGGCGTGGTCAATTACG
ECTV-Mos 087 - C		TTACTTCTTACAAGTTTTAACTTTTTTACGAACAA

Primer Name	Epitope Tag	Sequence 5' → 3'
ECTV-Mos 089		
ECTV-Mos 089 - N	6 x histidine	CACCATGGCACACCATCACCACCATCATATGGAAATGGATAAGCGTATG
ECTV-Mos 089 - C		TTAACAAGTGTCTTTTATATATTCGTAATCTATGCC
ECTV-Mos 091		
ECTV-Mos 091 - N	6 x histidine	CACCATGGCACACCATCACCACCATCATATGTCCATCAATATCGATATAAAAA
ECTV-Mos 091 - C		TTACTTAGTTACTATGTTGTTTATGTCTTTTCTTTCC
ECTV-Mos 096		
ECTV-Mos 096 - N	6 x histidine	CACCATGGCACACCATCACCACCATCATATGTCGAGCTTTGTTACCAAT
ECTV-Mos 096 - C		TTATGAGTCGACGATATTCGCGAGA
ECTV-Mos 098		
ECTV-Mos 098 - N	6 x histidine	CACCATGGCACACCATCACCACCATCATATGGGAATTACAATGGATGAG
ECTV-Mos 098 - C		TCATTTACTATTAACTAGCATATTATA
ECTV-Mos 099		
ECTV-Mos 099 - N	6 x histidine	CACCATGGCACACAATCACCACCATCATATGACCTTTTACAGATCTAGTATAATTAG
ECTV-Mos 099 - C		CTAATCAATAAATCCATCCGTTAATTTTTTA
ECTV-Mos 103		
ECTV-Mos 103 - N	6 x histidine	CACCATGGCACACCATCACCACCATCATATGGCTAAGCGAGTAAGCC
ECTV-Mos 103 - C		TTACAATAAACTCCGTAGAGAAATATCTATAATTTGT

Primer Name	Epitope Tag	Sequence 5' → 3'
ECTV-Mos 104		
ECTV-Mos 104 - N	6 x histidine	CACCATGGCACACCATCACCACCATCATATGAATCTACGATTATGTAGCGG
ECTV-Mos 104 - C		TTATACGTCTAATGAGCAAGTAGAAAACCTCT
ECTV-Mos 108		
ECTV-Mos 108 - N	6 x histidine	CACCATGGCACACCATCACCACCATCATATGGCAGACACAGACGATATTA
ECTV-Mos 108 - C		TTAGAATTTATACGAATATCGTTCTCTAAATGTAACA
ECTV-Mos 109		
ECTV-Mos 109 - N	6 x histidine	CACCATGGCACACCATCACCACCATCATATGGACAAACTTAGAGTTCTATACG
ECTV-Mos 109 - C		TTAGAATTTATACGAATATCGTTCTCTAAATGTAACA
ECTV-Mos 111		
ECTV-Mos 111 - N	6 x histidine	CACCATGGCACACCATCACCACCATCATATGTTCGAACCAGTACCAGATC
ECTV-Mos 111 - C		CTAAGTGAAGTATTTTAGTAACGTATCCTTATCGC
ECTV-Mos 114		
ECTV-Mos 114 - N	6 x histidine	CACCATGGCACACCATCACCACCATCATATGACGACCGTACCAGTGAC
ECTV-Mos 114 - C		TTAAATAATTTTAATTCGTTTAACGAATATCTTGAG
ECTV-Mos 118		
ECTV-Mos 118 - N	6 x histidine	CACCATGGCACACCATCACCACCATCATATGTTCGTAGACGATAATTCGTT
ECTV-Mos 118 - C		TTACTTATCATTTACTAGACGAAAAGGTGGTG

Primer Name	Epitope Tag	Sequence 5' → 3'
ECTV-Mos 122		
ECTV-Mos 122 - N	6 x histidine	CACCATGGCACACCATCACCACCATCATATGGATAGTACCAACGCGC
ECTV-Mos 122 - C		TTAACTCGCAAAATCGTTAAGAAGTTTAAGC
ECTV-Mos 123		
ECTV-Mos 123 - N	6 x histidine	CACCATGGCACACCATCACCACCATCATATGATAACTTTATTTTTAATCCTATGTT
ECTV-Mos 123 - C		TTAGGTAGTAAAAAATAAGTCAGAATATGCCCTAT
ECTV-Mos 126		
ECTV-Mos 126 - N	6 x histidine	CACCATGGCACACCATCACCACCATCATATGGATAATCTATTTACCTTTCTACA
ECTV-Mos 126 - C		TCATTTTAGAAGCAATTCTTTTAGACGATC
ECTV-Mos 128		
ECTV-Mos 128 - N		CACCATGGAGGTCACGAACCTTATTGAAAA
ECTV-Mos 128- C	hemagluttinin	CTAAGCGTAATCTGGAACATCGTATGGGTAAGTAGATATTGGTAGAAGATATGC
ECTV-Mos 131		
ECTV-Mos 131 - N	6 x histidine	CACCATGGCACACCATCACCACCATCATATGCAGTATCCGCGGG
ECTV-Mos 131 - C		TTATAATATATTAGAAGCTGACAAAATTTTTTTACAC
ECTV-Mos 134		
ECTV-Mos 134 - N	6 x histidine	CACCATGGCACACCATCACCACCATCATATGAATTGTTTTCAAGAAAAACAG
ECTV-Mos 134 - C		TTATGATACATTTTTTGACGACGATGATT

Primer Name	Epitope Tag	Sequence 5' → 3'
ECTV-Mos 141		
ECTV-Mos 141 - N	6 x histidine	CACCATGGCACACCATCACCACCATCATATGGCGGCCGAATGG
ECTV-Mos 141 - C		TTAATTACCAGTTGCTCGCACATTAGT
ECTV-Mos 141		
ECTV-Mos 141 - N	myc	CACCATGGAGCAGAAACTCATCTCTGAAGAGGATCTGATGGCGGCCGAATG
ECTV-Mos 141 - C		TTAATTACCAGTTGCTCGCACATTAGT
ECTV-Mos 145		
ECTV-Mos 145 - N	6 x histidine	CACCATGGCACACCATCACCACCATCATATGGCGTTTGATATATCAGTTAA
ECTV-Mos 145 - C		TTATACATCCGTTTCCCTGTCGGTT
ECTV-Mos 147		
ECTV-Mos 147 - N	6 x histidine	CACCATGGCACACCATCACCACCATCATATGACCTATATATTTATTTTCAGTTTTAT
ECTV-Mos 147 - C		TTACATCCACAGTTGCCCCACTG
ECTV-Mos 150		
ECTV-Mos 150 - N	6 x histidine	CACCATGGCACACCATCACCACCATCATATGATATCTTCACGTGGATATAGG
ECTV-Mos 150 - C		TCAACTACCTATAAAACTCTCCAAACACTTTAGA
ECTV-Mos 152		
ECTV-Mos 152 - N	6 x histidine	CACCATGGCACACCATCACCACCATCATATGAACTTTCAAGGACTTGTGTT
ECTV-Mos 152 - C		TTACATAACTCCATTCATTAATACGCGC

Primer Name	Epitope Tag	Sequence 5' → 3'
ECTV-Mos 153		
ECTV-Mos 153 - N	6 x histidine	CACCATGGCACACCATCACCACCATCATATGGCGATGTTTTACACACA
ECTV-Mos 153 - C		TTAAACTTTTATATATGACACCCATTCATCTGG
ECTV-Mos 160		
ECTV-Mos 160 - N	6 x histidine	CACCATGGCACACCATCACCACCATCATATGGAATCCTTCAAGTATTGTTT
ECTV-Mos 160 - C		TCAATCTTGTATAAACAGTCTACGTAGTCTGTCA
ECTV-Mos 161		
ECTV-Mos 161 - N	6 x histidine	CACCATGGCACACCATCACCACCATCATATGGATATCTTCAGGGAGATC
ECTV-Mos 161 - C		TTAATTAGTTGTTGGAGAGCAATATCTACCA
ECTV-Mos 167		
ECTV-Mos 167 - N	6 x histidine	CACCATGGCACACCATCACCACCATCATATGGAATACAATACCATTTACACC
ECTV-Mos 167 - C		TTAGTAGATGGGTAGTGTATCGTGTACTATATAACTATTC
ECTV-Mos 168		
ECTV-Mos 168 - N	6 x histidine	CACCATGGCACACCATCACCACCATCATATGTCTACTTGGCATGTTGTCA
ECTV-Mos 168 - C		TTATTGTGGATAGCAGTATTTCCCTATAAAAA
VACV-WR 148		
VACV-WR 148 - N		CACCATGGAGGTCACGAACCTTATTGAAAA
VACV-WR 148 - C	hemagglutinin	TTAAGCGTAATCTGGAACATCGTATGGGTAAGACGTCGCATCTCTCTCTGTTTC

Agarose gel electrophoresis

PCR products and plasmid DNA were resolved by agarose gel electrophoresis. Gels were prepared by dissolving OmniPur Agarose (EMD Chemicals Inc., Gibbstown, NJ, USA) in Tris-acetate buffer (TAE; 40 mM Tris-acetate, 1 mM EDTA) for a final agarose concentration of 1%. DNA samples were mixed with 6 x DNA loading buffer (0.25% bromophenol blue, 0.25% xylene cyanol FF, 40% sucrose, 50 mM EDTA) prior to loading on the gel. Mini gels were loaded with 2 - 10μl of each sample and 0.4 μg of 1 Kb Plus DNA Ladder (Cat # 10787018, Invitrogen Life Technologies). Electrophoresis was performed at 100 volts (Bio-Rad Power Pac 300; Bio-Rad, Richmond, CA, USA) for 30 minutes in TAE buffer. Following electrophoresis, the DNA was stained for approximately 15 minutes in buffer containing 0.5 μg/ml ethidium bromide, visualized using a MultiImage Light Cabinet (Alpha Innotech, San Leandro, CA, USA) and photographed.

Purification of PCR products

PCR products were purified using the QIAquick PCR Purification kit (Cat # 28104 QIAGEN, Chatsworth, CA, USA) according to the manufacturer's instructions. After purification, DNA was eluted from the QIAquick column by application of 50 μl Buffer EB (10 mM Tris-HCl, pH 8.5) and stored at -20°C.

Cloning of recombinant genes into the pENTR/SD/D-Topo Entry Vector

Purified PCR products were introduced into the cloning site of pENTR/SD/D-Topo entry vector (Kan^R) according to the instructions in the pENTR/SD/D-Topo Cloning Kit (Cat # 0219, Invitrogen Life Technologies) (Figure 5). Briefly, 2.5 ng fresh PCR product, 1 µl salt solution (250 mM NaCl, 10 mM $MgCl_2$), and 250 ng pENTR/SD/D-Topo entry vector were mixed together and brought up to a final volume of 5 µl with water. A negative control, in which the PCR product was omitted from the reaction mixture, was included the first time the reaction was performed. The reactions were mixed gently and allowed to incubate at room temperature for 5 minutes. Directionality of cloning was achieved through the unique design of the entry vector and use of topoisomerase I, which is covalently bound to the 3' phosphate of the linearized entry vector. The entry vector contains a single-strand GTGG overhang on the 5' end and a blunt end on the 3' end. The four-nucleotide overhang invades the double-stranded DNA of the PCR product and anneals to the CACC sequence incorporated in the 5' primer. Topoisomerase then ligates the PCR product in the correct orientation. After incubation, the reaction mixture was frozen at -20°C or used to transform One Shot TOP10 *E. coli* cells (Invitrogen Life Technologies).

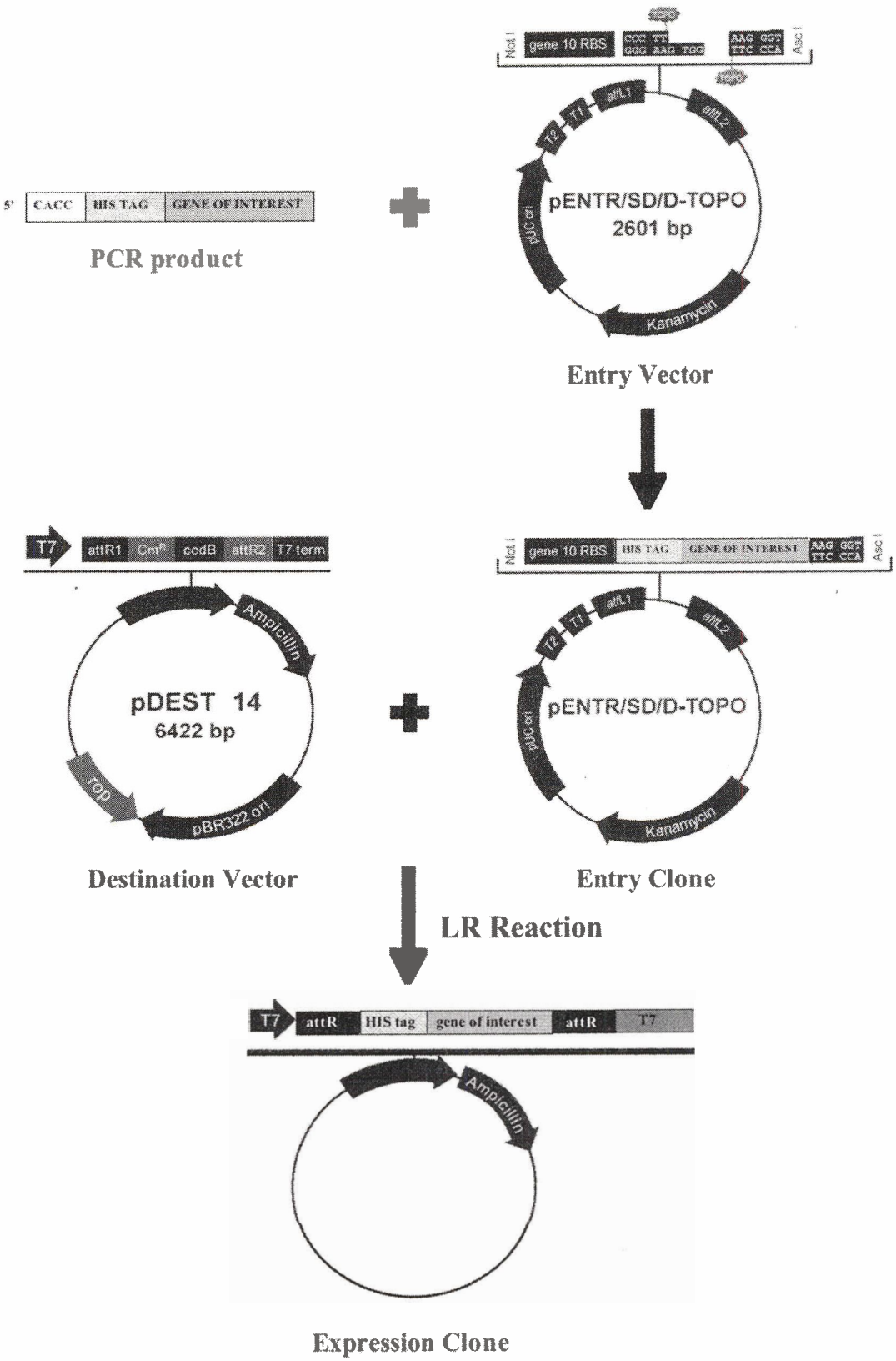

Figure 5. Cloning strategy for the production of pDEST14 expression clones.

Transformation of E. coli cells

2 µl of pENTR/SD/D-Topo entry vector or pDEST14 expression clone DNA was added to 1.5 ml screw-top microfuge tubes containing 50 µl of thawed, chemically competent One Shot TOP10 *E. coli* (Cat # 440301, Invitrogen Life Technologies) or One Shot BL21-AI Chemically Competent *E. coli* (Cat # 440184, Invitrogen Life Technologies), respectively, and swirled gently to mix. The cells were incubated on ice for 30 minutes then heat-shocked at 42°C for 30 seconds without agitation. The microfuge tubes were returned to ice, and 250 µl room temperature SOC medium (0.5% yeast extract, 2% tryptone, 10 mM NaCl, 2.5 mM KCl, 10 mM $MgCl_2$, 10 mM $MgSO_4$, 20 mM glucose) was added. The vials were shaken horizontally (200 rpm) at 37°C for 30 or 60 minutes in an Innova 4000 Shaking Incubator (New Brunswick Scientific Co. Inc., Edison, NJ, USA) to permit expression of the antibiotic resistance gene prior to plating 150 µl of the transformation reaction onto pre-warmed Luria Bertani (LB; 10g tryptone, 5g yeast extract, 10 g NaCl, in a total of 1 L of distilled water, adjusted to pH 7.0 with 5 M NaOH) 2% agar plates containing the appropriate antibiotic.

Isolation and purification of plasmid DNA

Single colonies were used to inoculate Luria Bertani broth containing the appropriate antibiotic and grown overnight at 200 rpm, 37°C in a shaking incubator. Plasmid DNA was isolated using the QIAprep Spin Miniprep Kit (Cat # 27104, QIAGEN) as outlined in the QIAprep Spin Miniprep Kit manual. This DNA isolation procedure is based on rapid alkaline lysis, as described by Birnboim and Doly (1979). After isolation and

purification, DNA was eluted from the QIAprep spin column by application of 50 µl sterile water.

Quantitation of DNA

A solid-state fluorimeter (SSF-600, Tyler Research Instruments Corporation, Edmonton, AB, Canada) was zeroed with ethidium bromide solution (5 mM Tris pH 8.0, 0.5 mM EDTA, 0.5 ng/ml EtBr), and calibrated with a standard containing 50 µg herring sperm DNA in 2 ml ethidium bromide solution. DNA sample concentration was determined by adding 1 µl of the sample DNA to 2 ml of ethidium bromide solution and comparing to the standard.

Identification of positive clones

Entry clones containing insert in the correct orientation in the pENTR/SD/D-Topo entry vector were identified by PCR analysis. A small amount of colony was removed from the transformation plate with a sterile toothpick and resuspended in 100 µl sterile water in a 1.5 ml Micro Tube. Typically, 1 µl of this cell suspension was used as template in the following PCR reaction: 1 x PCR buffer, 1 unit *Taq* polymerase (cloned in our laboratory), 0.1 mM dNTP mix, 0.1 µM gene-specific N-primer and 0.1 µM vector-specific M13 reverse primer (Cat # 460691, Invitrogen Life Technologies). Thermocyler conditions were as previously described. PCR products were analyzed by agarose gel electrophoresis.

DNA sequencing

Plasmid DNA from positive clones were checked by DNA sequencing to verify that errors had not been introduced by *Pfu* polymerase during PCR. High quality DNA suitable for sequencing was prepared using a QIAprep Spin Miniprep Kit (QIAGEN) according to the manufacturer's instructions. Approximately 1 μg of plasmid DNA was provided to the University of Victoria Centre for Environmental Health Sequencing Group. Sequences were obtained using a LI-COR fluorescent DNA sequencer. Raw data was analyzed with the EditView program (version 4.11, Applied Biosystems, Foster City, CA, USA).

Subcloning of recombinant genes into pDEST14 Destination Vector

For expression of the recombinant proteins, expression clones were constructed by transferring recombinant genes from the pENTR/SD/D-Topo entry clone to the pDEST14 Destination Vector (Amp^R) via the LR recombination reaction. The reaction strategy to produce a pDEST14 expression clone is given in Figure 5. LR reaction conditions were followed as per manufacturer instructions outlined in the Gateway Technology Cloning Manual (Invitrogen Life Technologies); however, reaction volumes were halved to minimize cost. To perform the LR reaction, typically 100 ng pENTR/SD/D-Topo entry clone, 150 ng pDEST14 destination vector (Invitrogen Life Technologies), 2 μl LR Reaction Buffer (Invitrogen Life Technologies), 5 μl TE buffer (TE; 10 mM Tris-Cl, pH 7.5, 1 mM EDTA pH 8.0), and 2 μl LR Clonase Enzyme Mix (Invitrogen Life Technologies) were mixed together in a 1.5 ml Micro Tube and allowed to incubate at

room temperature for 1 hour. To stop the reaction, 2 µl proteinase K solution (2 µg/ml in: 10 mM Tris-HCl pH 7.5, 20 mM $CaCl_2$, 50% glycerol) was added and the reaction was incubated at 37°C for 10 minutes. BL21-AI *E. coli* cells (Cat # C607003, Invitrogen Life Technologies) were transformed with 1 µl LR reaction for expression of the recombinant proteins.

Expression and purification of recombinant proteins

4 x 2 L Erlenmeyer flasks containing 500 ml LB broth plus 100 µg/ml ampicillin were inoculated with 12 ml of overnight culture and grown at 200 rpm, 37°C, in the shaking incubator until the OD_{600} was 0.4 (approximately 2 hours) as measured using a Beckman DU-65 Spectrophotometer (Beckman Coulter Inc.). The flask was rapidly cooled on ice to room temperature prior to the addition of 20 % L-arabinose to a final concentration of 0.2%. Expression of the recombinant protein from the expression vector is regulated by the *ara*BAD promoter (P_{BAD}), which controls expression of the T7 RNA polymerase in BL21-AI cells. In the presence of arabinose, the P_{BAD} promoter permits expression of the T7 RNA polymerase, and therefore transcription of the gene of interest. After induction with arabinose, the cells were grown for an additional 4 hours at 25-28°C to permit recombinant protein expression after which the cells were harvested by centrifugation at 5000 x g in a Beckman J2-HC centrifuge (JA-14 rotor) for 10 minutes at 4°C. The supernatants were discarded and the pellet resuspended in 40 ml lysis / purification buffer (50 mM $NaPO_4$, 0.5 M NaCl pH 7.0, 1 mM PMSF). The cells were lysed by passing the cell suspension through a French Pressure Cell Press (American Instrument Company, Silver Spring, Maryland, USA) at 1260 psi a total of 3 times. Insoluble material was

removed by centrifugation at 12,000 x g for 45 minutes at 4°C. The clarified extract was loaded onto 2 ml nitrilotetraacetic agarose columns (Cat # R90101, Ni-NTA resin, Invitrogen Life Technologies) at a flow rate of 0.5 ml/min for 80 minutes on a Bio-Rad Biologic low pressure chromatography system (Bio-Rad). Contaminating proteins were removed by washing the column with low pH lysis / purification buffer (pH 5.0) for 45 min at 0.5 ml/min. The histidine-tagged proteins were eluted with an elution buffer (50 mM $NaPO_4$, 0.5 M NaCl pH 7.0, 1mM PMSF) gradient from 0 mM to 300 mM imidazole over 2 hours at 0.5 ml/min, collecting 2 ml fractions. EDTA and glycerol were added to the fractions (final concentrations of 1mM and 10%, respectively) to prevent degradation and aggregation of the proteins, which were then stored at -20°C. Fractions containing significant amounts of purified protein were identified by SDS-PAGE.

Polyacrylamide gel electrophoresis

Sodium dodecyl sulfate polyacrylamide gel electrophoresis (SDS-PAGE) was performed using an Xcell *SureLock* Mini-cell apparatus (Invitrogen Life Technologies). Protein samples were prepared by adding NuPAGE LDS sample buffer (to a final concentration of 1 x); Cat # NP0007, Invitrogen Life Technologies), DTT (dithiothreitol; to a final concentration of 10 mM) and heating to 70°C for 10 minutes. If cell lysate was run on the gel, DNA was sheared with an 18-gauge syringe needle prior to loading. 5 μL BenchMark Protein Marker (Cat # 10747012, Invitrogen Life Technologies) or 10 μL SeeBlue Plus2 (Cat # LC5925, Invitrogen Life Technologies) protein molecular weight standard was used if the gel was to be stained with Coomassie blue or used in western blot analysis, respectively. Protein samples and protein standards were loaded onto pre-

cast NuPAGE Novex 4 - 12% Bis-Tris 12 well gels (Cat # NP0322BOX, Invitrogen Life Technologies) and run at 200 volts for 35 minutes in MES running buffer (0.05 M 2-(N-morpholino) ethane sulfonic acid, 0.05M tris base, 3.47 mM SDS, 1.025 mM EDTA, pH 7.3). Gels to be stained with Coomassie blue were placed in fixing solution (50% methanol, 10% acetic acid, 40% water) for 30 minutes, stained in Coomassie blue G-250 (0.1% Brilliant Blue G, 25% methanol, and 5% acetic acid) for 1 hour and then placed in destaining buffer (10% methanol, 10% acetic acid, 80% water) until background was sufficiently reduced (4 hours to overnight). Gels were digitally photographed using the Odyssey Infrared Imaging System (model 9120, Li-COR Biosciences, Lincoln, NB, USA), and dried in BioDesignGelWrap membrane (Cat# G101, BioDesign Inc., Carmel, NY, USA).

Bradford assays

Protein concentrations were determined using a Bradford assay in which 1.5 ml Bradford Reagent (Cat # B6916, Sigma) was added to 50 µl of bovine serum albumin (BSA) standards (serially diluted from 2 mg/ml to 0.25 mg/ml) or protein samples in disposable cuvettes. The samples were gently mixed and incubated for 20 minutes at room temperature to allow colour development. The absorbance of the samples was read at 595 nm on a Beckman DU-65 Spectrophotometer (Beckman Coulter Inc.). The concentrations of the protein samples were determined by construction of a standard curve using the absorbance readings for the BSA standards.

Western blots

Purified protein or cellular lysates were separated by SDS-PAGE on 4 - 12% acrylamide gels. Proteins were transferred to a Trans-Blot nitrocellulose membrane (Cat # 12011, Bio-Rad) in transfer buffer (20% methanol, 25 mM Tris base, 192 mM glycine, 0.035 mM SDS) at 80 volts for 90 minutes using a Bio-Rad mini trans-blot cell apparatus (Bio-Rad). Membranes were blocked with Odyssey Blocking Buffer (Cat # 9270000, Li-COR Biosciences) for 1 hour at room temperature and then incubated with primary antibody diluted in Odyssey Blocking Buffer 1:1500 for 1 hour at 4°C. Membranes were washed 4 x 5 minutes with PBS (phosphate buffered saline; 137 mM NaCl, 2.7 mM KCl, 4.3 mM $Na_2HPO_4 \bullet 7H_2O$, 1.4 mM KH_2PO_4 pH 7.3) + 0.1% TWEEN-20 and then incubated in secondary antibody 1:2500 dilution in Odyssey Blocking Buffer for 1 hour at 4°C. Histidine-tagged proteins were detected and visualized using mouse IgG_1 anti-penta histidine primary antibody (Cat # 34660, QIAGEN) and rabbit anti-mouse IgG (H&L) IRDye 800 conjugate secondary antibody (Cat # 610432020, Rockland Immunochemicals Inc., Gilbertsville, PA, USA). Myc-tagged ECTV-Mos 141 protein was detected and visualized using rabbit polyclonal anti-myc primary antibody (Cat # 2272, Cell Signaling Technology, Beverly, MA, USA) and goat anti-rabbit IgG (H&L) IRDye 800 conjugate secondary antibody (Cat # 611132122, Rockland Immunochemicals Inc.). Hemagglutinin-tagged proteins, ECTV-Mos 128 and VACV-WR 148, were detected and visualized using mouse IgG_1 anti – hemagglutinin Alexa Fluor 488 conjugate antibody (Cat # A21287, Molecular Probes Inc., Eugene, OR, USA) and rabbit anti-mouse IgG (H&L) IRDye 800 conjugate secondary antibody (Cat #

610432020, Rockland Immunochemicals Inc.). Actin was detected and visualized using rabbit IgG anti-actin primary antibody (Cat # A5060, Sigma-Aldrich) and goat anti-rabbit IgG (H&L) IRDye 800 conjugate secondary antibody (Cat # 611132122, Rockland Immunochemicals Inc.). After incubation in secondary antibody, membranes were washed 4 x 5 minutes each in PBS + 0.1% TWEEN-20 and then once in PBS alone for 5 minutes at room temperature. Blots were allowed to dry and then visualized and digitally photographed using the Odyssey Infrared Imaging System (Li-COR Biosciences).

Ectromelia virus (Moscow) genome map

The Viral Orthologs Clusters Database (VOCs) was used to create the genomic map of ECTV-Mos. Genes were selected for display and coloured based on their degree of conservation in 42 sequenced poxvirus genomes (Table 1). The resulting JPEG file was modified in OmniGraffle Professional software.

Homology modeling of ECTV-Mos 141[3]

The ECTV-Mos 141 primary protein sequence (NP_671660.1) was submitted to the SWISS-MODEL (Schwede et al., 2003) server using the "First Approach" mode with default settings. The server identified 4 profilin proteins as having a high degree of sequence identity with ECTV-Mos 141 based on BLASTp results (Altschul et al., 1990): human platelet profilin 1 (1FIL), human profilin (1FIK), human profilin NMR structure (1PFL), and bovine profilin bound with actin (1HLU). SWISS-MODEL created a multiple sequence alignment of ECTV-Mos 141 and the 4 template proteins using the

SIM sequence alignment program (Huang, X and M. Webb, 1991), and used the alignment in the ProModII (Peitsch, 1996) modeling program to build the ECTV-Mos 141 homology model. WHAT_CHECK (Hooft et al., 1996) and VADAR (Willard et al., 2003) protein verification tools were used to analyze the protein structure quality. Images of the homology model were generated using the Protein Explorer macromolecular visualization tool (Martz, 2002).

---

[3] This work was performed by Shan Sundararaj (current address: Department of Computing Science and Biological Sciences, University of Alberta, Edmonton, Alberta, Canada)

Mammalian cell culture

Tissue culture reagents were obtained from Gibco BRL Inc. (Gaithersburg, MD, USA) unless otherwise stated. The African green monkey kidney cell line BS-C-1 (ATCC CCL 26), was grown in complete Dulbecco's modified Eagle medium (D-MEM; 5.56 mM D-glucose, 4 mM L-glutamine, 0.0196 mM pyroxine hydrochloride, 1 mM sodium pyruvate and 44.05 mM $NaHCO_3$) supplemented with 10% newborn bovine serum, 50 U/ml penicillin, 50 μg/ml streptomycin and 5 ml/L (100X) GlutaMAX-II, in a humidified 37°C, 7% CO_2 incubator (Sanyo CO_2 Incubator, Caltec Scientific Ltd., Vancouver, BC, Canada). Cells were passaged by harvesting confluent monolayers from T75 tissue culture flasks (Falcon, Beckton Dickinson Labware, Franklin Lakes, NJ, USA) followed by seeding approximately 20% of the cells back to the flasks. Briefly, the medium was decanted into neutral buffer formalin (NBF; 4% formaldehyde pH 7.0, 0.145 M NaCl, 0.03 M Na_2HPO_4, 0.03 M $NaH_2PO_4 \bullet H_2O$) and the cells washed with pre-warmed, 37°C PBS. The cells were removed from the monolayer by the addition of 5 ml of 1 x PBS containing approximately 0.75 μg/ml trypsin and incubated at 37°C until the cells began to round up and detach. 5 ml of complete D-MEM + serum was added to inhibit trypsin activity and cell clumping. The cell suspension was transferred to 15 ml conical tubes, pelleted by centrifugation at 400 x g for 5 minutes (Beckman GS-15 Centrifuge, Beckman Instruments) and resuspended in 5 ml of complete D-MEM. 20% of the cells were added to a T75 flask containing 14 ml complete D-MEM then returned to the CO_2 incubator.

Virus infection and transfection of mammalian cells

This protocol was adapted from Fuerst et al., 1986. When BS-C-1 cells had reached approximately 90% confluency, the growth medium was removed and an appropriate volume of complete D-MEM containing virus at the desired multiplicity of infection (MOI) was added. For 100 mm and 6 well tissue culture dishes and chamber slides, the infection volumes were 3 ml, 500 µl and 200 µl respectively. Virus absorption was allowed to proceed at 37°C for 1 hour with gentle rocking every 10 minutes, the virus inoculum was removed and replaced with complete D-MEM + serum (10 ml, 2 ml and 200 µl, respectively). The infected cells were incubated at 37°C for an additional 2 hours before transfection with plasmid DNA.

During the last hour of infection, plasmid DNA was prepared for transfection of the BS-C-1 cells. For 100 mm and 6 well tissue culture dishes and chamber slides, the cells were transfected with a total of 25 µg, 2.5 µg or 200 ng pDEST14 expression clone DNA, respectively. The appropriate amount of DNA was brought up to a final volume of 700 µl, 230 µl, or 93 µl, respectively, with sterile water and mixed with 75 µl, 25 µl, or 17 µl of 2.5 M $CaCl_2$, respectively. The DNA / $CaCl_2$ solution was added dropwise to 750 µl, 250 µl, or 25 µl, respectively of 2 x HBS (HEPES-buffered saline solution; 0.28 M NaCl, 0.05 M HEPES, 1.5 mM Na_2HPO_4, pH 7.5, filter sterilized through a 0.45 µm filter), vortexed, and incubated at room temperature for 1 hour. After the 2 hour infection incubation, the medium was removed from the cells and the DNA precipitate was added dropwise over cells. The precipitate was left on cells for 15 minutes with occasional rocking, and then 10 ml, 1.5 ml, and 200 µl, respectively, of pre-warmed 37°C complete

D-MEM was added to the dishes or chamber slides and cells were incubated an additional 4 hours in the CO_2 incubator. The medium was removed, cells were washed 2 x with PBS, and an appropriate amount of pre-warmed complete D-MEM + serum was added to the dishes or chambers, and the cells were incubated overnight in the CO_2 incubator.

Immunoprecipitation

Protocol was adapted from Husain and Moss, 2003. BS-C-1 (passage 7) cells were seeded in 9 x 100 mm tissue culture dishes and grown to 90% confluency (approximately 6.3×10^7 cells / dish). Cells were infected with a recombinant VACV strain WR vTF7-3 (passage 3, ATCC VR-2153) expressing a T7 polymerase, at a multiplicity of infection (MOI) of 10 and transfected with 25 μg ECTV-Mos 141 (histidine-tagged) pDEST14 Expression Clone plasmid DNA per 100 mm dish. Cells were incubated overnight in a humidified 37°C, 7% CO_2 incubator. The next day (~16 hours later), the tissue culture dishes were removed from the incubator and placed on ice, the growth medium was removed, and the cells were washed 4 x with 10 ml ice-cold PBS. 350 μl ice-cold non-denaturing lysis buffer (50 mM Tris-HCl pH 7.5, 300 mM NaCl, 1% Triton X-100, 10 mM imidazole) containing protease inhibitor cocktail (Cat # 1836153, Roche Applied Science) was added to each 100 mm tissue culture dish. After a 10 minute incubation in lysis buffer on ice, cells were removed from the monolayer using a cell scraper, and transferred to a 30 ml glass centrifuge tube. The cell suspension (~3.15 ml) was mixed gently incubated an additional 30 minutes on ice. The lysate was cleared by centrifuging at 20,000 x g for 10 min at 4°C. The supernatant was transferred to a new tube and 15 μl Protein G-Plus Agarose (Cat # sc2002, Santa Cruz Biotechnology, Santa Cruz, CA, USA)

was added to pre-clear the extract. After rotating the tube at 4°C for 1 hour, the Protein G-Plus Agarose was pelleted by centrifuging at 1000 x g for 1 minute. The supernatant was removed and dispensed into a fresh centrifuge tube and Penta-His Antibody (Cat # 34660, mouse Penta-His Antibody IgG_1, QIAGEN) was added to a concentration of 5 μg/ml. The tube was rotated for 3 hours at 4°C before 60 μl Protein G-Plus Agarose was added and the incubation continued overnight. The next day (~ 16 hours later), the Protein G-Plus Agarose was pelleted by centrifuging at 1000 x g for 1 minute and the supernatant was removed. The agarose was resuspended in 3 ml of wash buffer (0.1% Triton X-100, 50 mM Tris-Cl, pH 7.5, 300 mM NaCl), mixed gently, and centrifuged at 1000 x g to pellet the agarose. The agarose was washed as above a total of 4 times before a final wash with PBS and resuspension in 80 μl of 1 x NuPAGE LDS sample buffer (Cat # NP0007, Invitrogen Life Technologies), 10 mM DTT (dithiothreitol) and heated to 70°C for 10 minutes. A control was performed which followed the identical protocol with the exception that cells were transformed with herring sperm DNA instead of pDEST14 expression clone DNA.

Mass spectrometry

Coomassie blue-stained bands were excised from the gel using a new scalpel and were prepared and analyzed by the Genome BC Proteomics Centre. The gel slices were subjected to an automated in-gel trypsin digestion, and were analyzed by MALDI-TOF using a Voyager-DE STR mass spectrometer (Applied Biosystems, Foster City, CA, USA). The Mascot search engine (Perkins et al., 1999) was used to identify the primary

protein sequences of the samples from the mass spectrometry data by searching primary sequence databases.

Far Western analysis

Protocol was adapted from Einarson and Orlinick, 2002. 2 μg of each of porcine muscle tropomyosin (Cat # T2400, Sigma-Aldrich), ECTV-Mos 141(histidine-tagged profilin homolog, metal chelation chromatography purified), rabbit muscle actin (Cat # A2522, Sigma-Aldrich), RelA (histidine-tagged bacterial protein, a gift from Dr. Edward Ishiguro, Dept. Biochemistry and Microbiology, University of Victoria), and Bovine Serum Albumin (BSA; Cat # A9647, Sigma-Aldrich) were separated by SDS-PAGE. After transfer to a nitrocellulose membrane, proteins were refolded by a denaturation and renaturation cycle in guanidine hydrochloride as described by Rea et al., 2004. The membrane was washed twice in 50 ml of denaturation buffer (6 M guanidine hydrochloride, 20 mM HEPES pH 7.5, 50 mM KCl, 10 mM $MgCl_2$, 1 mM DTT, 0.1% Nonidet P-40) for 10 minutes at 4°C with gentle agitation. The denaturation buffer was diluted 1:1 with basic buffer (20 mM HEPES pH 7.5, 50 mM KCl, 10 mM $MgCl_2$, 1 mM DTT, 0.1% Nonidet P-40) and the membrane was washed as before. This dilution and wash cycle was repeated four more times until the final wash contained 175 mM guanidinium hydrochloride. Porcine muscle tropomyosin was used as the probe protein, and was diluted to a final concentration of 20 μg/ml in interaction buffer (1% nonfat dry milk in basic buffer, 5% glycerol, 1 mM PMSF) and was incubated with the membrane for 5 hours at 4°C with gentle agitation. The tropomyosin solution was removed and the membrane was washed 4 x 10 minutes in buffer #1 (0.2% Triton X-100 in PBS) at 4°C

with gentle agitation, followed by 2 x 10 minutes in buffer #2 (0.2% Triton X-100, 100 mM KCl in PBS) at 4°C with gentle agitation. The membrane was exposed to mouse monoclonal anti-tropomyosin IgG_1 primary antibody (Cat # T2780, Sigma-Aldrich) diluted 1:1000 in 1:1 Odyssey Blocking Buffer and PBS + 0.2% TWEEN-20, overnight at 4°C with gentle agitation. The next day the primary antibody was removed and the membrane was washed 4 x 5 minutes with PBS + 0.1% TWEEN-20. The membrane was then exposed to rabbit anti-mouse IgG (H&L) IRDye 800 conjugate secondary antibody (Cat # 610432020, Rockland Immunochemicals Inc.) at 1:2500 dilution for 1 hour at 4°C with gentle agitation. The secondary antibody was removed and the membrane was washed 4 x 5 minutes with PBS + 0.1% TWEEN-20 and once with PBS alone. The blot was visualized and digitally photographed using the Odyssey Infrared Imaging System (Li-COR Biosciences).

Immunofluorescence

Protocol was adapted from Ye et al., 2004. BS-C-1 cells (passage 12) were grown on cover slips to 80% confluency, infected at a MOI of 10 with recombinant VACV western reserve strain vTF7-3 (passage 3; ATCC VR-2153) expressing T7 RNA polymerase, and then transfected with a total of 200 ng pDEST14 expression clone plasmid DNA per chamber. After infection and transfection, cells were incubated overnight (approximately 16 hours) in the 37°C, CO_2 incubator. The next day, the growth medium was removed, cells were washed once with room temperature Tris-buffered saline (TBS; 150 mM Tris•HCl pH 7.4, 150 mM NaCl) and then fixed for 10 minutes in 4% paraformaldehyde (in PBS). The paraformaldehyde was removed, cells were washed 5 minutes with TBS,

permeabilized in 0.2% Triton X-100 (in PBS) for 5 minutes at room temperature and then washed 3 x 5 minutes each with TBS. Cells were quenched in fresh 0.1% sodium borohydride (in PBS) for 5 minutes, washed 3 x 5 minutes with TBS, blocked (in 10% fetal bovine serum, 1% BSA, 0.02% NaN3, in PBS) for 1 hour at room temperature with gentle agitation and then washed once for 5 minutes with TBS.

Prior to staining of the cells, all antibodies were centrifuged for 20 minutes at 12,000 x g in a microfuge refrigerated at 4°C to remove any aggregated material. Cells were incubated in primary antibody diluted in 1% BSA (in TBS) overnight at 4°C with gentle agitation. The next day (~16 hours) cells were washed 3 x 5 minutes with TBS and then incubated with secondary antibody diluted in 1% BSA (in TBS) at room temperature in the dark for 45 minutes. Proteins containing a myc tag were visualized using rabbit polyclonal anti-myc primary antibody (Cat # 2272, Cell Signaling Technology, Beverly, MA, USA) 1:100 dilution, and Alexa Fluor 568 conjugate goat anti-rabbit IgG (H+L) secondary antibody (Cat # A11011, Molecular Probes) 1:200 dilution. Proteins containing a hemagglutinin tag were visualized using Alexa Fluor 488 conjugate mouse monoclonal IgG_1 anti-hemagglutinin antibody (Cat # A21287, Molecular Probes) 1:200 dilution. Endogenous cellular tropomyosin was visualized using mouse monoclonal anti-tropomyosin IgG_1 primary antibody (Cat # T2780, Sigma-Aldrich) 1:200 dilution, and goat anti-mouse IgG (whole molecule) FITC conjugate secondary antibody (Cat # F2012, Sigma-Aldrich) 1:40 dilution. After incubation with secondary antibody, cells were washed 3 x 5 minutes each with TBS in low lighting, and DNA was visualized by incubation of cells with DAPI (4',6-Diamidino-2-phenyindole; Cat # D5964, Sigma-

Aldrich) at 1 ng/ml in TBS for 5 minutes in the dark. Controls cells for the co-localization of ECTV-Mos 141 with ATI proteins VACV-WR 148 and ECTV-Mos 128, were infected with vTF7-3, transformed with herring sperm DNA, and stained with primary and secondary antibodies and DAPI. Control cells for the co-localization of ECTV-Mos 141 with endogenous cellular tropomyosin were not infected with vTF7-3 but were transformed with herring sperm DNA and stained with primary and secondary antibodies and DAPI. After staining with DAPI, cells were washed 3 x 5 minutes each with TBS in low lighting and coverslips were mounted on slides using the Prolong Antifade Kit (Cat # P7481, Molecular Probes). Pictures of cells at 1000x magnification were taken using the Leica DM6000 B microscope (Leica Microsystems, Richmond Hill, ON, Canada) using the autoexposure option.

Protein sequence alignments

Primary protein sequences for: human profilin-1 (P07737), bovine profilin (P02584), murine profilin-1 (P62962), rat profilin-1 (AAH62405), ectromelia virus profilin homolog (NP_671660.1) and vaccinia virus profilin homolog (NP_063836.1) were retrieved from the National Center for Biotechnology Information (NCBI) website at http://www.ncbi.nlm.nih.gov/. Alignments of amino acid sequences were created with the Clustal W Multiple Sequence Alignment Program (Thompson et al., 1994) using default settings as described by Higgins et al., 1994.

A multiple sequence alignment from primary protein sequences was also created for three A-type inclusion (ATI) protein orthologs ECTV-Mos 128 (CAA49168), VACV-WR 148 (P21117) and CPXV-BR 158 (NP_619942) using the same method as above.

Chapter 3: Results

Selection of 56 conserved orthopoxvirus gene families for structural and functional characterization

Despite the large body of poxvirus genome sequence information now available, many poxvirus proteins, including a significant number that are present in all sequenced poxviruses, are either totally uncharacterized or merely have a predicted function based on sequence similarity (Upton et al., 2003). The goal of this thesis was to contribute to the understanding of poxvirus biology by beginning preliminary characterization of genes conserved between the orthopoxviruses, a genus of poxviruses containing viruses of human, veterinary and zoonotic importance (Bugert et al., 2000). The Viral Orthologs Clusters (VOCs) database (Upton et al., 2003), a repository for poxvirus genomic information, was used to identify 133 orthologous gene families conserved between the orthopoxviruses (see Materials and Methods for genomes searched). Many of these 133 gene families, however, have been well characterized in previous research, and further characterization would provide little or no additional insight into the poxvirus life cycle. As such, 56 gene families were chosen for characterization (Table 3) based both on a paucity of information available about the gene families in addition to their conservation in orthopoxviruses. Nearly half of these conserved orthopoxvirus gene families are involved in essential viral functions, such as DNA replication, mRNA transcription and virion maturation (Upton et al., 2003). Five of the 56 gene families encode proteins that are orthopoxvirus-specific and modulate host immune responses during the virus life cycle. These viral immunoregulatory proteins are involved in blocking the host

inflammatory and immune response to infection, and probably contribute significantly to the virulence of the virus in a natural infection (Seet et al., 2003). Interestingly, 15 of the 56 gene families in addition to being absolutely conserved within the orthopoxviruses are also found in all other sequenced poxviruses, from the insect-infecting entomopoxviruses to the vertebrate-infecting chordopoxviruses. The absolute conservation of these genes suggests that they are essential in the poxvirus life cycle, and further characterization may eventually lead to the identification of drug, antibody, vaccine and detection targets (Upton et al., 2003). Furthermore, 27 of the gene families chosen for characterization have a yet unidentified function, and further characterization of these genes may not only provide an excellent opportunity for significant contributions to the understanding of the poxvirus life cycle, but might also illuminate novel aspects of the virus-host relationship.

Table 3. Selection of 56 conserved orthopoxvirus gene families for characterization. Families are grouped according to the known function of their gene products during infection. Columns: Gene family no, VOCs gene family identification no.; Family name, function of gene product. Highlighted gene family numbers indicate the gene family is absolutely conserved in all sequenced poxviruses.

Replication	
Gene family no.	**Family name**
1009	Deoxyuridine triphosphatase
1081	Serine-threonine kinase II
1503	Ribonucleotide reductase-small subunit
1599	Glutaredoxin 1
1603	Thymidylate kinase
Transcription	
Gene family no.	**Family name**
1133	RNA polymerase subunit 7
1141	RNA polymerase subunit 18
1142	Nucleoside triphosphate pyrophosphohydrolase
1143	Nucleophosphohydrolase-pyrophosphohydrolase downregulator
1153	Late transcription factor 2
1197	RNA polymerase subunit 35
1225	RNA polymerase subunit 19
1228	Late transcription factor 3
1252	RNA polymerase subunit 30
1272	RNA polymerase subunit 22
1277	Late transcription elongation factor
1283	Core packaging / transcription
1287	Late transcription factor 1
1353	Late transcription factor 4
1758	Intermediate transcription factor 3 - small subunit
1946	Intermediate transcription factor 3 - large subunit
Host Response Modifier	
Gene family no.	**Family name**
1196	Serpin-1 (serine protease inhibitor)
1196	Serpin-2 (serine protease inhibitor)
1196	Serpin-3 (serine protease inhibitor)
1554	Interferon resistance - protein kinase R inhibitor
1605	Interleukin-1 signaling inhibitor

Table 3. Continued.

Virion Maturation	
Gene family no.	**Family name**
1065	Serine-threonine kinase
1192	ATPase - DNA packaging protein
1270	Tyrosine-serine phosphatase
1283	Core packaging / transcription
1351	Virion core protein
Limited Characterization	
Gene family no.	**Family name**
1001	Unknown - putative maturation protein
1116	Unknown
1131	Unknown
1148	Unknown
1202	Unknown
1217	Unknown
1224	Unknown
1238	Unknown - ubiquitin ligase
1260	Unknown
1268	Unknown - putative telomere binding protein
1309	Unknown
1367	Unknown - intracellular mature virus virion protein 13
1504	Unknown - Kelch-like
1545	Unknown
1546	Unknown
1564	Unknown
1569	Unknown - serine-threonine kinase
1584	Unknown
1595	Unknown - Schlafen-like
1609	Unknown - profilin homolog
1613	Unknown
1614	Unknown - cytoplasmic protein
1617	Unknown - Kelch-like
1673	Unknown - putative monoglyceride lipase
1745	Unknown - Kelch-like
1746	Unknown – Kelch-like

Cloning of gene targets

Following selection of the 56 gene targets for characterization, orthologous genes were identified in ectromelia virus strain Moscow (ECTV-Mos) (Tables 4 and 5), a virulent orthopoxvirus that is the causative agent of mousepox. Ectromelia virus has been used previously as a model for smallpox infection (Buller and Palumbo, 1991) as many proteins shared between ECTV and variola virus share greater than 90% amino acid identity (Chen et al., 2000). The polymerase chain reaction (PCR) was utilized to amplify the target genes from ECTV-Mos DNA and incorporate a 6 x histidine tag onto the amino terminus of each gene, via design of the primers (Figure 4), to aid in purification of the proteins. The only gene that could not be amplified was ECTV-Mos 098 (gene family no. 1142, nucleoside triphosphate pyrophosphohydrolase (NTP-PPH)), possibly because primers could not be fully optimized due to sequence-dependant design restrictions e.g. formation of hairpins. As this was a collaborative project, 23 of the amplified genes were sent to collaborators at the University of Alberta for cloning and characterization (Table 4).

Table 4. Twenty-three of the 56 conserved orthopoxviruses genes identified in ECTV-Mos were PCR-amplified and sent to collaborators at the University of Alberta for cloning and characterization. Columns: ECTV-Mos gene no., gene identification no. in ECTV-Mos; Start, first nucleotide of start codon; Stop, last nucleotide of stop codon; Gene family no., VOCs gene family identification no.; Family name, function of gene product.

ECTV-Mos gene no.	Start	Stop	Gene family no.	Family name
012	19658	20383	1238	Unknown – ubiquitin ligase
018	29158	27620	1745	Unknown - Kelch-like
023	35291	34170	1196	Serpin-3 (serine protease inhibitor)
024	37765	36932	1673	Unknown - putative monoglyceride lipase
026	40232	39789	1009	Deoxyuridine triphosphatase
027	41708	40260	1504	Unknown - Kelch-like
028	42678	41719	1503	Ribonucleotide reductase - small subunit
029	43927	43703	1564	Unknown
031	44528	44331	1614	Unknown - cytoplasmic protein
032	45224	44586	1001	Unknown - putative maturation protein
033	46530	45211	1065	Serine-threonine kinase
038	51705	51229	1148	Unknown
039	52407	51712	1309	Unknown
043	57098	56526	1554	Interferon resistance
044	57934	57155	1252	RNA polymerase subunit 30
053	68528	68202	1599	Glutaredoxin 1
067	82204	82395	1133	RNA polymerase subunit 7
131	150134	149217	1197	RNA polymerase subunit 35
150	168929	170620	1746	Unknown - Kelch-like
160	181212	182072	1569	Unknown - serine-threonine kinase
161	182164	183198	1196	Serpin-2 (serine protease inhibitor)
167	191522	193201	1617	Unknown - Kelch-like
168	193640	194572	1196	Serpin-1 (serine protease inhibitor)

Our laboratory retained the remaining 32 amplified genes for cloning and characterization (Table 5). Invitrogen's Gateway Technology was chosen for this high-throughput cloning project, since it is an efficient means of cloning genes into a variety of vectors for expression of protein in a wide range of expression systems. Additionally, the

technology employs the action of topoisomerase, an enzyme that facilitates the directional insertion of the gene into the entry vector, thereby reducing the number of genes inserted into the vector incorrectly. Gene targets were cloned into the pENTR/SD/D-Topo entry vector, creating entry clones that were subsequently sequenced to verify the absence of errors introduced by polymerase during PCR. Initially, cloning of the genes into the entry vector was problematic due to incompatible components within the Gateway system itself; however, after resolving these issues and optimizing the cloning reactions, cloning proceeded more efficiently. Of the 32 genes retained by our laboratory, 28 were successfully cloned into the pENTR/SD/D-Topo entry vector. Genes that could not be cloned into the entry vector include: ECTV-Mos 037 (function unknown), ECTV-Mos 089 (function unknown), ECTV-Mos 099 (nucleophosphohydrolase – pyrophosphohydrolase (NPH-PPH) downregulator) and ECTV-Mos 126 (intermediate transcription factor-large subunit). These genes consistently produced entry clones containing sequence errors introduced by *Pfu* polymerase during PCR amplification. These errors were not due to the length of the gene, since gene sizes ranged from 213bp (ECTV-Mos 037) to 1146bp (ECTV-Mos 126). Additionally, errors did not consistently occur at a specific area on the genes, which would be expected if the polymerase was stuttering and introducing errors at homonucleotide stretches (Sarisky and Weber, 1994). Although cloning of these genes was unsuccessful, viable entry clones could undoubtedly be created if more attempts were made. After gene targets were cloned into the entry vector, they were then subcloned, via a recombination reaction, into the pDEST14 destination vector to generate expression clones.

Table 5. Thirty-three of the 56 conserved orthopoxviruses genes identified in ECTV-Mos were retained by our laboratory for PCR-amplification and cloning. Columns: ECTV-Mos gene no., gene identification no. in ECTV-Mos; Start, first nucleotide of start codon; Stop, last nucleotide of stop codon; Gene family no., VOCs gene family identification no.; Family name, function of gene product.

ECTV-Mos gene no.	Start	Stop	Gene family no.	Family name
037	50964	50749	1613	Unknown
058	73312	73073	1367	Unknown – IMV virion protein 13
059	74479	73331	1268	Unknown – telomere binding protein
064	79883	80545	1277	Late elongation transcription factor
068	82397	82894	1131	Unknown
070	84005	84787	1287	Late transcription factor 1
073	86614	86877	1584	Unknown
075	87932	88687	1283	Unknown - core packaging / transcription
080	91031	91588	1272	RNA polymerase subunit 22
083	96532	96017	1270	Tyrosine-serine phosphatase
084	96546	97115	1116	Unknown
087	100663	101301	1353	Late transcription factor 4
089	102283	102723	1260	Unknown
091	105695	105255	1351	Virion core protein
096	111427	111912	1141	RNA polymerase subunit 18
098	112831	113472	1142	NTP-PPH
099	113469	114221	1143	PH-PPH downregulator
103	119172	118720	1153	Late transcription factor 2
104	119867	119193	1228	Late transcription factor 3
108	122979	123473	1225	RNA polymerase subunit 19
109	124588	123470	1224	Unknown
111	126798	127664	1758	Intermediate transcription factor 3-small subunit
114	130684	131640	1217	Unknown
118	133274	132990	1546	Unknown
122	136712	136479	1545	Unknown
123	137069	136713	1202	Unknown
126	138861	140009	946	Intermediate transcription factor 3-large subunit
134	151649	150840	1192	ATPase - DNA packaging protein
141	158771	159175	1609	Unknown - profilin homolog
145	161607	162329	1605	Interleukin - 1 signaling inhibitor
147	163180	163863	1603	Thymidylate kinase
152	172283	173182	1081	Serine - threonine kinase II
153	173249	174760	1595	Unknown - Schlafen-like

Location of gene target ortholog ORFs in the ECTV-Mos genome

It has long been observed that poxvirus genes centrally located in the genome tend to be relatively conserved within members of the *Chordopoxvirinae* family and encode proteins that perform common essential molecular functions such as DNA replication, mRNA transcription, and virion maturation. Terminally located genes tend to be more variable and express an array of proteins that mediate the biological specificity of infections through mechanisms such as host range restriction and modulation of host antiviral responses (Johnston and McFadden, 2003; Upton et al., 2003). A genome map of ECTV-Mos (Figure 6) generated in the VOCs database (Upton et al., 2003) shows the location of open reading frames (ORFs) in the genome, and the number of sequenced poxviral genomes in which the ortholog is conserved. Genes chosen for characterization in this thesis have been labeled. In agreement with previous analyses (Upton et al., 2003), 49 gene families absolutely conserved in all 42 sequenced poxvirus genomes are located centrally in the poxvirus genome (Figure 6 red arrows). It is interesting to note the location of the 27 gene families with unknown functions chosen for characterization in the present study. Six of these gene families, ECTV-Mos 32, 68, 75, 84, 114,123 are located centrally in the genome and are absolutely conserved in all sequenced poxviruses (Figure 6 labeled red arrows), suggesting that these genes encode proteins with essential functions in the virus life cycle. Similarly, 6 of the gene families located within this central core, ECTV-Mos 58, 59, 73, 89, 109, and 122 (Figure 6 labeled pink arrows) are conserved within all sequenced chordopoxviruses, indicating that these genes encode proteins highly advantageous to the viral life cycle within vertebrate cells. There are, however, exceptions to this trend because although ECTV-Mos 37, 38, 39 and 118 and

centrally located in the genome, these genes are conserved only within certain chordopoxviruses. This anomaly is likely not specific to the genome of ECTV because previous restriction endonuclease analyses of poxvirus genomes have shown that the central region of orthopoxviruses is highly conserved (Macket and Archard, 1975; Muller et al., 1977). Additionally, 11 of the gene families with unknown functions, ECTV-Mos 12, 18, 24, 27, 29, 31, 141, 150, 153, 160, 167, are located near the terminal regions of the genome (Figure 6 labeled green and blue arrows). Their location in the genome and conservation in a subset of sequenced chordopoxvirus genomes, principally the orthopoxviruses, suggests that these genes encode proteins that may have a role in virulence or host range restriction.

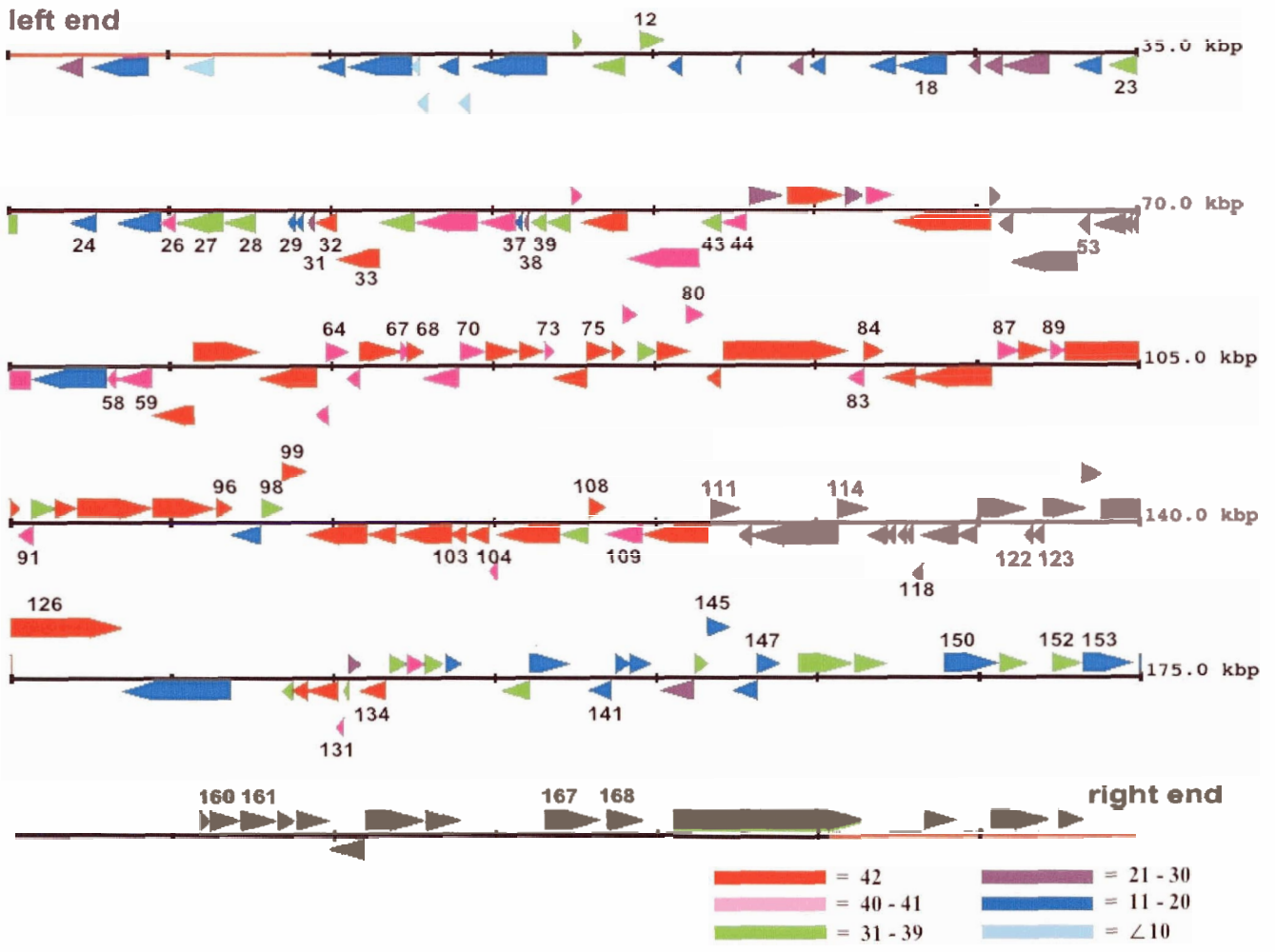

Figure 6. Organization of gene target ORFs in the ECTV-Mos genome. Coloured bars indicate ORFs and the number of viruses in which an ortholog is conserved. Red arrows indicate the 49 genes conserved in all 42 sequenced poxviruses. ORFs chosen for characterization (Table 3) have been labeled. ORFs transcribed rightward are shown above the line, and ORFs transcribed leftward are shown below the line.

Expression of recombinant proteins in E. coli

A prokaryotic expression system was chosen for expressing the recombinant proteins because the large number of proteins to be processed necessitated a relatively fast and inexpensive method to generate the large quantity of protein needed for structural analysis. The BL21-AI *E. coli* strain was utilized for these initial expression experiments because protein expression is tightly regulated from the arabinose-inducible *araBAD* promoter, keeping basal protein expression low, which is advantageous when expressing proteins that are potentially toxic in *E. coli*. In addition, this strain lacks the *lon* and Ompt T proteases, thereby reducing degradation of overexpressed heterologous proteins (Newman and Fuqua, 1999). The 28 pDEST14 expression clones generated in the Gateway cloning recombination reaction were introduced into BL21-AI *E. coli*, and the transformants treated with arabinose to induce expression of the recombinant proteins. After induction, cells were incubated for 5 hours before being disrupted using a French Pressure Cell Press. To visualize recombinant protein expression, the cell lysate was separated by SDS-PAGE and stained with Coomassie blue (Figure 7). Thirteen recombinant proteins expressed in *E. coli* including:

ECTV-Mos 064 (late transcription elongation factor)
ECTV-Mos 070 (late transcription factor 1)
ECTV-Mos 075 (involved in core packaging and transcription)
ECTV-Mos 080 (RNA polymerase subunit 22)
ECTV-Mos 087 (late transcription factor 4)
ECTV-Mos 096 (RNA polymerase subunit 18)
ECTV-Mos 108 (RNA polymerase subunit 19)
ECTV-Mos 109 (unknown)
ECTV-Mos 111 (intermediate transcription factor 3-small subunit)

ECTV-Mos 118 (unknown)
ECTV-Mos 134 (ATPase)
ECTV-Mos 141 (profilin homolog)
ECTV-Mos 145 (interleukin-1 signaling inhibitor)
ECTV-Mos 147 (thymidylate kinase)

Interestingly, *E .coli* transformed with the pDEST14 expression clone containing the ECTV-Mos 147 gene encoding thymidylate kinase exhibited slower growth compared to other cultures after induction of recombinant protein expression (data not shown) and is consistent with previous observations (Hughes et al., 1991; Su and Sclafani, 1991). Although bacteria also encode a thymidylate kinase, overexpression of the poxviral kinase or overexpression of the thymidylate kinase in general, appears to be toxic to bacteria. Observed sizes of overexpressed proteins were consistent with predicted protein sizes, except in the case of ECTV-Mos 087, which had a predicted protein size of 24 kDa and an observed protein size of 35 kDa. The ability of ECTV-Mos 087, virion late transcription factor 4, to self-interact has just recently been described by Dellis et al., 2004 and is suggested to be integral to the function of the protein during transcription. Therefore, the 35 kDa band is most likely an ECTV-Mos 087 protein dimer, although this conjecture must be confirmed using mass spectrometry in future experiments. Notably, the transcription factors and the RNA polymerase subunits expressed exceptionally well. All overexpressed proteins were confirmed to contain a histidine tag by performing a western blot on cell lysate using mouse monoclonal anti-histidine primary antibodies and goat anti-mouse IRDye 800 conjugated secondary antibodies (data not shown).

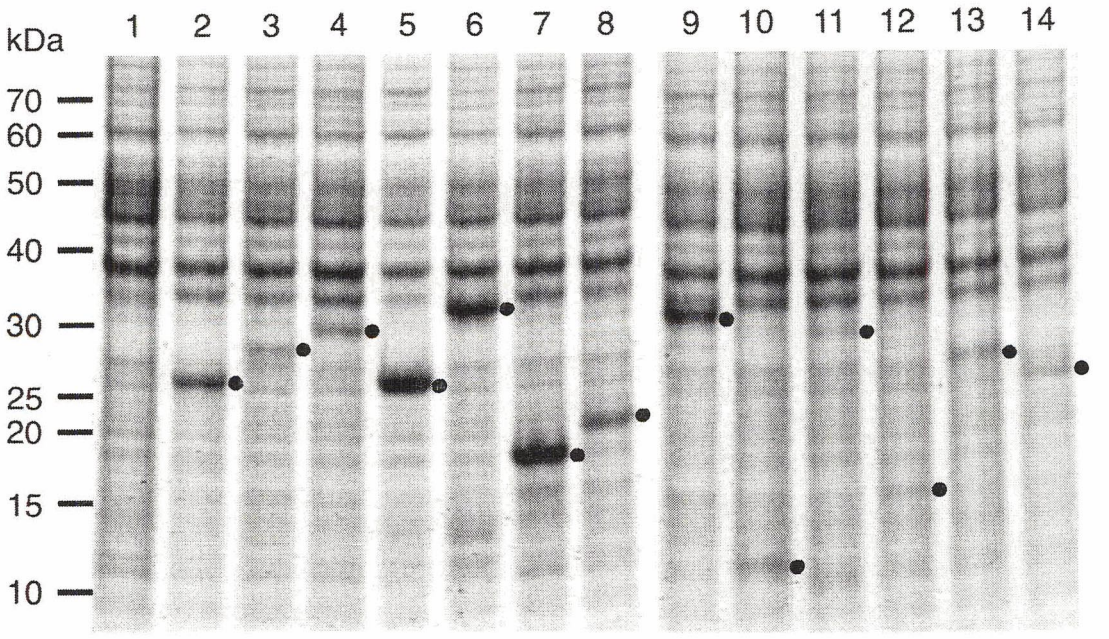

Figure 7. SDS-PAGE analysis of recombinant protein expression in *E. coli.* Five hours after induction of recombinant protein expression cells were lysed, and proteins were separated by SDS-PAGE and stained with Coomassie blue. Overexpressed proteins can be seen as unique bands beside the dots at the indicated molecular weights. Lane 1, uninduced cells (negative control). Lane 2, ECTV-Mos 064 at 27 kDa. Lane 3, ECTV-Mos 070 at 29 kDa. Lane 4, ECTV-Mos 075 at 31 kDa. Lane 5, ECTV-Mos 080 at 27 kDa. Lane 6, ECTV-Mos 087 at 35 kDa. Lane 7, ECTV-Mos 096 at 19 kDa. Lane 8, ECTV-Mos 108 at 23 kDa. Lane 9, ECTV-Mos 111 at 35 kDa. Lane 10, ECTV-Mos 118 at 12 kDa. Lane 11, ECTV-Mos 134 seen as a faint band at 31 kDa. Lane 12, ECTV-Mos 141 at 16 kDa. Lane 13, ECTV-Mos 145 at 29 kDa. Lane 14, ECTV-Mos 147 at 27 kDa.

To determine the solubility of the overexpressed proteins in the bacterial cells, the cell lysate was clarified by centrifugation to remove insoluble material. Clarified cell extract was separated by SDS-PAGE and stained with Coomassie blue (data not shown). Of the 13 proteins that expressed in *E. coli,* only four were found to be soluble: ECTV-Mos 070,

087, 108 and 141. The insoluble proteins were most likely contained within inclusion bodies, which are aggregates of unfolded protein in the cellular cytoplasm. Inclusion body formation is a common problem when overexpressing proteins in bacteria (Stevens, 2000), and is documented as particularly problematic when overexpressing poxvirus proteins (McDonald and Traktman, 1994; Slabaugh et al., 1993; Stuart et al., 1993). Several strategies were attempted to improve protein solubility (Stevens, 2000); including cooling cultures on ice to 25°C prior to induction of protein expression, inducing protein expression with half of the recommended amount of arabinose, and growing bacteria at 25°C-28°C overnight after induction. These strategies were aimed at decreasing the rate of bacterial growth and recombinant protein production, thereby decreasing inclusion body formation. These attempts were met with limited success, however, improving solubility to at most 10% (data not shown). Further experiments are required to optimize protein expression conditions to decrease or eliminate inclusion body formation. Alternatively, other expression systems, more amenable to the expression of poxvirus proteins, such as a baculovirus expression system or *in vitro* transcription/translation, could be sought and tested. The *E. coli* expression system, although not ideal for the overexpression of poxvirus proteins, was successfully employed to quickly screen a large number of proteins that could be expressed in a soluble form in an inexpensive expression system.

Purification of ECTV-Mos 141 protein, a profilin homolog

Of the 4 soluble recombinant proteins expressed in *E. coli* (Figure 7), ECTV-Mos 141, encoding a profilin homolog, has been the least studied and we therefore decided to focus

efforts on further characterizing this protein. Two papers published in the early 1990's (Machesky et al., 1994; Blasco et al., 1991) identified this family as homologous to cellular profilin, an actin-binding protein. Despite this initial characterization, however, the function of the poxvirus profilin homolog during natural infection is still unknown, and elucidating its function provides an opportunity to describe novel aspects of poxvirus biology. To begin structural analysis of the profilin homolog, ECTV-Mos 141 was purified to near homogeneity on a metal chelating column (Figure 8A). The apparent molecular mass of 16 kDa was consistent with the predicted molecular mass of 16.2 kDa; however, a second band at approximately 29 kDa was also present, suggesting self-association of the ECTV-Mos 141 protein. To confirm that the purified protein was ECTV-Mos 141, and to determine if the band at 29 kDa could be an ECTV-Mos 141 protein dimer, a western blot was performed on the purified protein using monoclonal mouse anti-histidine primary antibodies and rabbit anti-mouse IRDye 800 conjugated secondary antibodies (Figure 8B). Immunoreactive bands present on the blot at both 16 kDa and 29 kDa confirmed that histidine tagged ECTV-Mos 141 was purified, and suggests that this protein may form highly stable protein dimers, a characteristic of the protein that has not been described previously. A further experiment in which the 29 kDa band is excised from an SDS-PAGE gel and analyzed by mass spectrometry is needed to identify the proteins composing the band and to discount the possibility that ECTV-Mos 141 is associating with a bacterial protein of approximately the same size. Detailed protocols for the expression and purification of ECTV-Mos 141 were sent to collaborators at the University of Alberta where the structure of the protein will be determined by nuclear magnetic resonance (NMR).

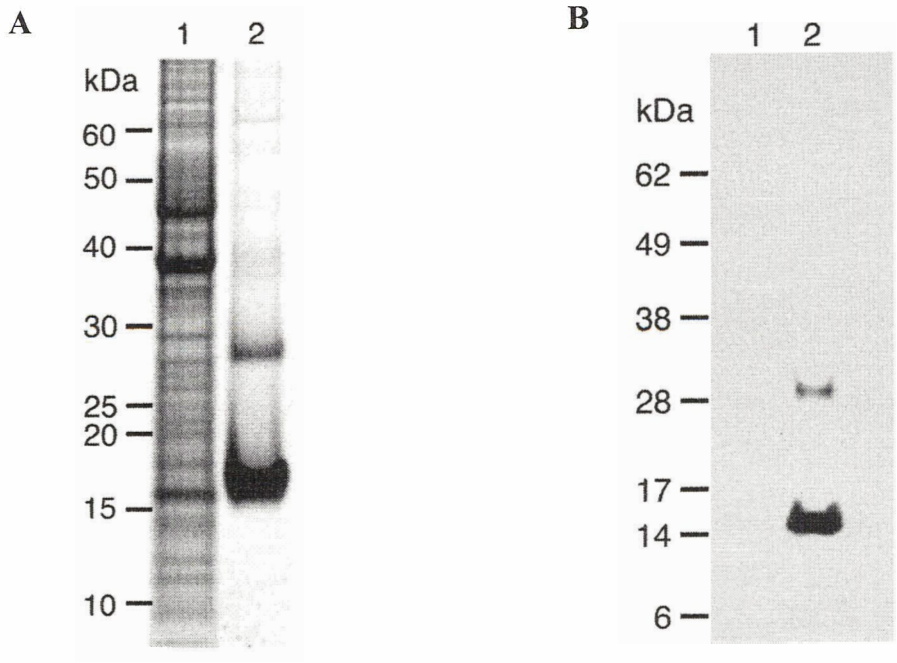

Figure 8. SDS-PAGE and western blot analysis of purified ECTV-Mos 141 protein. BL21-AI *E. coli* cells were transformed with pDEST14 expression clones carrying the histidine-tagged ECTV-Mos 141 gene. Recombinant protein expression was induced in broth cultures by addition of L-arabinose, and cultures were incubated overnight at 28°C. Cells were harvested, lysed and recombinant ECTV-Mos 141 was purified on a metal chelating column. **A.** Proteins were separated by SDS-PAGE and stained with Coomassie blue. Lane 1, whole cell lysate of BL21-AI *E. coli* cells expressing recombinant ECTV-Mos 141 at 16 kDa. Lane 2, purified ECTV-Mos 141 following elution of the protein off of the nickel chelating column. Two prominent bands are present, one at 16 kDa and the other at approximately 29 kDa. **B.** Western blot analysis of purified, ECTV-Mos 141 protein following separation by SDS-PAGE and transfer to a nitrocellulose membrane. Immunoblot was performed using mouse monoclonal anti-histidine primary antibodies and rabbit anti-mouse IRDye 800 conjugated secondary antibodies and was visualized using the Odyssey Infrared Imaging System. Lane 1, whole cell lysate of uninduced BL21-AI *E. coli* cells (negative control). No immunoreactive bands present. Lane 2, purified ECTV-Mos 141 protein showing immunoreactive bands at 16 kDa and 29 kDa.

Analysis of the orthopoxvirus profilin homolog protein family

Although the central region of orthopoxvirus genomes is highly conserved and displays a high degree of sequence identity at the amino acid level, the terminal regions of the genome are less well conserved (Macket and Archard, 1979; Muller et al., 1977). These variable regions in orthopoxvirus genomes contain deletions and insertions in one genome relative to the other, determining the species specific gene complement that is responsible for the virus host adaptation, virulence and ability to interfere with the host's defense machinery (Seet et al., 2003). ECTV-Mos 141 is located near the right hand terminal region in the ECTV-Mos genome (Figure 6). The extent of sequence conservation of the ECTV-Mos profilin homolog with orthologs in other orthopoxviruses was investigated by constructing an alignment of the protein family with sequences (Table 6) retrieved from the VOCs database (Upton et al., 2003).

Virus name	Gene name	GenBank ID	Protein ID
VARV-Bsh	A45R	439066	AAA60897.1
VARV-GAR	A50R	9633348	NP_050452.1
VARV-Ind	A47R	9627674	NP_042197.1
VACV-MVA	154R	2772795	AAB96534.1
VACV-Cop	A42R	335521	NP_063836.1
VACV-Tan	TA53R	6969841	AAF34053.1
VACV-WR	167	29692273	AA089446.1
VACV-Acambis	156	47088482	AAT10552.1
MPXV-Zre	A42R	17975065	NP_536579.1
MPXV-WRAIR	146	Not in GenBank	------
CMLV-M96	161	18640395	NP_570551.1
CMLV-CMS	158R	19718132	AAG37657.1
ECTV-Mos	141	22164747	NP_671660.1
ECTV-Nav	164	Not in GenBank	------
RPXV-Utr	150	44971513	AA649863.1
CPXV-BR	179	20178540	NP_619961.1
CPXV-GRI	A44R	30519536	CAD90711.1

Table 6. The poxvirus profilin homolog protein family. Columns: Virus name, abbreviation of virus name and strain; Gene name, name of gene in virus strain; GenBank ID, gene identification no. in GenBank; Protein ID, protein identification in NCBI. VARV (variola virus), VACV (vaccinia virus), MPXV (monkeypox virus), CMLV (camelpox virus), ECTV (ectromelia virus), RPXV (rabbitpox virus) and CPXV (cowpox virus).

The protein sequences were aligned using the ClustalW (Thompson et al., 1994) sequence alignment program (Figure 9). The amino acid sequences encoding the profilin homolog are 92% identical, excluding a five amino acid deletion in VACV-MVA and VACV-Acambis. The protein sequence is remarkably well conserved considering that in the conserved central region of the genome, ECTV-Mos shares 96-97% amino acid identity with VACV-Cop, VARV-Bsh and CPXV-BR (Chen et al., 2003). The

conservation of the protein in all sequenced orthopoxviruses in addition to the high sequence identity between orthologs suggests that this protein does perform a function during viral infection. Additionally, the situation of the gene in the variable, terminal regions of the orthopoxvirus genome suggests that the protein may perform a function in the biological specificity of the infection.

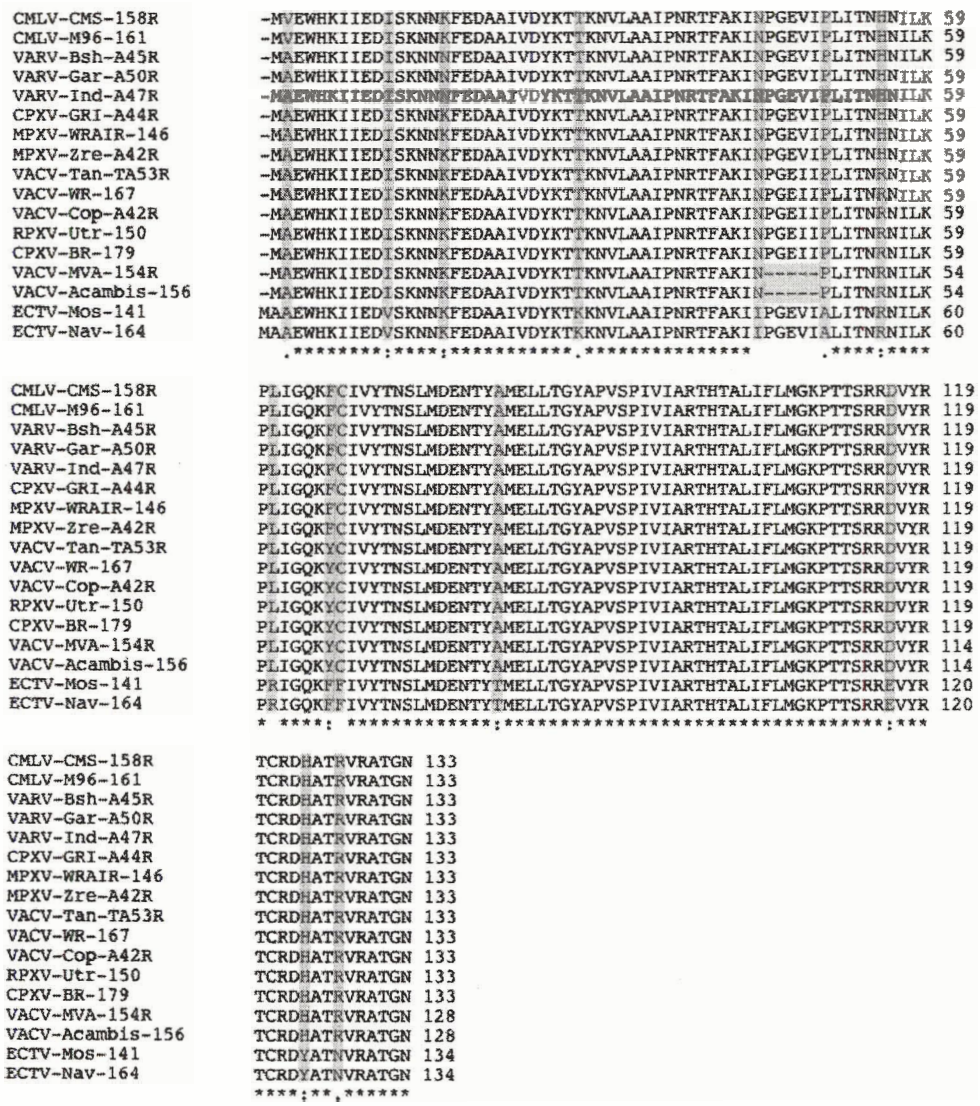

Figure 9. Protein sequence alignment of the orthopoxvirus profilin homolog protein family. The alignment was constructed using ClustalW. "*" indicates identical amino acid residues, ":" indicates conserved substitutions, "." indicates semi-conserved substitutions. Differences in amino acid residues are shaded.

Homology model of ECTV-Mos 141 protein

A 3-dimensional structure for the poxvirus profilin homolog has not yet been determined, however, the structures for a number of profilins, including both bovine (Cedergren-Zeppezauer et al., 1994) and human (Metzler et al., 1995) profilin have been solved. A homology model of the ECTV-Mos 141 protein (Figure 10B), was constructed in SWISS-MODEL (Schwede et al., 2003) using four human and bovine profilin template sequences: human profilin crystallized in high salt and low salt (1FIL and 1FIK, respectively), human profilin NMR (1PFL), and bovine profilin bound with actin (1HLU). Although the viral profilin homolog shares only 30% sequence identity with human and bovine profilin, the resulting model suggests that the three-dimensional structure of the protein is conserved and displays many of the features of a characteristic profilin fold, consisting of 4 alpha helices and 7 beta sheets (Figure 10B). This is consistent with previous reports that demonstrate profilins maintain very similar three-dimensional structures even if the amino acid sequence is poorly conserved between organisms (Mahoney et al., 1997). Two obvious differences between the structure of the template proteins and the model are a lack of alpha helix 3 and a shortened loop between the fifth and sixth beta sheets in ECTV-Mos 141. Absence of amino acid residues in ECTV-Mos 141 at positions that correspond to residues 57-60 and 91-93 in the mammalian profilins are the cause of these two structural differences.

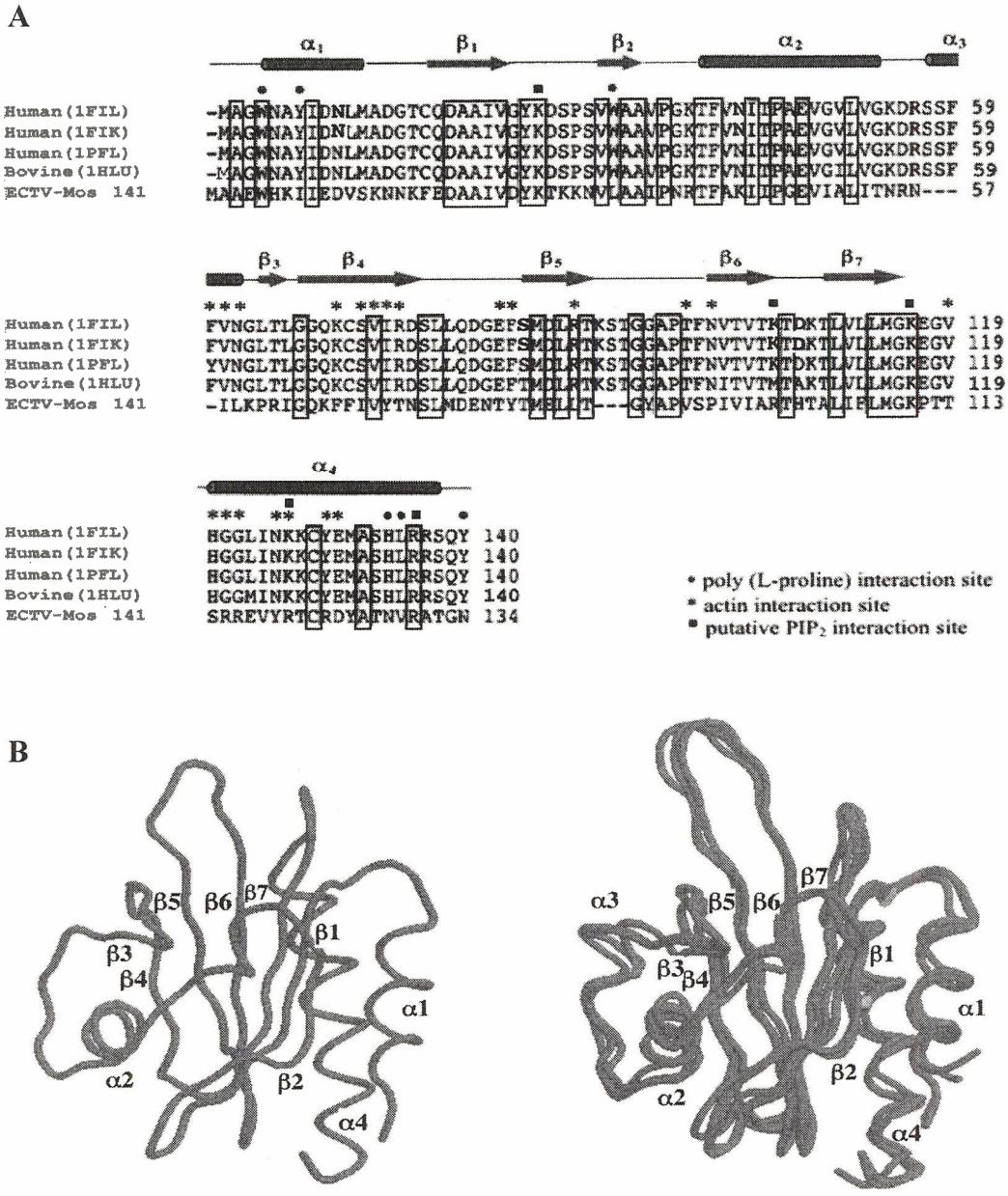

Figure 10. Homology model of ECTV-Mos 141 protein. **A**. Multiple sequence alignment of profilin protein sequences from human (1FIL, 1FIK, 1PFL), bovine (1HLU) and ECTV-Mos (NP_671660). Absolutely conserved residues are boxed. Residues implicated in secondary structure formation, and poly (L-proline), actin and PIP_2 interaction are indicated. **B**. Homology model of ECTV-Mos 141 (left) compared to known structures of template proteins (right). Secondary structural elements are labeled, "α" alpha helix, "β" beta sheet.

All known cellular profilins bind actin monomers, phosphatidylinositol 4,5-bisphosphate (PIP_2) and poly (L-proline) sequences (Witke, 2004). The poxvirus profilin homolog has been shown to have a similar affinity for PIP_2 as that of cellular profilin, however, it has a low affinity for actin monomers and no detectable affinity for poly (L-proline) (Machesky et al., 1994). To determine the reason for the observed differences and similarities in binding affinities for these ligands, the residues implicated in forming secondary structural elements and those known to be involved in binding actin, PIP_2 and phosphoinositides labeled in mammalian profilin are labeled on the multiple sequence alignment used in the construction of the ECTV-Mos 141 homology model (Figure 10A).

Residues that have been shown to be important for actin interaction in bovine profilin have been marked with an asterix, "*" (Figure 10A) and are bovine F59, V60, N61, K69, S71, V72, I73, R74, E82, F83, R88, T97, N99, V118, H119, G121, M122, N125, K125, Y128, and R129 (Schutt et al., 1993). The ECTV-Mos profilin homolog sequence displays important differences in several of these residues. ECTV-Mos R115 corresponds to a highly conserved glycine at position 121 in the α-helix of bovine profilin that contacts actin directly. The bulky side chain of this arginine residue could prevent close contact between the two proteins. Similarly, the large side chains of ECTV-Mos Y81 and Y119, compared to bovine F83 and N125, could interfere sterically with binding to actin if the backbone conformation of the two profilins were the same.

Mammalian profilins have a highly conserved hydrophobic patch of amino acids, which are predominantly aromatic, brought together by the folding of the polypeptide chain and

are identified in Figure 10A by a dot, "●". These aromatic residues have been directly implicated in the binding of poly (L-proline) and correspond to bovine profilin W4, Y7, W32, H134, L135, and Y140 (Bjorkegren et al., 1993). The ECTV-Mos profilin homolog lacks four of these aromatic residues. Bovine profilin has a tyrosine instead of an isoleucine at ECTV-Mos position 8, a tryptophan instead of leucine at ECTV-Mos 141 position 33, a histidine instead of an asparagine at ECTV-Mos 141 position 128, and a tyrosine instead of an asparagine at ECTV-Mos 141 position 134.

Although the PIP_2 binding site on profilin is not as well defined as that for actin or poly (L-proline), five residues in human profilin that form a highly positive electrostatic surface potential have been implicated in PIP_2 binding (Skare and Karlsson, 2002) and are identified in Figure 10A with squares, "■". These residues are K26, K105, K116, K126 and R136 in human profilin, which correspond to residues K27, R99, K110, R120 and R130 in ECTV-Mos 141. If the ECTV-Mos profilin homolog has the same three-dimensional arrangement as that for human profilin, these amino acid residues will form a surface with a highly positive electrostatic surface potential, suitable for binding of PIP_2.

Coimmunoprecipitation of ECTV-Mos 141 and ECTV-Mos 141-interacting proteins from poxvirus-infected cells

To determine what, if any, proteins interact with ECTV-Mos 141 *in vivo* during viral infection, an immunoprecipitation was performed to isolate ECTV-Mos 141 and ECTV-Mos 141-interacting proteins from poxvirus infected cells. A vaccinia virus (vTF7-3)

transient expression system was used to overexpress histidine-tagged ECTV-Mos 141 in BS-C-1 cells, an African green monkey kidney cell line. BS-C-1 cells were transfected with pDEST14 expression plasmids containing the histidine-tagged ECTV-Mos 141 gene under the control of the T7 promoter and were then infected with recombinant VACV-WR expressing the T7 RNA polymerase (vTF7-3). At a late time during infection (~16 hours) cells were lysed under non-denaturing conditions and histidine-tagged ECTV-Mos 141 and ECTV-Mos 141-interacting proteins were isolated by incubating Protein G-Plus agarose and mouse monoclonal anti-histidine antibodies with the cell lysate. A control, in which BS-C-1 cells were transfected with herring sperm DNA instead of pDEST14 expression plasmid, was run in parallel to identity proteins interacting non-specifically with the antibodies or the Protein G-Plus agarose. In future experiments, however, the pDEST14 plasmid containing no insert should be used as control DNA. Immunoprecipitated proteins were separated by SDS-PAGE and stained with Coomassie blue (Figure 11). Proteins interacting specifically with ECTV-Mos 141 were identified on the gel, excised, and sent for identification by mass spectrometry analysis.

Coimmunoprecipitated proteins were identified as VACV-WR 148, an 84 kDa viral A-type inclusion protein (protein accession no. AA089427.1), and α tropomyosin, a 38 kDa cellular actin-binding protein (protein accession no. AAA61226). In addition, the capture of ECTV-Mos 141 was confirmed. One band present at approximately 29 kDa in Lane 2 labeled as "Unknown" was not excised from the gel for identification by mass spectrometry, but may be an ECTV-Mos 141 dimer, as self-association of the protein was

also observed in Figure 8 . The interaction of ECTV-Mos 141 with cellular tropomyosin and the viral A-type inclusion protein observed in this experiment is novel.

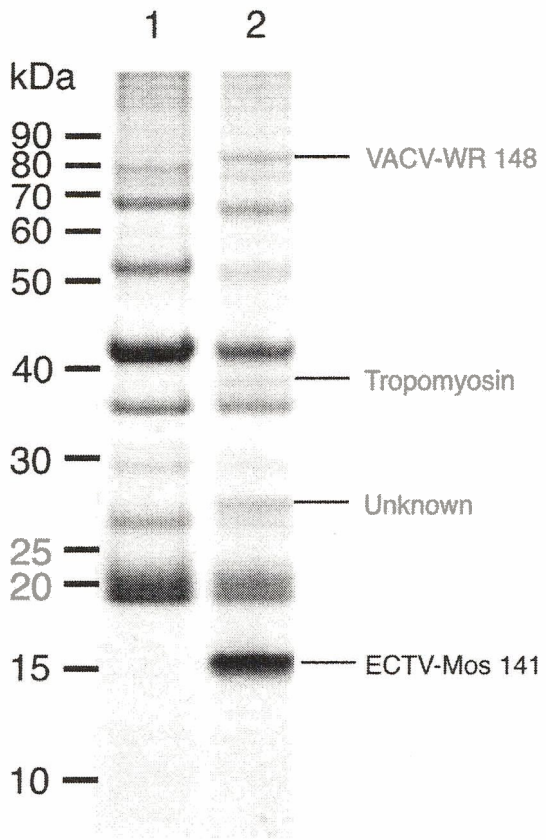

Figure 11. Coimmunoprecipitation and identification of proteins interacting with ECTV-Mos 141 during viral infection. A vTF7-3 transient expression system was used to overexpress histidine-tagged ECTV-Mos 141 in BS-C-1 cells. Mouse monoclonal anti-histidine antibodies and Protein G-Plus agarose were used to immunoprecipitate ECTV-Mos 141 and ECTV-Mos 141-interacting proteins from cell lysate. Proteins were separated by SDS-PAGE and stained with Coomassie blue. Lane 1, proteins interacting non-specifically with antibodies and agarose were identified by performing the immunoprecipitation on cell lysate containing no recombinant ECTV-Mos 141(negative control). Lane 2, proteins isolated from immunoprecipitation on cells expressing recombinant ECTV-Mos 141. Three bands at 16 kDa, 38 kDa and 84 kDa were excised from the gel and identified by mass spectrometry as indicated.

As the poxvirus profilin homolog is known to bind actin weakly (Machesky et al., 1994), there was a possibility that actin also coimmunoprecipitated with ECTV-Mos 141, and that tropomyosin, which is an actin-binding protein, may have been pulled-down with actin and not through a direct interaction with ECTV-Mos 141. To determine if actin did coimmunoprecipitate, a western blot was performed using polyclonal anti-actin primary antibodies and goat anti-rabbit IRDye 800 conjugated secondary antibodies and was visualized using the Odyssey Infrared Imaging System (Figure 12). Actin was not detected in the coimmunoprecipitated proteins, suggesting that tropomyosin co-immunoprecipitated through a direct interaction with ECTV-Mos 141. An immunoreactive band in Lane 3 at approximately 17 kDa, corresponds to the molecular mass of Protein G. It appears as though even after separation on an SDS-PAGE gel and transfer to a membrane under denaturing conditions, this protein retains its ability to bind to antibodies.

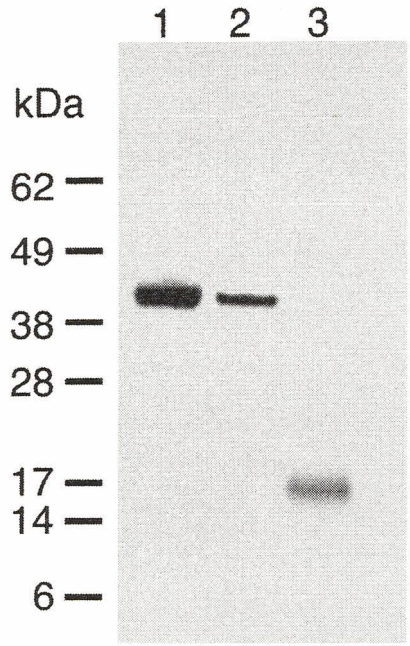

Figure 12. Western blot for detection of actin in coimmunoprecipitated proteins. Lane 1, purified rabbit muscle actin showing an immunoreactive band at 42 kDa (positive control). Lane 2, cell lysate from which ECTV-Mos 141 and ECTV-Mos 141-interacting proteins were isolated. An immunoreactive band is present at approximately 42 kDa confirming the presence of actin in the cell lysate (positive control). Lane 3, proteins that coimmunoprecipitated with ECTV-Mos 141. Absence of an immunoreactive band at 42 kDa indicating no actin is present.

ECTV-Mos 141 and tropomyosin interact directly

To eliminate the possibility that the interaction between tropomyosin and the ECTV-Mos profilin homolog detected in the immunoprecipitation experiment was mediated through the histidine tag on the ECTV-Mos 141 protein, a far western analysis was performed to show specific interaction of the proteins. Equal amounts of purified porcine muscle

tropomyosin, ECTV-Mos 141, rabbit muscle actin, relA (a histidine-tagged bacterial enzyme), and bovine serum albumin (BSA) protein were separated by SDS-PAGE and transferred to a nitrocellulose membrane. Proteins were then refolded on the membrane though a guanidine hydrochloride denaturation and renaturation process. The membrane was incubated with purified porcine muscle tropomyosin diluted in interaction buffer and protein-protein interactions were allowed to form overnight at 4°C. A western blot using mouse monoclonal anti-tropomyosin primary antibodies and rabbit anti-mouse IRDye 800 conjugated secondary antibodies was performed to detect tropomyosin localization on the membrane. The blot was visualized using the Odyssey Infrared Imaging System as shown (Figure 13A). Tropomyosin interacts with ECTV-Mos 141, as shown by the presence of an immunoreactive band at 15 kDa in Lane 2, but does not interact with histidine-tagged RelA in Lane 5 or BSA in Lane 4. These results suggest that the interaction between ECTV-Mos 141 and tropomyosin is not mediated through the histidine tag on ECTV-Mos 141 and must represent interaction between functional domains of the proteins. An interaction between tropomyosin and the ECTV-Mos 141 dimer at 29 kDa was not detected, however, this may be due to the relatively small amount of the dimerized protein present on the gel. To control for the amount of protein loaded onto the SDS-PAGE gel for the far western analysis, a second gel was loaded with equal amounts of the same proteins and was stained with Coomassie blue (Figure 13B). This confirms that any protein interactions, or lack thereof, were not the result of over- or under-loading of the gel.

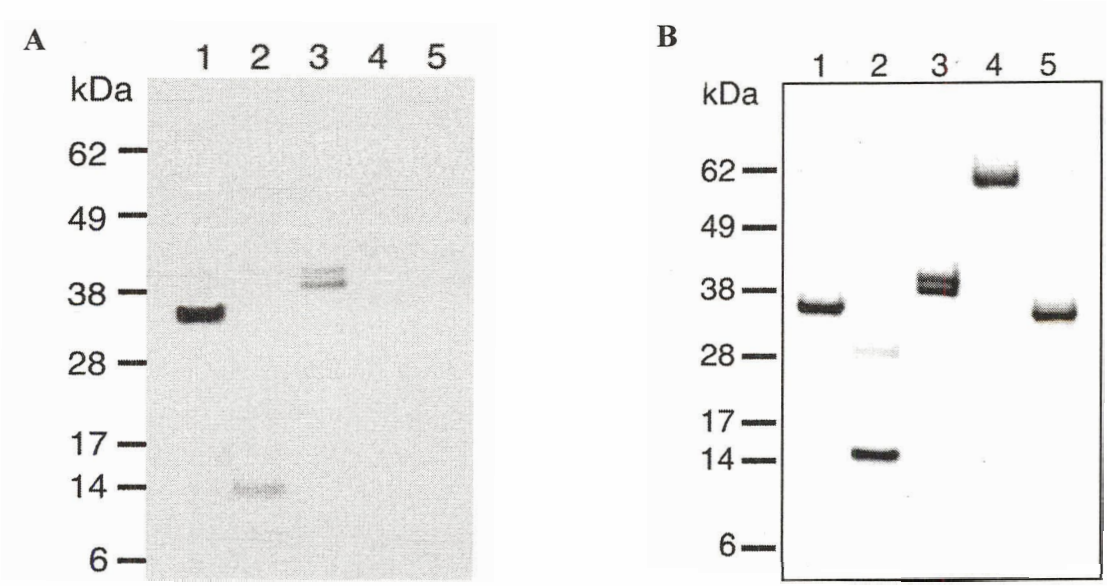

Figure 13. Far western analysis of the interaction between ECTV-Mos 141 and tropomyosin. **A.** Far western analysis showing specific interaction between ECTV-Mos 141 and tropomyosin. Proteins were separated by SDS-PAGE, transferred to a nitrocellulose membrane and refolded. The membrane was incubated with purified porcine muscle tropomyosin overnight, and tropomyosin localization on the membrane was detected with mouse anti-tropomyosin primary antibodies and rabbit anti-mouse IRDye conjugated secondary antibodies. The blot was visualized with the Odyssey Infrared Imaging System. Lane 1, purified porcine muscle tropomyosin showing an immunoreactive band at 37 kDa (positive control). Lane 2, purified ECTV-Mos 141 showing an immunoreactive band at 15 kDa, representing tropomyosin – ECTV-Mos 141 interaction. Lane 3, purified rabbit muscle actin showing immunoreactive bands at 42 kDa and 43 kDa, representing tropomyosin interaction with different actin isoforms, respectively (positive control). Lane 4, and Lane 5 contain histidine-tagged relA and bovine serum albumin, respectively. No immunoreactive bands are present (negative control). **B.** SDS-PAGE separated proteins stained with Coomassie blue. Lane assignments are as described in A. Equal amounts of protein were loaded in each lane.

Analysis of Orthopoxvirus A-type inclusion proteins

Results from the coimmunoprecipitation experiment (Figure 11) suggest that the ECTV-Mos profilin homolog interacts *in vivo* with VACV-WR 148 (A-type inclusion protein) during viral infection. All known orthopoxviruses encode an A-type inclusion protein that is expressed late in infection, at roughly the same time as the profilin homolog (Meyer and Rziha, 1993). A-type inclusion proteins are present in all orthopoxviruses in one of two forms; a full-length protein found in cowpox virus (CPXV) and ECTV, and a truncated form of the protein found in most other orthopoxviruses. Full-length A-type inclusion proteins form large bodies in the cytoplasm that may contain IMV, and are thought to be important in survival and dissemination of the virions (Ichihashi et al., 1971). The truncated A-type inclusion proteins, however, have no known function, although the conservation of these truncated genes suggests the protein does confer an advantage to the virus during its life cycle. A protein sequence alignment of three A-type inclusion protein orthologs, from CPXV-BR, ECTV-Mos, and VACV-WR was performed using the ClustalW multiple sequence alignment program (data not shown). A graphical representation of the sequence alignment is shown in Figure 14.

CPXV encodes the full-length, complete A-type inclusion protein, and consists of a large amino terminus, 10 tandem repeats, and a smaller carboxy terminus (Funahashi et al., 1988). ECTV encodes the only other known full-length A-type inclusion protein, however, six of the tandem repeats have been deleted from the centre of the protein and the carboxy terminus of the protein shares only 60% sequence identity with CPXV (Osterrieder et al., 1993). All poxvirus A-type inclusion proteins have a highly conserved

amino terminus, sharing >70% sequence identity (data not shown). The A-type inclusion proteins encoded by VACV (de Carlos and Paez, 1991), camelpox virus (CMPXV) (Meter and Rziha, 1993), variola virus (VARV) (Fenner et al., 1989) and monkeypox virus (MPXV) (Fenner et al., 1989) are truncated within the first four tandem repeats (Osterrieder, 1994).

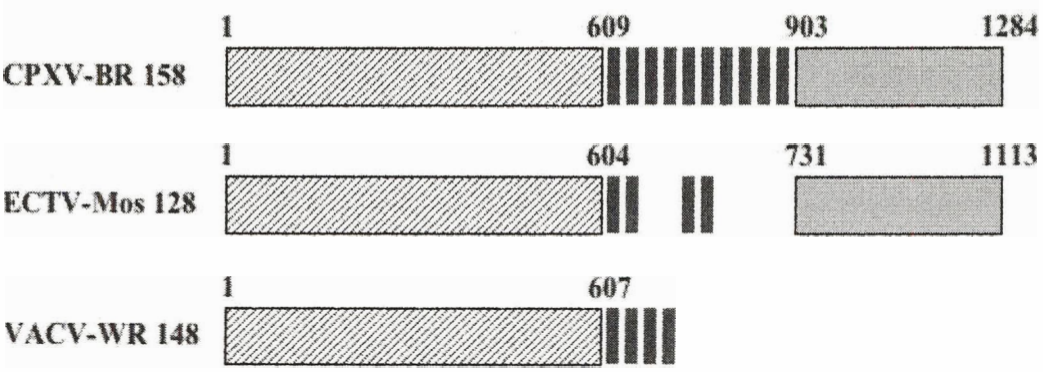

Figure 14. Graphical representation of a protein sequence alignment between A-type inclusion proteins: CPXV-BR 158 (protein accession no. NP_671647.1), ECTV-Mos 128 (protein accession no. NP_671647.1) and VACV-WR 148 (protein accession no. AA089427.1). The amino termini of the proteins (striped bar) are well conserved, however, proteins differ in conservation of 10 tandem repeats (black bars) and presence of a carboxy terminus (solid grey bar). Numbers indicate amino acid residues at the beginning and end of the amino and carboxy termini. Tandem repeats are 27 - 31 amino acid residues in length.

Localization of the ECTV-Mos profilin homolog and viral A-type inclusion proteins in vivo

The coimmunoprecipitation of the ECTV-Mos profilin homolog and VACV-WR 148 ATI protein (Figure 11), suggested that the proteins interact *in vivo* during viral infection. To determine if ECTV-Mos 141 and VACV-WR 148 colocalize in poxvirus-infected cells, epitope-tagged versions of the proteins were overexpressed *in vivo* using a vTF7-3 transient expression system and localization of the proteins was investigated by indirect immunofluorescence. Hemagglutinin-tagged VACV-WR 148 and myc-tagged ECTV-Mos 141 were PCR-amplified from crude viral DNA and from viral genomic DNA fragments, respectively, incorporating epitope tags via the design of the primers (Figure 4). Histidine-tagged proteins were not used in localization experiments because this would cause a higher background staining with antibodies due to the fact that eukaryotic cells express a number of proteins containing poly-histidine (Jones et al., 2004). The epitope-tagged genes were then cloned into the pDEST14 destination vector under the control of the T7 promoter. BS-C-1 cells were transfected with equal amounts of both expression clones and then infected with vTF7-3, a recombinant vaccinia virus that expresses the T7 RNA polymerase. Cells were incubated approximately 16 hours and then fixed. Localization of myc-tagged ECTV-Mos 141 was determined by incubation of the cells with rabbit polyclonal anti-myc primary antibodies and Alexa Fluor 568 conjugated goat anti-rabbit secondary antibodies, while localization of hemagglutinin-tagged VACV-WR 148 was determined using Alexa Fluor 488 conjugated mouse monoclonal anti-hemagglutinin antibodies. Cellular and viral DNA in the infected cells was visualized by DAPI staining.

Both VACV-WR 148 (Figure 15C) and ECTV-Mos 141 (Figure 15D) are cytoplasmic proteins that are excluded from the nucleus as shown by DAPI staining (Figure 15B). The proteins appear to colocalize in higher concentrations in a least two areas in the cytoplasm (Figure 15E arrows 1 and 2). These areas could be inclusion bodies formed by the aggregation of truncated VACV-WR 148 A-type inclusion protein. The aggregation of truncated A-type inclusion proteins to form inclusion bodies has been documented previously in the literature (Patel et al., 1986) however these bodies are thought to be unstable and formed rarely. Although no photographs of such inclusion bodies have been published, they are described as being small and irregularly shaped, matching the morphology of the putative inclusion bodies in Figure 15E (arrows 1 and 2). Two areas of concentrated viral DNA (Figure 15B arrows 1 and 2) also show colocalization to the putative inclusion bodies, suggesting that although inclusion bodies formed by truncated A-type inclusion proteins are unstable, intracellular mature virions (IMV) can still be sequestered in these bodies. A viral factory, which is a discrete area in the cytoplasm that contains actively replicating viral DNA (Figure 15B arrow 4), does not colocalize to the putative inclusion bodies. Interestingly, there is a structure near the cell periphery (Figure 15E arrow 3) to which ECTV-Mos 141 and VACV-WR 148 colocalize. This structure resembles protrusions from the cell surface induced by cell associated virions (CEV) during infection that are important for the intercellular spread of the virus (Goudin et al., 2005).

Figure 15 (following page). ECTV-Mos 141 colocalizes with VACV-WR 148, a truncated A-type inclusion protein, *in vivo*. Hemagglutinin-tagged VACV-WR 148 and myc-tagged ECTV-Mos 141 were overexpressed in BS-C-1 cells using a vTF7-3 transient expression system. Cells were fixed and then stained with antibodies, as described in the text, to localize recombinant proteins. Indirect fluorescence microscopy was used to visualize and photograph the cells. **A**, control cells, infected with virus and transfected with calf thymus DNA, show little background staining with antibodies (negative control). **B**, DAPI staining of cellular nuclei and viral DNA. A viral factory is indicated by arrow 4. Discrete areas of concentrated viral DNA in the cytoplasm are indicated with arrows 1 and 2. **C** and **D**, VACV-WR 148 and ECTV-Mos 141, respectively, are cytoplasmic proteins. Arrows 1,2 and 3 indicate where proteins colocalize. **E**, merged view of panels B, C and D. Arrows 1 and 2 indicate areas where VACV-WR 148, ECTV-Mos 141 and viral DNA colocalize to putative inclusion bodies. Arrow 3 indicates where VACV-WR 148 and ECTV-Mos 141 colocalize to putative protrusions from the cell surface.

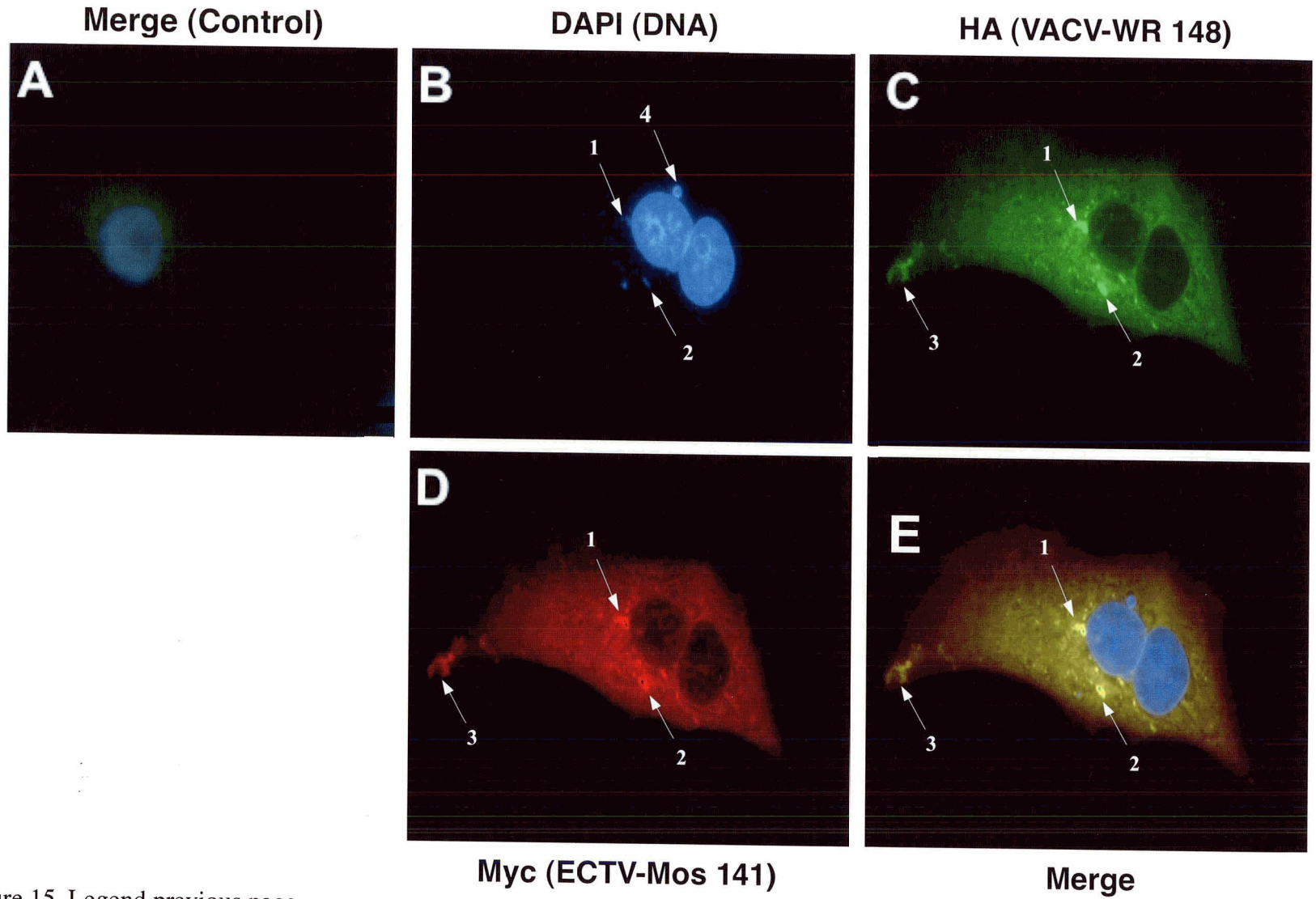

Figure 15. Legend previous page.

To further characterize the interaction between the ECTV-Mos profilin homolog and poxvirus A-type inclusion proteins, the ability of ECTV-Mos 141 to colocalize with the full-length ECTV-Mos 128 A-type inclusion protein *in vivo* was investigated. Hemagglutinin-tagged ECTV-Mos 128 was PCR-amplified from ECTV-Mos genomic DNA fragments and cloned into the pDEST14 destination vector. Hemagglutinin-tagged ECTV-Mos 128 and myc-tagged ECTV-Mos 141 were overexpressed and localized in BS-C-1 cells using the same vTF-3 transient expression system and antibodies as previously described.

ECTV-Mos 128 has been shown previously (Osterrieder et al., 1994) to form large, round inclusion bodies in the cytoplasm of the host cell, and these bodies are clearly visible in Figure 16C. The ECTV-Mos 128 A-type inclusion protein appears to be completely localized to these inclusions in the cytoplasm which are excluded from the nucleus as seen by DAPI staining (Figure 16B). Although the ECTV-Mos profilin homolog is largely colocalizing to these inclusion bodies (Figure 16D), a portion of the protein remains distributed throughout the cytoplasm suggesting that the protein may be interacting with other proteins in the cytoplasm, which is consistent with the finding that ECTV-Mos 141 also interacts with cellular tropomyosin (Figure 11). Viral DNA (Figure 16C arrows 1 and 2) does not appear to localize to the inclusion bodies.

Taken together, the results of these two immunofluorescence experiments suggest that ECTV-Mos 141 localizes to inclusion bodies formed by both truncated and full-length versions of the viral A-type inclusion protein in the cytoplasm of the host cell. As the

amino terminus and first 2 tandem repeats are the only domains shared between these two A-type inclusion proteins, it is reasonable to conclude that either, or both, of these regions on the protein contain the site of interaction with the profilin homolog. These results also confirm previous findings (Patel et al., 1986) suggesting that truncated A-type inclusion proteins have the ability to form A-type inclusion bodies. The association of ECTV-Mos 141 and IMV with these bodies, however, is a novel finding. In addition, the colocalization of the viral profilin homolog and truncated A-type inclusion protein to protrusions from the cell surface suggests that these proteins may be involved in intercellular transport of the virus.

Figure 16 (following page). ECTV-Mos 141 colocalizes with ECTV-128, a full length A-type inclusion protein, *in vivo*. Hemagglutinin-tagged ECTV-Mos 128 and myc-tagged ECTV-Mos 141 were overexpressed in virus-infected BS-C-1 cells using a vTF7-3 transient expression system. Cells were fixed and stained with antibodies, as described in the text, to localize recombinant proteins. Indirect fluorescence microscopy was used to visualize and photograph the cells. **A**, control cells, infected with virus and transfected with calf thymus DNA, show little background staining with antibodies (negative control). **B**, DAPI staining of cellular nuclei, and viral DNA. Areas containing viral DNA are indicated by arrows 1 and 2. **C**, ECTV-Mos 128 forms large inclusion bodies throughout the cytoplasm. **D**, ECTV-Mos 141 localizes to inclusion bodies but remains, in part, distributed throughout the cytoplasm. **E**, merged view of panels B, C and D showing localization of ECTV-Mos 141, but not viral DNA, to inclusion bodies.

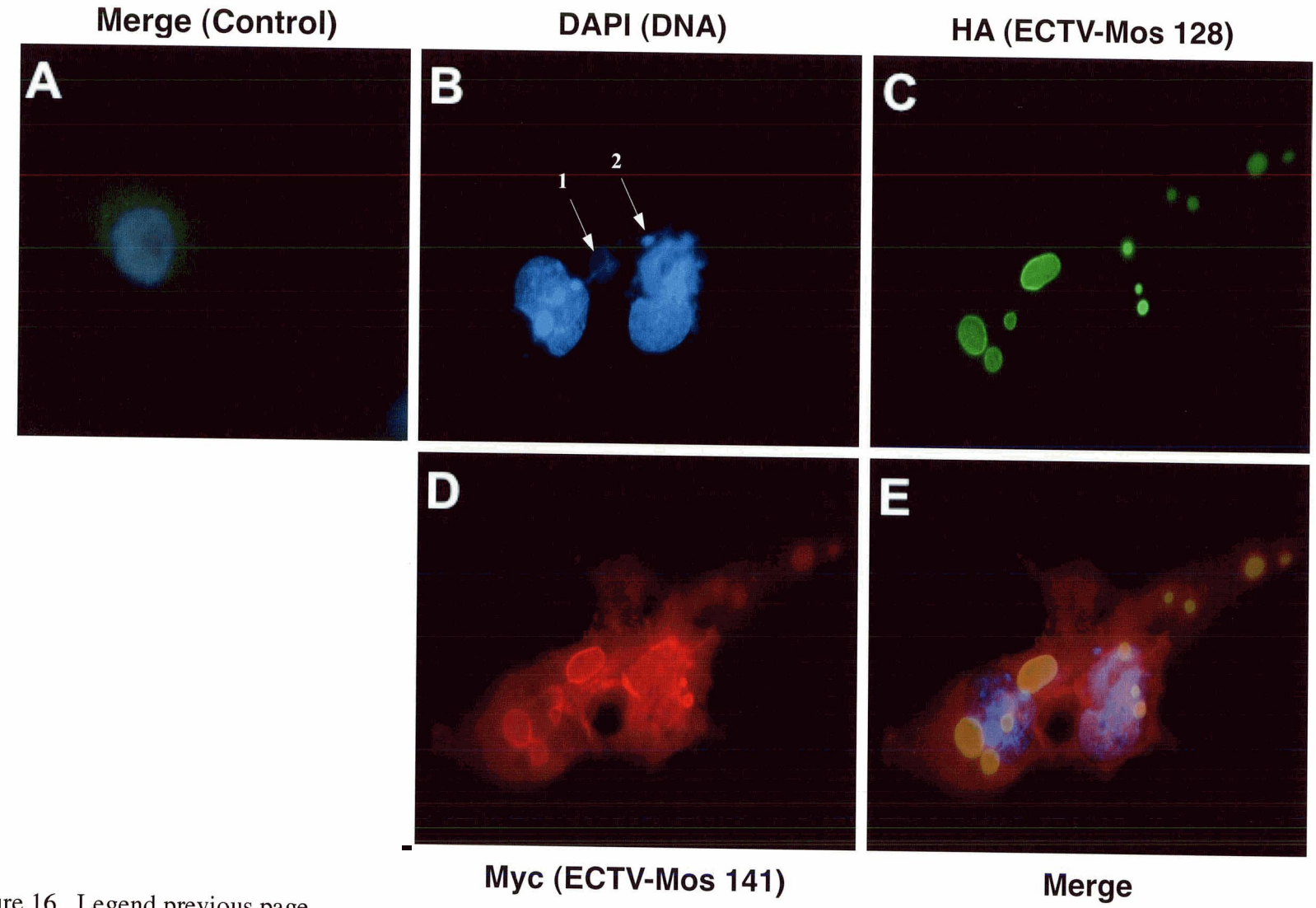

Figure 16. Legend previous page.

Localization of the ECTV-Mos profilin homolog and cellular tropomyosin in vivo

The results of the immunoprecipitation experiment (Figure 11) and far western analysis (Figure 13) suggest that the ECTV-Mos profilin homolog and cellular tropomyosin interact *in vivo* during viral infection. To investigate this interaction further, localization of the proteins in infected BS-C-1 cells was determined using indirect immunofluorescence. ECTV-Mos 141 was overexpressed in BS-C-1 cells using a vTF7-3 transient expression system and was localized using antibodies as previously described, while endogenous cellular tropomyosin was visualized using mouse monoclonal anti-tropomyosin primary antibodies and goat anti-mouse FITC conjugated secondary antibodies.

Tropomyosin is a cytoplasmic protein (Figure 17C) that is excluded from the nucleus as shown by DAPI staining (Figure 17B). The ECTV-Mos profilin homolog and endogenous cellular tropomyosin colocalize to structures resembling actin tails (Figure 17E arrow 1) and to protrusions from the cell surface (Figure 17E arrow 2). Actin tails are formed just after budding of the virus from the cell and support protrusions from the cell surface that are important for intercellular spread of the virus (Gouin et al, 2005). Interestingly, it appears as though small inclusion bodies are forming throughout the cytoplasm (Figure 17E arrow 3) by aggregation of the truncated A-type inclusion protein encoded by vTF7-3, the recombinant vaccinia virus used in the transient expression system. These inclusion bodies are more spherical than the irregularly shaped inclusion bodies formed during overexpression of the truncated A-type inclusion protein VACV-WR 148, suggesting that overexpression of the protein may affect the morphology of the

inclusion body. It would be expected that viral DNA would localize to these putative inclusion bodies, as viral DNA was shown to localize to the inclusion bodies formed by VACV-WR 148. The large amount of viral DNA present in the cytoplasm in the vicinity of the putative inclusion bodies, however, makes localization of the DNA difficult to determine with certainty.

Together, these results suggest that ECTV-Mos 141 and cellular tropomyosin interact during viral infection and that these proteins may have a role in intercellular transport of the virus.

Figure 17 (following page). ECTV-Mos 141 and cellular tropomyosin colocalize *in vivo*. Myc-tagged ECTV-Mos 141 was overexpressed in virus-infected BS-C-1 cells using a vTF7-3 transient expression system. Cells were fixed and stained with antibodies, as described in the text, to localize recombinant proteins. Indirect fluorescence microscopy was used to visualize and photograph the cells. **A**, uninfected control cells stained with anti-tropomyosin antibodies, show a relatively uniform distribution of endogenous tropomyosin throughout the cytoplasm. **B**, DAPI staining of the cellular nucleus and viral DNA. **C** and **D,** endogenous tropomyosin and ECTV-Mos 141 are distributed throughout the cytoplasm but localize to structures resembling actin tails (arrow 1) and to protrusions from the cell surface (arrow 2). ECTV-Mos 141 is also localizing to areas in the cytoplasm that resemble inclusion bodies formed by truncated A-type inclusion protein, VACV-WR-148 (arrow 3). **E**, merged view of panels B, C and D showing colocalization of tropomyosin and ECTV-Mos 141 to structures at the cell periphery, indicated by arrows 1,2. Arrow 3 indicates location of a putative inclusion body.

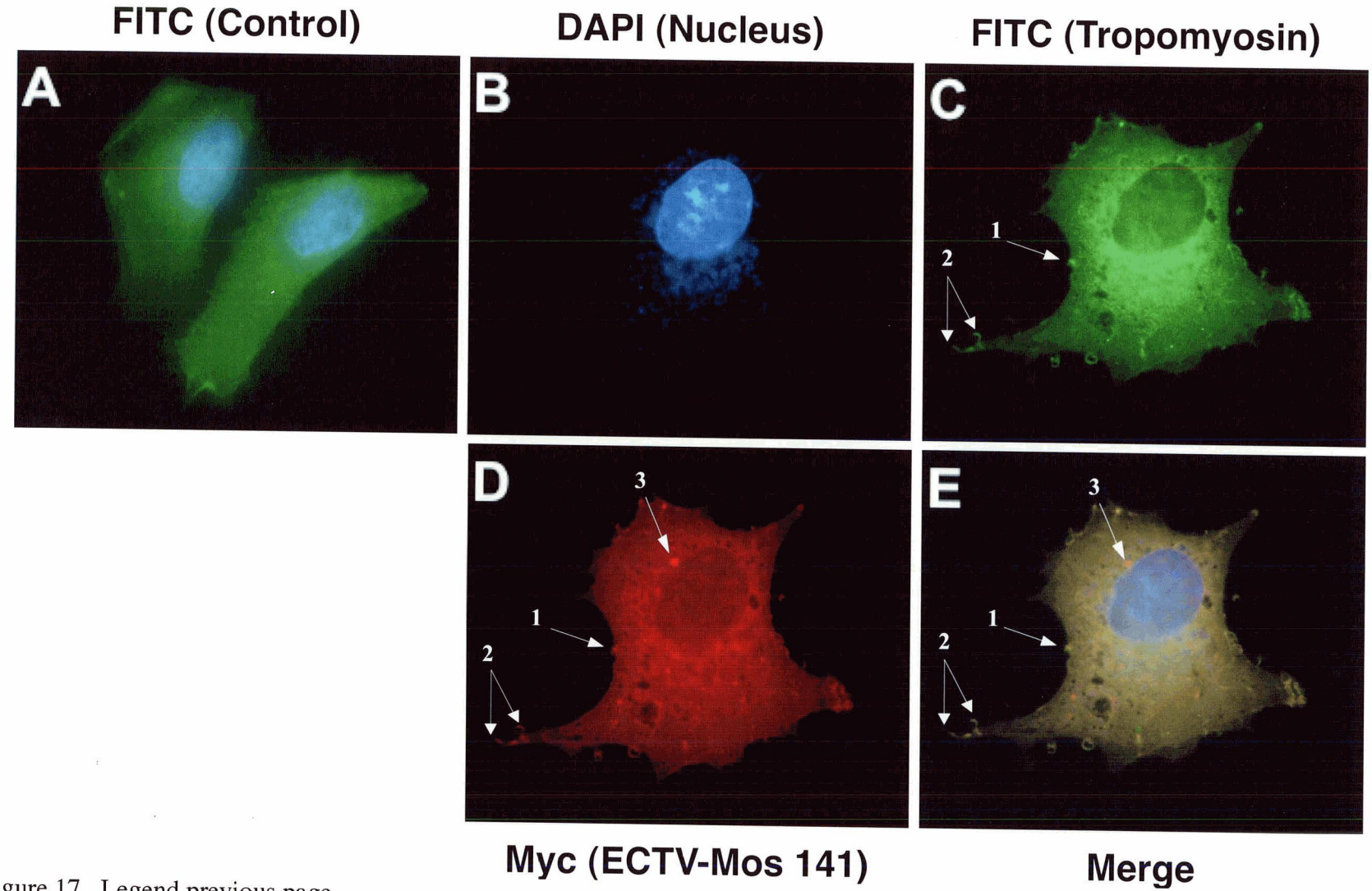

Figure 17. Legend previous page.

Chapter 4: Discussion

The goal of this thesis was to identify and begin preliminary characterization of gene families conserved between the orthopoxviruses, a genus of poxviruses containing viruses of medical and veterinary importance. The identification of fifty-six highly conserved orthopoxvirus gene families (Table 3) was achieved by coupling the large body of poxvirus genome sequence information now available with software designed specifically for poxvirus genome analysis (Upton et al., 2003). All of these families have had little or no previous characterization and approximately half have a yet unknown function. The genes encoding proteins with an unidentified function were particularly interesting because characterization of these proteins provides a unique opportunity to describe novel aspects of the virus life cycle and virus-host interactions. The localization of gene target ORFs (Figure 6) in the genome of ECTV-Mos 141 revealed that six of these families with an unknown function are absolutely conserved in all poxviruses and are located centrally within the genome, indicating an essential function for the encoded proteins. An additional six gene families with unknown function are similarly centrally located in the genome and are highly conserved within the chordopoxviruses, suggesting that the encoded protein is advantageous for viral replication in vertebrate cells. Furthermore, approximately eleven of these completely uncharacterized families are located in the terminal regions of the genome and are primarily conserved within the orthopoxviruses, indicating that these proteins may be involved in host range restriction or virulence (Johnston and McFadden, 2003; Upton et al., 2003). These results, coupled with the cloning of 28 of the gene targets (Table 5) into expression vectors, provide a

basis for further characterization of the proteins. Additionally, gene families identified in this study that are unique to the orthopoxviruses may prove to be potential drug, vaccine and detection targets.

This study focused on the preliminary characterization of ECTV-Mos 141, a gene encoding a protein homologous to mammalian profilin 1, an actin binding protein (Blasco et al., 1991). During infection, poxviruses utilize the cellular cytoskeleton to move virus components and virions to different locations throughout the cytoplasm (Ward, 2005). An intensive area of poxvirus research has been delineating the mechanisms by which these viruses are able to control the actin and microtubule cytoskeletons to facilitate their own life cycle (Newsome et al., 2004). An excellent candidate for the involvement of a viral protein in these processes would be the profilin homolog, as its cellular counterpart is known to be involved in the regulation of the actin cytoskeleton (Witke, 2004).

The profilin homolog is found exclusively within the orthopoxviruses (Table 6), and an alignment of the profilin homolog protein family demonstrates that the protein sequence is highly conserved between the viruses comprising this genus, sharing over 92% sequence identity (Figure 9). The absolute conservation of the profilin homolog in orthopoxviruses, in addition to the high degree of amino acid identity shared between the protein orthologs, suggests the protein does have a function during viral infection.

It has been known for some time that certain dsDNA viruses, including poxviruses, express proteins homologous to immune signaling molecules or receptors found in their

vertebrate hosts (Hughes and Friedman, 2005). The genes encoding these homologous proteins were most likely acquired by the virus through horizontal gene transfer from the host, and maintained as they increase the fitness of the virus (Shackelton and Holmes, 2004; Hughes and Friedman, 2004; McLysaght et al., 2003). Although many proteins essential to the viral life cycle are also shared between poxviruses and vertebrate cells, such as RNA polymerase subunits and ribonucleotide reductase, they do not show evidence of recent horizontal gene transfer and likely form part of the ancient viral genome. Interestingly, a recent evolutionary analysis of the poxvirus genome provides evidence suggesting that the gene encoding the profilin homolog was acquired by an ancestral orthopoxvirus through a horizontal gene transfer event (McLysaght et al., 2003). A BLASTp (Altschul et al., 1990) search of the NCBI protein sequence databases revealed that the ECTV-Mos profilin homolog shares a higher amino acid identity (30%) with human and bovine profilin 1than with profilin from any other organism (data not shown). These observations together suggest that the gene encoding the profilin homolog was likely acquired by an ancestral orthopoxvirus from a mammalian host in a horizontal gene transfer event.

The observation that the ECTV-Mos 141 gene is located in the terminal regions of the ECTV-Mos genome (Figure 6), in addition to evidence indicating it has been acquired by horizontal gene transfer (McLysaght et al., 2003), suggests that this protein does not have an essential function during the viral life cycle. This hypothesis is consistent with previous reports that the profilin homolog is not essential for virus replication in cell culture (Blasco et al., 1991), although it is suspected that the profilin homolog confers an

advantage to the virus at some point during its life cycle. If the profilin homolog has a nonessential function that increases the fitness of the virus in its host, such as involvement in modulation of the host immune responses, this function may only become apparent during natural infection.

It has been demonstrated that profilins maintain very similar three-dimensional structures even if the amino acid sequence is poorly conserved between organisms. The conservation of the characteristic profilin fold is important in binding of actin, poly (L-proline and phosphoinosities (Mahoney et al., 1997). In agreement with these previous observations, a homology model of ECTV-Mos 141 (Figure 10B) suggests that although mammalian profilin and the viral profilin homolog share only 30% sequence identity (Figure 10A), ECTV-Mos 141 likely shares a structure similar to that of its mammalian counterpart. There are, however, differences between the proteins in both the structure (Figure 10B) and in the composition of residues comprising ligand binding domains (Figure 10A), which might have important implications in the function of the profilin homolog. The low affinity of ECTV-Mos 141 for actin in comparison to all other known profilins (Machesky et al., 1994) can be explained in part by the acquisition of residues in the profilin homolog with bulkier side chains at R116, Y81 and Y119 compared with the corresponding residues, G121, F83 and N125 in bovine profilin, which may prevent close contact between the profilin homolog and actin (Schutt et al. 1993). Similarly, absence of alpha helix 3 in the viral profilin homolog, shown to be important for actin interaction in bovine profilin may also account for decreased affinity for actin (Schutt et al., 1993). Additionally, the viral profilin homolog does not bind poly (L-proline) sequences, which

may be due to the loss of several aromatic residues at I8, L33, N129, N134, corresponding to bovine profilin Y7, W32, H134 and Y140, shown to be involved in forming this interaction (Bjorkegren et al., 1993). Interestingly, the VACV profilin homolog maintains an ability to bind phosphoinosities with an affinity comparable to that of mammalian profilin (Machesky et al., 1994), possibly through the conservation of positively charged basic residues at K27, R99, K110, R120 and R130. These positively charged basic residues have been shown to form a positive electrostatic surface potential on human profilin that is suitable for the binding of PIP_2. It is not yet clear what advantage the loss of affinity for actin and poly (L-proline) coupled with the retention of affinity for phosphoinositides confers upon the viral profilin homolog during viral infection. The loss of affinity for poly (L-proline) may affect localization of the profilin homolog *in vivo*. Cellular profilins bind to the proline-rich sequences of several proteins, such as WASP and VASP, which are intimately involved in actin polymerization, and therefore may act to localize profilin to the sites of rapid actin assembly (Paavilainen et al., 2004). The loss of affinity for poly (L-proline) and may allow the profilin homolog to disperse into other areas of the cell where actin is not being rapidly assembled to perform functions advantageous to the virus life cycle, while still maintaining an ability to modulate actin regulatory proteins through interaction with phosphoinositides.

Further evidence supporting the hypothesis that the profilin homolog may not interact with the actin cytoskeleton directly comes from observations made during purification of ECTV-Mos 141 from *E. coli* overexpressing the protein. The profilin homolog demonstrates ability to self-associate, as putative dimers of the purified protein were

visible on a Coomassie stained SDS-PAGE gel (Figure 7A), and on a western blot using antibodies directed against the epitope tag on the protein (Figure 7B). Although there have been no previous reports of the poxvirus profilin homolog having the ability to self-interact, multimerization has been described for human platelet profilin (Babich et al., 1996). Human profilin 1 forms both dimers and tetramers after purification that are readily visible on an SDS-PAGE gel, and it has been demonstrated that the tetramers are the high affinity actin binding form (Babich et al., 1996). The inability to detect viral profilin homolog tetramers during SDS-PAGE analysis of the purified protein (Figure 7A) suggests another reason why the protein has a lower affinity for actin compared to cellular profilin, and supports the suggestion that the profilin homolog does not interact with actin directly during infection. The interpretation of this experiment depends on the assumption that the properties of the recombinant ECTV-Mos profilin homolog are representative of the native protein. Although it has not yet been possible to purify native protein from virus infected cells, other reports which have extensively characterized recombinant human profilins produced in *E. coli* have not found substantial functional or structural differences compared to native proteins (Federov et al., 1994; Vinson et al., 1993). Future experiments are required to confirm the formation of ECTV-Mos 141 dimers on the SDS-PAGE gel, and in addition, more sensitive detection methods should be employed to confirm the absence of profilin homolog tetramers.

Surprisingly, the profilin homolog coimmunoprecipitated with α–tropomyosin 1 and VACV-WR 148, a truncated viral A-type inclusion protein from VACV-infected cells (Figure 11). The interactions between ECTV-Mos 141 and tropomyosin was shown to be

specific and not mediated through actin or the eptiope tag on ECTV-Mos 141 in subsequent control experiments (Figures 12 and 13). Although the function of α-tropomyosin 1 is poorly understood in non-muscle cells, it has been linked to intracellular transport of cellular vesicles via actin microfilaments (Liu and Bretscher, 1992). The coimmunoprecipitation of the ECTV-Mos profilin homolog with a cellular protein implicated in intracellular trafficking of cellular cargo lends further evidence to the hypothesis that the profilin homolog may be involved in the manipulation of the cytoskeleton by orthopoxviruses for the transportation of viral cargo.

The colocalization of the profilin homolog with tropomyosin during viral infection *in vivo* was determined using indirect immunofluorescence (Figure 17). Proteins were shown to colocalize to structures at the periphery of the cell resembling actin tails (Figure 17 arrow 1), and at virus-induced protrusions from the cell surface (Figure 17 arrow 2), which are important for intercellular spread of the virus (Smith et al., 2002). Although the profilin homolog has been shown to be nonessential for the formation of these protrusions in cell culture (Blasco et al., 1991), the possibility exists that the profilin homolog may affect these processes during natural infection of a host, and the localization of ECTV-Mos 141 to these structures *in vivo* supports this prospect.

The interaction between the poxvirus profilin homolog and viral A-type inclusion proteins has been detected in a yeast 2-hybrid analysis (McCraith et al., 2000), however the immunoprecipitation data presented in this thesis is the only known work demonstrating that these proteins interact during viral infection *in vivo*. Most

orthopoxviruses, including vaccinia, variola and monkeypox, contain a truncated A-type inclusion protein that has a highly conserved N-terminal domain, sharing greater than 70% amino acid identity (Figure 14) (Osterrieder, 1994). Although no function has yet been ascribed to the truncated A-type inclusion proteins, the high accumulation of this protein in infected cells (about 4% of total cellular protein) and the conservation of this gene in all known orthopoxviruses, suggests that the protein is maintained because its confers some advantage to the virus (de Carlos and Paez, 1991).

Colocalization of the ECTV-Mos profilin homolog and both the truncated and full-length A-type inclusion proteins, was investigated *in vivo* using indirect immunofluoresence. The profilin homolog was shown to colocalize with both the truncated and full-length A-type inclusion proteins. Association of the profilin homolog and the truncated A-type inclusion protein occurs at higher concentrations in several areas throughout the cytoplasm (Figure 15E arrows 1 and 2), and may be colocalizing to inclusion bodies formed by the aggregation of the truncated A-type inclusion protein. Although inclusion bodies formed by truncated A-type inclusion proteins are rarely formed and are purportedly unstable, they have been described previously in the literature (de Carlos and Paez, 1991). Interestingly, IMV also appear to be localizing to these putative inclusion bodies (Figure 15E arrows 1 and 2), an observation that has not been previously documented in the literature. It is possible that truncated A-type inclusion proteins are able to form inclusion bodies into which IMV can be sequestered, although the inherent instability of these bodies makes this event difficult to visualize. The profilin homolog and the truncated A-type inclusion protein also colocalize at the cell periphery to

structures resembling virus-induced protrusions (Figure 15 arrow 3), although the significance of protein colocalization at these locations remains unclear.
Similarly, the profilin homolog also associated with large inclusion bodies formed by a full-length A-type inclusion protein (Figure 16E), although some of ECTV-Mos 141 remained distributed throughout the cytoplasm suggesting that the profilin homolog may be interacting with other proteins, possibly tropomyosin, in the cytoplasm.

Although the vTF7-3 transient expression system is commonly employed in poxvirology to investigate localization of proteins *in vivo* (Fuerst et al., 1996), further experiments with additional controls are needed to confirm the results of these immunofluorescence experiments and to discount the possibility that colocalization of ECTV-Mos 141, with tropomyosin, and the A-type inclusion proteins *in vivo* is an artifact of overexpression of the viral proteins. Similar localization experiments performed using recombinant viruses encoding epitope-tagged versions of the viral proteins would be more representative of the levels of these proteins produced during natural infection and would provide a clearer picture of where protein colocalization occurs. Additionally, localization of actin within the cell is needed to confirm the identity of the structures putatively described as actin tails and virus-induced protrusions from the cell surface.

The function of the viral profilin homolog during natural viral infection of a host remains unclear. The association of the viral profilin homolog with A-type inclusion proteins and tropomyosin, offers few insights into the function of the viral profilin homolog, as the functions of these proteins are also poorly understood. However, a clue to this puzzle

may be slowly emerging. It is now understood that intracellular enveloped virions (IEVs) are transported to the cell periphery along the microtubule cytoskeleton powered by kinesin motor proteins (Rietdorf et al., 2001), as simple diffusion through the viscous cytoplasm would be a slow and inefficient process (Sodeik, 2000). For the same reasons that active transport mechanisms are needed to move IEVs to the plasma membrane, similar mechanisms may be necessary for the retrograde transport of both IMVs and the viral A-type inclusion proteins to the sites where these proteins colocalize (McKelvey et al., 2002). It has been suggested that certain high molecular weight, non-muscle tropomyosins, may be involved in organelle transport that utilizes both microtubules and actin filaments (Pelham et al., 1996; Liu et al., 1992). By overexpressing tropomyosin 3 in mammalian cells, dramatic retrograde translocation and accumulation of organelles into the perinuclear area is observed, although the mechanism through which tropomyosin brings about this effect is far from clear (Pelham et al., 1996). It is possible that the viral profilin homolog and tropomyosin may be involved in the retrograde transport of the A-type inclusion proteins to the sites where they will colocalize with IMV. The interaction with tropomyosin mediated through the profilin homolog may also act to tether the A-type inclusion bodies to the cytoskeleton. The localization of the viral profilin homolog, the truncated A-type inclusion protein, and tropomyosin to structures resembling actin tails and virus-induced protrusions from the cell surface may indicate that these proteins are involved in intercellular transport of virions. Until further experiments are conducted that characterize the interactions between these proteins in greater depth, one can only speculate on the functional significance of this complex.

Although a specific function cannot yet be attributed to the profilin homolog, these results lay the foundation for further characterization of the protein and suggest that the protein may be involved in utilizing the cellular cytoskeleton for transport of intracellular transport of viral proteins and for the intercellular transport of virions.

Conclusion

This thesis focused on the further characterization of a highly conserved orthopoxvirus gene encoding a profilin homolog. The variety of cellular processes influenced by cellular profilin includes regulation of actin polymerization and modulation of actin binding proteins. The ability of poxviruses to utilize the cellular cytoskeleton for the transport of virions and viral components during viral infection suggests that the profilin homolog may play a role in these processes.

Although it is still not possible to assign a role to the profilin homolog in poxvirus infection, this work has contributed to the overall picture by demonstrating that the ECTV-Mos 141 interacts directly with cellular tropomyosin and viral A-type inclusion proteins *in vivo*. The significance of this interaction remains unclear, but suggests that the profilin homolog may be important for intracellular transport of viral proteins in the cytoplasm on the cellular microtubule cytoskeleton. The profilin homolog also co-localizes with tropomyosin and the truncated A-type inclusion protein to structures at the cell periphery important for intercellular transport of the virus, implicating the proteins in this process. A homology model of the ECTV-Mos profilin homolog demonstrates that the protein maintains many features of the characteristic profilin fold found in all profilins to date (Nodelman et al., 1999). In contrast to all other known profilins, however, the viral profilin homolog displays a decreased affinity for actin and loss of affinity for poly (L-proline) (Machesky et al., 1994), a result of the mutation or deletion of key residues involved in forming these interactions. The maintenance of the

phosphoinositide binding domain in the profilin homolog suggests that the protein could maintain an ability to modulate actin regulatory proteins.

I hope that this thesis lays the foundation for further characterization of the profilin homolog, as many aspects of this preliminary characterization suggest an important role for the protein during the viral life cycle. Illuminating the mechanisms by which poxviruses manipulate the cytoskeleton will not only result in a deeper understanding of the virus-host relationship, but may also give a fresh insight into mechanisms by which cells organize and control the actin and microtubule cytoskeletons. In addition, the cloning of 28 of the 56 conserved orthopoxvirus genes identified at the onset of this project is the first step in further characterization of these genes, which will undoubtedly resulting in an enhanced understanding of poxvirus biology.

Literature Cited

Afonso, C.L., G. Delhon, E. R. Tulman, Z. Lu, A. Zsak, V. M. Becerra, L. Zsak, G. F. Kutish, and D. L. Rock. 2005. Genome of Deerpox Virus. *Journal of Virology*. 79:966-977.

Afonso, C.L., E.R. Tulman, Z. Lu, L. Zsak, N.T. Sandybaev, U.Z. Kerembekova, V.L. Zaitsev, G.F. Kutish, D.L. Rock. 2002a. The genome of camelpox virus. *Virology*. 295:1-9.

Afonso, C.L., E.R. Tulman, Z. Lu, L. Zsak, F.A. Osorio C. Balinsky, G.F. Kutish and D.L. Rock. 2002b. The genome of swinepox virus. *Journal of Virology*. 76:783-790.

Afonso, C.L., E.R. Tulman, Z. Lu, L. Zsak, G.F. Kutish and K.L. Rock. 2000. The genome of fowlpox virus. *Journal of Virology*. 74:3815-3831.

Afonso, C.L., E.R. Tulman, Z. Lu, E. Oma, G.F. Kutish and D.L. Rock. 1999. The genome of *Melanoplus sanguinipes* entomopoxvirus. *Journal of Virology*. 73:533-552.

Altschul, S.F., T.L. Madden, A.A. Schaffer, J. Zhang, Z. Zhang, W. Miller and D.J. Lipman. 1997. Gapped BLAST and PSI-BLAST: a new generation of protein database search programs. *Nucleic Acids Research*. 25:3389-3402.

Altschul, S.F., W. Gish, W. Miller, E.W. Myers and D.J. Lipman. 1990. "Basic local alignment search tool." *Journal of Molecular Biology*. 215:403-410.

Antoine, G., F. Scheiflinger, F. Dorner, and F.G. Falkner. 1998. The complete genomic sequence of the modified vaccinia Ankara strain: comparison with other orthopoxviruses. *Virology*. 244:365396.

Arif, B.M. 1984. The entomopoxviruses. *Advances in Virus Research.* 29:195-213.

Babich, M., L. Foti, L. Sykaluk and C. Clark. 1996. Profilin forms tetramers that bind to G-actin. *Biochemical and Biophysical Research Communications.* 218:125-131.

Baroudy, B.M., S. Venkatesan and B. Moss. 1982. Incompletely base-paired flip-flop terminal loops link the two DNA strands of the vaccinia virus genome into one uninterrupted polynucleotide chain. *Cell.* 28:315-324.

Barquet, N., and P. Domingo. 1997. Smallpox: the triumph over the most terrible of the ministers of death. *Annals of Internal Medicine.* 127:635-642.

Bawden, A. L., K. J. Glassberg, J. Diggans, R. Shaw, W. Farmerie and R. W. Moyer. 2000. Complete genomic sequence of the Amscata moorei entomopoxvirus: analysis and comparison with other poxviruses. *Virology.* 274:120-139.

Bearer, E. L. and P. Satpute-Krishnan. 2002. The role of the cytoskeleton in the life cycle of viruses and intracellular bacteria: tracks, motors, and polymerization machines. *Current Drug Targets for Infectious Disorders.* 2:247-264.

Beaud, G. 1995. Vaccinia virus DNA replication: A short review. *Biochimie.* 77:774-779.

Bharadwaj, S., S. Hitchcock-DeGregori, A. Thorburn and G.L. Prasad. 2004. N terminus is essential for tropomyosin functions. *The Journal of Biological Chemistry.* 279:14039-14048.

Birnboim, H.C., and J. Doly. 1979. A rapid alkaline extraction procedure for screening recombinant plasmid DNA. *Nucleic Acids Research.* 7:1513-23.

Bjorkegren C., M. Rozycki, C.E. Schutt, U. Lindberg and R. Karlsson. 1993. Mutagenesis of human profilin locates its poly(L-proline)-binding site to a hydrophobic patch of aromatic amino acids. *FEBS Journal.* 333:123-126.

Blasco, R. and B. Moss. 1992. Role of cell-associated enveloped vaccinia virus in cell-to-cell spread. *Journal of Virology*. 66:4170-4179.

Boone, R.F. and B. Moss. 1978. Sequence complexity and relative abundance of vaccinia virus mRNA's synthesized in vivo and in vitro. *Journal of Virology*. 26:554-569.

Bray, M., and C.J. Roy. 2004. Antiviral prophylaxis of smallpox. *Journal of Antimicrobial Chemotherapy*. 54:1-5.

Broyles, S. Vaccinia virus transcription. 2003. *Journal of General Virology*. 84:2293-2303.

Brunetti,C.R., H. Amano, Y. Ueda, J. Qin, T. Miyamura, T. Suzuki, X. Li, J.W. Barrett and G. McFadden. 2003. Complete Genomic Sequence and Comparative Analysis of the Tumorigenic Poxvirus Yaba Monkey Tumor Virus. *Journal of Virology*. 77:13335-13347.

Bugert, J.J. and G. Darai. 2000. Poxvirus homologues of cellular genes. *Virus Genes*. 21:111-133.

Buller, R.M. and G.J. Palumbo. 1991. Poxvirus pathogenesis. *FEMS Microbiology Reviews*. 55:80-122.

Cameron, C., S. Hota-Mitchell, L. Chen, J. Barrett, J.X. Cao, C. Macaulay, D. Willer, D. Evans, and G. McFadden. 1999. The complete DNA sequence of myxoma virus. *Virology*. 264:298-318.

Carlsson, L., L.E. Nystrom, I. Sundkvist, F. Markey and U. Lindberg. 1977. Actin polymierization is influenced by profilin, a low molecular weight protein in non-muscle cells. *Journal of Molecular Biology*. 115:465-483.

Carroll, M.W., B. Moss. 1997. Poxviruses as expression vectors. *Current Opinion in Biotechnology*. 8:573-577.

Chen, N., R.M. Buller, E.M. Wall and C. Upton. 2000. Analysis of host response modifier ORFs of ectromelia virus, the causative agent of mousepox. *Virus Research.* 66:155-173.

Chen, W., R. Drillien, D. Spehner and R.M. Buller. 1992. Restricted replication of ectromelia virus in cell culture correlates with mutations in virus-encoded host range gene. *Virology.* 187:433-442.

de Carlos, A. and E. Paez. 1991. Isolation and characterization of mutants of vaccinia virus with a modified 94-kDa inclusion protein. *Virology.* 185:768-778.

Delhon,G., E.R. Tulman, C.L. Afonso, Z. Lu, A. de la Concha-Bermejillo, H.D. Lehmkuhl, M.E. Piccone, G.F. Kutish and D.L. Rock. 2004. Genomes of the Parapoxviruses Orf Virus and Bovine Papular Stomtatitis Virus. *Journal of Virology.* 78:168-177.

des Gouttes Olgiati, B.G. Pogo and S. Dales. 1976. Biogenesis of vaccinia: specific inhibition of rapidly labeled host DNA in vaccinia inoculated cells. *Virology.* 71:325-335.

De Silva, F. S. and B. Moss. 2005. Origin-independent plasmid replication occurs in vaccinia virus cytoplasmic factories and requires all five known poxvirus replication factors. *Virology Journal.* 2:23.

Doms, R. W., R. Blumenthal and B. Moss. 1990. Fusion of intra- and extracellular forms of vaccinia virus with the cell membrane. *Journal of Virology.* 64:4884-4892.

Dong, J., B. Radau, A. Otto, E. Muller, C. Lindschau and P. Westermann. 2000. Profilin I attached to the Golgi is required fro the formation of constitutive transport vesicles at the trans-Golgi network. *Biochimica et Biophysica Acta.* 1497:253-260.

Du, S. and P. Traktman. 1996. Vaccinia virus DNA replication: two hundred base pairs of telomeric sequence confer optimal replication efficiency on minichromosome templates. *Proceedings of the National Academy of Sciences USA*. 93: 9693-9698.

Dubochet, J., M. Adrian, K. Richter, J. Garces and R. Wittek. 1994. Structure of intracellular mature vaccinia virus observed by cryoelectron microscopy. *Journal of Virology*. 68:1935-1941.

Dunlop, L.R., K.A. Oehlberg, J.J. Reid, D. Avci and A.M. Rosengard. 2003. Variola virus immune evasion proteins. *Microbes and Infection*. 5:1049-1056.

Einarson, M.B. and J.R. Orlinick. 2002. Identification of protein-protein interactions with glutathione-S-transferase fusion proteins. In " Erica Golemis (ed), Protein-protein interactions." Cold Spring Harbor Laboratory Press, Cold Spring Harbor, NY, USA, pp. 37-57.

Ellner, P.D. 1998. Smallpox: gone but not forgotten. *Infection*. 26:263-269.

Esteban, M. and D.H. Metz. 1973. Early virus protein synthesis in vaccinia virus infected cells. *Journal of General Virology*. 19:201-206.

Fedorov, A.A. K.A. Magnus, H. Graupe, E.E. Lattman, T.D. Pollard and S.C. Almo. 1994.

Fenner, F., R. Wittek and K.R. Dumbell. 1989. *In* " The Orthopoxviruses. New York&London: Academic Press, San Diego, CA, USA. pp. 198-239.

Frischknecht, F., V. Moreau, S. Rottger, S. Gonfloni, I. Rechman, G. Superti-Furga and M. Way. 1999. Actin-based motility of vaccinia virus mimics receptor kinase signaling. *Nature*. 401:926-929.

Fuerst, T.R, P.L. Earl and B. Moss. 1986. Eukaryotic transient-expression system based on recombinant vaccinia virus that synthesizes bacteriophage T7 polymerase. *Proceedings of the National Academy of Sciences USA*. 83:8122-8126.

Funahashi, S., T. Sato and H. Shida. 1988. Cloning and characterization of the gene encoding the major protein of the A-type inclusion body of cowpox virus. *Journal of General Virology*. 69:35-47.

Goebel, S.J., G.P. Johnson, M.E. Perkus, S.W. Davis, J.P. Winslow and E. Paoletti. 1990. The complete DNA sequence of vaccinia virus. *Virology*. 179:247-266.

Gouin, E. M.D. Welch and P. Cossart. 2005. Actin-based motility of intracellular pathogens. *Current Opinion in Microbiology*. 8:35-45.

Gubser, C. and G.L. Smith. 2002. The sequence of camelpox virus shows it is most closely related to variola virus, the cause of smallpox. *Journal of General Virology*. 83:855-872.

Haarer, B. and S. Brown. 1990. Structure and function of profilin. *Cell Motility and the Cytoskeleton*. 17:71-74.

Hall. A. 2004. Src launches vaccinia. *Science*. 306:65-67.

Harrison, S.C., B. Alberts, E. Ehrenfeld, L. Enquist, H. Fineberg, S.L. McKnight, B. Moss, M. O'Donnell, H. Ploegh, S.L. Schmid, K.P. Walter, J. Theriot. 2004. Discovery of antivirals against smallpox. *Proceedings of the National Academy of Sciences*. 101:11178-11192.

Higgins, D., J. Thompson, J.D Thompson, D.G. Higgins, T.J. Gibson. 1994. CLUSTAL W: improving the sensitivity of progressive multiple sequence alignment through sequence weighting, position-specific gap penalties and weight matrix choice. *Nucleic Acids Research*. 22:4673-4680.

Hiller, G. and K. Weber. 1985. Golgi-derived membranes that contain an acylated viral polypeptide are used for vaccinia virus envelopment. *Journal of Virology*. 55:651-659.

Hooft, R.W.W., G. Vriend, C. Sander and E.E. Abola. 1996. Errors in protein structures. *Nature*. 381:272-272.

Huang, X., and M. Webb. 1991. A time-efficient, linear-space local similarity algorithm. *Advances in Applied Mathematics*. 12:337-357.

Hughes, A. and R. Friedman. 2005. Poxvirus genome evolution by gene gain and loss. *Molecular Phylogenetics and Evolution*. 35:186-195.

Hughes, S.J., L.H. Johnston, A. de Carlos and G.L. Smith. 1991. Vaccinia virus encodes an active thymidylate kinase that complements a *cdc8* mutant *of saccharomyces cerevisiae*. *The Journal of Biological Chemistry*. 30:20103-20109.

Husain, M. and B. Moss. 2005. Role of receptor-mediated endocytosis in the formation of vaccinia virus extracellular enveloped particles. *Journal of Virology*. 79:4080-4089.

Husain, M. and B. Moss. 2003. Intracellular trafficking of a palmitoylated membrane-associated protein component of enveloped vaccinia virus. 2003. *Journal of Virology*. 77:9008-9019.

Ichihashi, Y. 1996. Extracellular enveloped vaccinia virus escapes neutralization. *Virology*. 217:478-485.

Ichihashi, Y., S. Matsumoto, and S. Dales. 1971. Biogenesis of poxviruses: role of A-type inclusions and host cell membranes in virus dissemination. *Virology*. 46:507-532.

Jones, A.L., M.D. Hulett and C.R. Parish. Histidine-rich glycoprotein binds to cell-surface heparan sulfate via its N-terminal domain following Zn2+ chelation. *Journal of Biological Chemistry*. 279:30114-3022.

Kamal, A. and L. Goldstein. 2002. Principles of cargo attachment to cytoplasmic motor proteins. *Current Opinion in Cell Biology*. 14:63-68.

Kara, P.D., C.L. Afonso, D.B. Wallace, G.F. Kutish, C. Abolnik, Z. Lu, F.T. Vreede, L.C.F. Taljaard, A. Zsak, G.J. Viljoen and D.L. Rock. 2003. Comparative sequence analysis of the South African vaccine strain and two virulent field isolates of Lumpy skin disease virus. *Archives of Virology*. 148:1335-1356.

Keck, J.G., C.J. Baldick Jr. and B. Moss. 1990. Role of DNA replication in vaccinia virus gene expression: a naked template is required for transcription of three late trans-activator genes. *Cell*. 61:801-809.

Kyte, J., and R.F. Doolittle. 1982. A simple method for displaying the hydopathic character of a protein. *Journal of Molecular Biology*. 157:105-132.

Laidlaw, S.M.and M.A. Skinner. 2004. Comparison of the genome sequence of FP9, an attenuated, tissue culture-adapted European strain of Fowlpox virus, with those of virulent American ad European viruses. *Journal of General Virology*. 85:305-322.

Landy, A. 1989. Dynamic, structural, and regulatory aspects of lambda site-specific recombination. *Annual Review of Biochemistry*. 58:913-945.

Langford, G.M. 1995. Actin-and microtubule-dependent organelle motors: interrelationship between the two motility systems. *Current Opinions in Cell Biology*. 7:82-88.

Lee, H.J., K. Essani and G.L. Smith. 2001. The genome sequence of Yaba-like disease virus, a yatapoxvirus. *Virology*. 281:170-192.

Locker, J K., A. Kuehn, S. Schleich, G. Rutter, H. Hohenberg, R. Wepf and G. Griffiths. 2000. Entry of the two infectious forms of vaccinia virus at the plasma membrane is signaling-dependent for the IMV but not the EEV. *Molecular Biology of the Cell.* 11:2497-2511.

Lorenzo, M., E. Herrera, R. Blasco and S. Isaacs. 1998. Functional analysis of vaccinia virus B5R protein: role of the cytoplasmic tail. *Virology.* 252:450-457.

Machesky, L. N.B. Cole, B. Moss and D. Pollard. 1994. Vaccinia virus expresses a novel profilin with a higher affinity for polyphosphoinosities than actin. *Biochemistry.* 33:10815-10824.

MacLeod, A.R., and C. Gooding. 1988. Human hTMα gene: expression in muscle and nonmuscle tissue. *Molecular and Cellular Biology.* 8:433-440.

Mahalingam, S., I. Damon and B. Lidbury. 2004. 25 years since the eradication of smallpox: why poxvirus research is still relevant. *TRENDS in Immunology.* 25:636-639.

Mahoney, N.M., P.A. Janmey and S.C. Almo. 1997. Structure of the profilin-poly-L-proline complex involved in morphogenesis and cytoskeletal regulation. *Nature Structural Biology.* 4:953-960.

Makett, M. and L.C. Archard. 1979. Conservation and variation in Orthopoxvirus genome structure. *Journal of General Virology.* 45:683-701.

Martz, E. 2002. Protein Explorer: easy yet powerful macromolecular visualization. *Trends in Biochemical Sciences.* 27:107-109.

Massung, R.F., L.I. Liu, J. Qi, J.C. Knight, T.E. Yuran, A.R. Kerlavage, J.M. Parsons, J.C. Venter and J.J. Esposito. 1994. Analysis of the complete genome of smallpox variola major virus strain Bangladesh – 1975. *Virology.* 201:215-240.

McCraith, S., T. Holtzman, B. Moss and S. Fields. 2000. Genome-wide analysis of vaccinia virus protein-protein interactions. *Proceedings of the National Academy of Sciences USA*. 97:4879-4884.

McDonald, W.F. and P. Traktman. 1994. Overexpression and purification of the vaccinia virus DNA polymerase. *Protein Expression and Purification*. 5:409-421.

McFadden, F. 2005. Poxvirus tropism. *Nature Reviews in Microbiology*. 3:201-213.

McKelvey, T., S. Andrews, S. Miller, C. Ray, and D. Pickup. 2002. Identification of the orthopoxvirus *p4c* gene, which encodes a structural protein that directs intracellular mature virus particles into A-type inclusions. *Journal of Virology*. 76:11216-11225.

McLysaght, A., P. Baldi and B. Gaut. 2003. Extensive gene gain associated with adaptive evolution f poxviruses. *Proceedings of the National Academy of Sciences USA*. 100:15655-15660.

Meyer, H. and H.J. Rziha. 1993. Characterization of the gene encoding the A-type inclusion protein of camelpox virus and sequence comparison with other orthopoxviruses. *Journal of General Virology*. 74:1679-1684.

Miner, J.N. and D.E. Hruby. 1990. Vaccinia virus: A versatile tool for molecular biologists. *Trends in Biotechnology*. 8:20-25.

Miyagi, Y., T. Yamashita, M. Fukaya, T. Sonoda, T. Okuno, K. Yamada, M. Watanabe, Y. Nagashima, I. Aoki, K. Okuda, M. Mishina and S. Kawamoto. 2002. Delphilin: a novel PDZ and formin homology domain-containing protein that synaptically colocalizes and interacts with glutamate receptor δ2 subunit. *Journal of Neuroscience*. 22:803-814.

Moritz, R., J. Eddes, J. Hong, G. Reid and R. Simpson. 1995. Rapid separation of proteins and peptides using conventional silica-based supports: identification of 20 gel proteins following in-gel proteolysis. *In* " J.W. Crabb (ed.), Techniques in protein chemistry." Academic Press, San Diego, CA, USA, vol. 6. pp. 311-319.

Moss, B. 2001. *Poxviridae*: The viruses and their replication. *In* Fundamental Virology. B.N. Fields, D.M. Knipe, and P.M. Howley, editors. Lippincott-Raven Publishers, Philadelphia. 1163-1197.

Moss, B. and P.L. Earl. 1998. Expression of proteins in mammalian cells using vaccinia viral vectors. Overview of the vaccinia virus expression system. *In* "Current Protocols in Molecular Biology." John Wiley & Sons, Inc. Publishers, Hoboken, NJ, USA, Vol. 3, pp. 16.15.1-16.15.5.

Muller, H.K., R. Wittek, W. Schaffner, D. Schumperli, A. Menna, R. Wyler. 1978. Comparison of five poxvirus genomes by analysis with restriction endonucleases HindIII, BamI and EcoRI. *Journal of General Virology*. 38:135-147.

Newman, J.R and C. Fuqua. 1999. Broad-host-range expression vectors that carry the L-arabinose-inducible *Escherichia coli araBAD* promoter and the *araC* regulator. *Gene*. 227:197-203.

Newsome, T.P., N. Scaplehorn and M. Way. 2004. SRC mediates a switch from microtubule-to actin-based motility of vaccinia virus. *Science*. 306:2264-2267.

Niemialtowski M., I. Spohr de Faundez, M. Gierynska, E. Malicka, F. Toka, A. Schollenberger and A. Popis. 1994. The inflammatory and immune response to mousepox (infectious ectromelia) virus. *Acta virologica*. 38:299-307.

Osterrieder, N., H. Meyer and M. Pfeffer. 1994. Characterization of the gene encoding the A-type inclusion body protein of Mousepox virus. *Virus Genes*. 8:125-135.

Paavilainen, V., E. Bertling, S. Falck and P. Lappalainen. 2004. Regulation of cytoskeletal dynamics by actin-monomer-binding proteins. *TRENDS in Cell Biology*. 14:386-394.

Payne, L.G. 1980. Significance of extracellular virus in the in vitro and in vivo dissemination of vaccinia virus. *Journal of General Virology*. 50:89-100.

Peitsch, M.C. 1996. ProMod and Swiss-Model: Internet-based tools for automated comparative protein modeling. *Biochemical Society Transactions*. 24:274-279.

Pelham, R., J. Jung-Ching Lin, and Y. Wang. 1996. A high molecular mass non-muscle tropomyosin isoform stimulates retrograde organelle transport. *Journal of Cell Science*. 109:981-989.

Perkins, D.N., D.J. Pappin, D.M. Creasy and J.S. Cottrell. 1999. Probability-based protein identification by searching sequence databases using mass spectrometry data. *Electrophoresis*. 20:3551-3567.

Perkus, M.A., J. Tartaglia and E. Paoletti. 1995. Poxvirus-based vaccine candidates for cancer, AIDS, and other infectious diseases. *Journal of Leukocyte Biology*. 58:1-13.

Perry, S.V. 2001. Vertebrate tropomyosin: distribution, properties and function. *Journal of Muscle Research and Cell Motility*. 22:5-49.

Ploubidou, A., V. Moreau, K. Ashman, I. Reckmann, C. Gonalez and M. Way. 2000. Vaccinia virus infection disrupts microtubule organization and centrosome function. *The EMBO Journal*. 19:3932-3944.

Rea, G., P. Iacovacci, P. Ferrante, M. Zelli, B. Brunetto, D. Lamba, A. Boffi, C. Pini, R. Federico. 200. Refolding of the Cupressus arizonica major pollen allergen Cupa1.0 overexpressed in Escherichia coli. *Protein Expression and Purification*. 37: 419-425.

Rietdorf, J. A. Ploubidou, I. Reckmann, A. Holmstrom, F. Frischknecht, M. Zetti, T. Zimmermann and M. Way. 2001. Kinesin-dependent movement on microtubules precedes actin-based motility of vaccinia virus. *Nature Cell Biology*. 3:992-1000.

Roper, R.L. 2004. Rapid preparation of vaccinia virus DNA template for analysis and cloning by PCR. *Methods in Molecular Biology*. 269:213-218.

Sanchez, G., A. Bosch and R.M. Pinto. 2003. Genome variability and capsid structural constraints of hepatitis a virus. *Journal of Virology*. 77:452-459.

Sanderson , C. M., M. Hollinshead and G. L. Smith. 2000. The vaccinia virus A27L protein is needed for the microtubule-dependent transport of intracellular mature virus particles. *Journal of General Virology*. 83:2915-2931.

Sarisky, R.T. and P.C. Weber. 1994. Role of anisomorphic DNA conformations in the negative regulation of herpes simplex virus type 1 promoter. *Virology*. 204;569-579.

Schutt, C., J.C. Myslik, M.D. Rozychi, N.C.W. Goonesekere and U. Lindberg. 1993. The structure of crystalline profilin-beta-actin. *Nature*. 365:810-816.

Schwede T., J. Kopp, N. Guex and M.C. Peitsch. 2003. SWISS-MODEL: an automated protein homology-modeling server. *Nucleic Acids Research*. 31:3381-3385.

Seet B.T., J.B. Johnston, C.R. Brunetti, J.W. Barrett, H. Everett, C. Cameron, J. Sypula, S.H. Nazarian, A. Lucas and G. McFadden. 2003. Poxviruses and immune evasion. *Annual Reviews of Immunology*. 21:377-423.

Senkevich, T.G. and B. Moss. 2005. Vaccinia virus H2 protein is an essential component of a complex involved in virus entry and cell-cell fusion. *Journal of Virology*. 79:4744-4754.

Senkevich, T.G., E.V. Koonin, J.J. Bugert, G. Darai, and B. Moss. 1997. The genome of molluscum contagiosum virus: analysis and comparison with other poxviruses. *Virology*. 233:19-42.

Shackelton, L. and E. Holmes. 2004. The evolution of large DNA viruses: combining genomic information of viruses and their hosts. *TRENDS in Microbiology*. 12:458-465.

Shchelkunov, S. N., A.V. Totmenin, I.V. Babkin, P.F. Safronov, O.I. Ryazankina, N.A. Petrov, V.V. Gutorov, E.A. Uvarova, M.V. Mikheev, J.R. Sisler, J.J. Esposito, P.B. Jahrling, B. Moss and L.S. Sandakhchiev. 2001. Human monkeypox and smallpox viruses: genomic comparison. *FEBS Letters*. 509:66-70.

Shchelkunov, S. N., A.V. Totmenin, I.V. Babkin, P.F. Safronov, O.I. Ryazankina, N.A. Petrov, V.V. Gutorov, E.A. Uvarova, M.V. Mikheev, J.R. Sisler, J.J. Esposito, P.B. Jahrling, B. Moss and L.S. Sandakhchiev. 1996a. Study of the structure-activity organization of the smallpox viral genome. V. Sequencing and analysis of the nucleotide sequence of the left terminus of the India-1967 strain genome. *Molecular Biology* (Moscow). 30:595-612.

Shchelkunov, S. N., A.V. Totmenin, I.V. Babkin, P.F. Safronov, O.I. Ryazankina, N.A. Petrov, V.V. Gutorov, E.A. Uvarova, M.V. Mikheev, J.R. Sisler, J.J. Esposito, P.B. Jahrling, B. Moss and L.S. Sandakhchiev. 1996b. Analysis of the nucleotide sequence of 23.8 kbp from the left terminus of the genome of variola major virus strain India-1967. *Virus Research*. 40:169-183.

Shen, Y. and J. Nemunaitis. 2004. Fighting cancer with vaccinia virus: teaching new tricks to an old dog. *Molecular Therapy*. 11:180-195.

Shine, J., and Dalgarno, L. 1975. Terminal-sequence analysis of bacterial ribosomal RNA. Correlation between the 3'-terminal polypyrimidine sequence of 16-S RNA and translational specificity of the ribosome. *European journal of Biochemistry*. 57:221-230.

Skare, P., J.P. Kreivi, A. Bergstrom and R. Karlsson. 2003. Profilin I colocalizes with speckles and Cajal bodies: a possible role in pre-mRNA splicing. *Experimental Cell Research.* 286:12-21.

Skare, P. and R. Karlsson. 2002. Evidence for two interaction regions for phosphatidylinositol (4,5)-bisphosphate on mammalian profilin I. *FEBS Letters.* 522:199-124.

Slabaugh, M.B., R.E. Davis, N.A. Roseman and C.K. Mathews. 1993. Vaccinia virus ribonucleotide reductase expression and isolation of the recombinant large subunit. *Journal of Biological Chemistry.* 268:17803-17810.

Smith, L. and M. Law. 2004. The exit of vaccinia virus from infected cells. *Virus Research.* 106:189-197.

Smith G.L., B.J. Murphy and M. Law. 2003. Vaccinia virus motility. *Annual Review of Microbiology.* 57:323-342.

Smith. G.L., A. Vanderplasschen and M. Law. 2002. The formation and function of extracellular enveloped vaccinia virus. *Journal of General Virology.* 83: 2915-2931.

Sodeik, B. 2000. Mechanisms of viral transport in the cytoplasm. *TRENDS in Microbiology.* 8:465-472.

Stevens, R.C. 2000. Design of high-throughput methods of protein production for structural biology. *Structure.* 8:R177-R185.

Stuart, D.T., C. Upton, M.A. Higman, E.G. Niles and G. McFadden. 1993. A poxvirus-encoded uracil DNA glycosylase is essential for virus viability. *Journal of Virology.* 67:2503-2512.

Su, J.Y. and R.A. Sclafani. 1991. Molecular cloning and expression of the human deoxythymidylate kinase gene in yeast. *Nucleic Acids Research.* 19:823-827.

Sutter, G. and B. Moss. 1992. Nonreplicating vaccinia vector efficiently expresses recombinant genes. *Proceedings of the National Academy of Sciences, USA.* 89:10847-10851.

Szajner,P., A.S. Weisberg and B. Moss. 2001. Unique temperature-sensitive defect I vaccinia virus morphogenesis maps to a single nucleotide substitution in the A30L gene. *Journal of Virology.* 75:11222-11226.

Thompson, J.D., D.G. Higgins and T.J. Gibson. 1994. CLUSTAL W: improving the sensitivity of progressive multiple sequence alignment through sequence weighting, position-specific gap penalties and weight matrix choice. *Nucleic Acids Research.* 22:4673-4680.

Tulman,E.R., C.L. Afonso, Z. Lu, L. Zsak, G.F. Kutish and D.L. Rock. 2004. The genome of canarypox virus. *Journal of Virology.* 78:353-366.

Tulman, E.R., C.L. Afonso, Z. Lu, L. Zsak, J.H. Sur, N.T. Sandybaev, U.Z. Kerembekova, V.L. Zaitsev, G.F. Kutish and D.L. Rock. 2002. The genomes of sheeppox and goatpox viruses. *Journal of Virology.* 76:6054-6061.

Tulman, E.R., C.L. Afonso, Z. Lu, L. Zsak, G.F. Kutish and D.L. Rock. 2001. Genome of lumpy skin disease virus. *Journal of Virology.* 75:7122-7130.

Upton, C., S. Slack, A.L. Hunter, A. Ehlers, and R.L. Roper. 2003. Poxvirus Orthologous Clusters: toward defining the minimum essential poxvirus genome. *Journal of Virology.* 77:7590-7600.

Vanderplasschen, A. and G. L. Smith. 1997. A novel virus binding assay using confocal microscopy demonstrates that the intracellular and extracellular vaccinia virions bind to different cellular receptors. *Journal of Virology.* 71:4032-4041.

Wang, X., M. Kibschull, M.M. Laue, B. Lichte, E. Petrasch-Parwez and M.W. Kilimann. 1999. Aczonin, a 550-kD putative scaffolding protein of presynaptic active zones, shares homology regions with Rim and Bassoon and binds profilin. *Journal of Cell Biology*. 147:151-162.

Ward, B.M. 2005. Visualization and characterization of the intracellular movement of vaccinia virus intracellular mature virions. *Journal of Virology*. 79:4755-4763.

Willard, L., A. Ranjan, H. Zhang, H. Monzavi, R. Boyko, B. Sykes and D. Wishart. 2003. VADAR: a web server for quantitative evaluation of protein structure quality. *Nucleic Acids Research*. 31:3316:3319.

Willer, D.O., G. McFadden and D.H. Evans. 1999. The complete genome sequence of shope (rabbit) fibroma virus. *Virology*. 264:319-343.

Witke, W. 2004. The role of profilin complexes in cell motility and other cellular processes. *TRENDS in Cell Biology*. 14:461-469.

Witke, W. 1998. In mouse brain profilin I and profilin II associate with regulators of the endocytic pathway and actin assembly. *European Journal of Molecular Biology*. 17:967-976.

Yamamoto, M., D.H. Hilgemann, S. Feng, H. Bito, H. Ishihara, Y. Shibasaki, H.L. Yin. 2001. Phosphatidylinositol 4,5-bisphosphate induces actin stress-fiber formation and inhibits membrane ruffling in CV1 cells. *Journal of Cell Biology*. 152:867-876.

Ye, Y., Y. Shibata, C. Yun, D. Ron and T.A. Rapoport. 2004. A membrane protein complex mediates retro-translocation from the ER lumen into the cytosol. *Nature*. 429:841-847.